Andrew Ross

Nonlinear Manoeuvring Models for Ships: a Lagrangian Approach

PhD-thesis 2008:114

**Department of Engineering Cybernetics,
Faculty of Information, Technology,
Mathematics, and Electrical Engineering**

Contents

Department of Engineering Cybernetics
Faculty of Information Technology, Mathematics, and Electrical Engineering
Norwegian University of Science and Technology
NO-7491 Trondheim
Norway

NTNU Philosophiae Doctor 2008:114
ITK Report 2008:6-W

ISBN 978-82-471-8298-7 (printed)
ISBN 978-82-471-8303-8 (electronic)
ISSN 1503-8181

Abstract

This thesis analyses manoeuvring ships. Good modelling is vital for effective control system design and simulation. Such models are invaluable tools in areas such as training and decision support. This thesis prioritises physical reasoning in the ship model, and contributes with the following:

- A physically motivated ship model
- A new, compact derivation of the equations of motion with memory effect for ships

The first contribution is a model developed from longstanding analyses in low aspect–ratio aerodynamics. The hull of a ship is treated as an aircraft wing flipped onto its side. An advanced mathematical model structure is then derived. The model copes with the four degrees of freedom of most interest in manoeuvring: surge, sway, roll, and yaw. The effects of sway velocity and yaw rate arrive naturally from these analyses. The goal is to arrive at a model structure, and to enumerate this structure from experiment. That is, the structure is what is sought, and not methods for computing its parameters.

Using experimental data from planar motion mechanism tests, this model is verified and validated. It matches up very closely with what is observed in experiment. Furthermore, the model is compared to a pre–existing commercial model, and shows considerably greater accuracy. The model is additionally verified through full–scale tests on a modern trimaran design.

The Lagrangian formulation in this field dates back many decades. This thesis contains the derivation for the nonlinear equations of motion for a ship manoeuvring through waves. The equations arise from applying Kirchhoff's equations to a convolution integral formulation of the added mass.

Acknowledgments

Thanks are due to many. I am grateful to Prof. Thor I. Fossen. After supervising me during my Master's thesis in 2002, he invited me to return to Trondheim to pursue a PhD. His supervision has been exemplary at each and every stage, and for this I offer my sincerest gratitude.

I am thankful to have had the privelige of so many good colleagues during my studies. Cooperation with my co–supervisor, Dr. Tristan Perez, has always been fruitful and he has ever been a pleasure to work with. Thanks also to Dr. Kari Unneland, my unfortunate office–mate with whom many useful, funny and interesting conversations were had. A special measure of thanks go to my friend, Prof. Jèrôme Jouffroy, for his emphasis on the higher concepts of science. I am very grateful to Morten Breivik for the interest showed in my historical review, and for the numerous comments offered. Thanks are given to Ravi Kota and Reza Taghipour for discussions on hydrodynamics. Additional gratitude is offered to Austal Ships for supplying the full–scale test data.

Final thanks are offered to several friends: Sigmund Ås, Kurt Schmidt, Riccardo Basani, Bas Olsman, and Dave O'Brien.

This thesis is dedicated to my mother, Edith Ross, and to my late father, George Ross.

Andrew Ross
Trondheim, May 2008

Chapter 1

Introduction

Seagoing vessels have always carried the vast bulk of tradeable goods across our planet. In ancient times, a single vessel journeying from the Far East carried as much spice as all the beasts of burden did in an entire year (Pereira 2006). Today, lumbering oil tankers carry the lifeblood of our economies across the globe. Ferries of increasing performance and efficiency move huge numbers of people and traffic daily. High performance naval vessels, from small agile coastal patrol vessels, through frigates and destroyers, all the way up to vast nuclear aircraft carriers, are put to use in both defensive and offensive capacities year–round.

The past decades have seen mammoth developments in both control theory and computerisation. These advances filtered into an array of fields; marine cybernetics being one prime example. Cybernetics was defined by Wiener (1948) to be *"the science of control and communication in the animal and the machine"*. Marine cybernetics is the study of complex dynamical systems as they relate to the marine discipline. This science consists of control theory and systems theory applied to a vast array of topics. These range from analyses of ships, boats and submarines to remote and autonomous underwater vehicles. Wiener claimed both animal and machine in this field of study. Marine cybernetics might seem to be machine rather than animal, but the studies of how fish swim and the design of biomimetic underwater vehicles make it clear that marine cybernetics encompasses both.

The work within this thesis analyses manoeuvring ships. These analyses are vital for the accurate modelling of any vessel, be it a riverboat, coastal or ocean–going vessel. The myriad of control problems, from a simple manoeuvring task through to complex guidance manoeuvres necessitate

such work.

Many fields of guidance, navigation and control are dependent on accurate models. Fields such as path following, collision avoidance or formation control are limited in scope if the assumptions made about the model are unphysical. The problem of navigation is quite meaningless if there is no knowledge of the capabilities of whatever is navigating. Inaccurate modelling of a vessel puts limitations on the control system, making an already onerous task all the greater, and limiting the capabilities of the vessel.

For many years, the primary concern in developing models of ships has been mathematical convenience: a model with "nice" properties. This motivation has given rise to models with simple linear damping terms, and models which are heavily decoupled using diagonal mass and damping matrices. This statement is not to belittle these approaches, but such simplifications sacrifice accuracy for utility, and forfeit the ability to cope with changing operating conditions. These models are limited to manoeuvres around fixed operating points, or to only modest manoeuvres.

Contrary to such approaches, this thesis attempts to explain the forces acting on a ship from the standpoint of physical motivation. That is, the work in this thesis introduces concepts for physical rather than mathematical reasons. The result is a model sufficiently advanced to capture much of the behaviour of displacement and semi–displacement vessels in heavy manoeuvring problems. By applying lift and drag theory sectionally, the effects that surge, sway and yaw have on the vessel arise naturally.

The treatment is carried out in four degrees of freedom: surge, sway, roll and yaw. Heave and pitch are neglected. The end result is a model highly capable of modelling a ship manoeuvring aggressively across a very large speed range.

The viability of this model is tested by considering a set of planar motion mechanism tests. Data at one speed range were used to verify the effectiveness of the model. Data at a separate speed range were then used to validate the model as working across a wide speed range. For further verification, data from full–scale trimaran trials are used.

In addition to this work, a new formulation of the equations of motion appears. This formulation is based on Lagrangian dynamics. By applying Kirchhoff's equations to a convolution formulation of the added–mass, a wholly new structure to the equations of motion is found. This structure allows manoeuvring through waves to be contemplated, without being restricted to any limited coordinate system.

The results give strong indications that the physics of manoeuvring is

being dealt with quite comprehensively.

Before the main topic of this thesis is delved into, the field must be placed in context. This introduction is broadly divided into two sections. The first deals with the history of dynamics, while the second is a review of manoeuvring theory as it has developed and how it exists today.

1.1 History of Dynamics

The field of dynamics is among the most important in history. Human *interest* in the field extends deep into pre–history. The knowledge of which direction and speed to run at to catch one animal, or to escape from another, is innate to humans. The development of weaponry for hunting and fighting demonstrates interest in the dynamical aspects of the motion of bodies. The use of ranged weaponry predates modern man. Javelins[1] dated to 400,000 B.C. were discovered in a mineshaft in modern day Germany, and were used by *homo–heidelbergensis*, a predecessor and contemporary of early man. The ancient world is replete with innovative and inventive applications of dynamics: from slings to ballistæ, to vending machines for holy water.

Take what the pre–eminent physicist and philosopher of science, Ernst Mach, wrote of Newton's contributions (Mach 1883):

> Newton discovered universal gravitation and completed the formal enunciation of the mechanical principles now generally accepted. Since his time no essentially new principle has been stated. All that has been accomplished in mechanics since his day has been a deductive, formal, and mathematical development of mechanics on the basis of Newton's Laws.[2]

The sentiments expressed by Mach are held by most in the fields of mechanics. When they are not held, the disagreement is usually slight. As common as these sentiments may be, it is still necessary to examine whether they are factual or not.

The motivation for writing this section of the introduction stems from the sentiments of the great physicist, mathematician, historian of science,

[1] A javelin is distinct from a spear. It is designed to be front–weighted and lighter to make it suitable for throwing. In contrast, spears are weighted for ease of carrying.

[2] That general relativity has since superseded classical mechanics is of no importance here.

and polemicist, Clifford Truesdell[3]. In his essay *A Program toward Rediscovering the Rational Mechanics of the Age of Reason* (Truesdell 1968), he wrote:

> The scientists, in so far as they take any note of history at all, not only have shared the historians' neglect of the later [i.e., after Newton] mathematical development of mechanics but also, in the main, have ignored what the historians have learned about the earlier periods and have rested content with Mach's whole view or a rudimentary abstract of it.

Whether reading a textbook on robotics, marine engineering, aerospace engineering or, indeed, on mechanics *itself*, the statement above is often too true.

Discussions of dynamics almost invariably begin by citing the work of Sir Isaac Newton (1687) in his *Principia*, and only seldomly proceed further than this opus: *petitio Principia*, if the reader will excuse the Dog Latin.

The neglect of the history of the field is extant from the beginning of a university education. It is as if classical mechanics arose from a combination of thin air and the genius of Newton. This hagiography does a great disservice to at least four parties: firstly, to the scholars whose works predate Newton; secondly, to Newton's contemporaries and successors, who actually *synthesised* the dynamics that we know and apply today; thirdly, to the present–day students who pursue a true history of dynamics; and fourthly to Newton himself, whose memory is sullied by the misrepresentation of his work.

This neglect leads us to question why this history is being contemplated here. What is the problem?

The problem is that the history of science, a large and growing field, seems to filter none of its knowledge to the practitioners of science. Scientific careers can be built on advanced topics with absolutely no concept of what lies in the foundations.

The history of a science is vital to a true and humble understanding of that science. Being taught a subject and simply assuming it true is more like theft than the pursuit of knowledge.

In truth, history of a science can only really be grasped and analysed *after* the subject itself is known to a good degree. However, once that science is understood and a university degree comes to its end, there is no

[3]The term "natural philosopher" ought to suffice, but unfortunately has not enjoyed popular or correct usage in recent times (Noll 2006).

drive to put the learning into a historical perspective. A modern engineering degree is then more like an advanced tradeschool diploma than the higher form of learning and understanding that it ought to be, and that it used to be.

A cursory glance at history seems sufficient nowadays, but should it be? The development of dynamics is a much longer, halting and laborious story that neither began nor ended with Isaac Newton.

1.1.1 Before Newton

An analysis of motion ought to begin with the Ancient Greeks[4]. Since the influence of the Greeks lasted two millennia, it is inconceivable to describe the growth of dynamics *without* mentioning them.

The dominant figure in the ancient development of dynamics was Aristotle (384 BC– 322 BC). His writings (Aristotle *ca.* 330 B.C.) on this and on many other subjects held sway over much of science for the next two thousand years. Much of his reasoning on motion stemmed from the faulty concept of the classical elements (fire, air, water and earth). Each of these is given its own natural place in the world: fire at the top; air underneath fire; water below air; and finally earth resting beneath them all.

Whenever an element was taken from its natural place it would endeavour to return. This reasoning explained why an air bubble breathed underwater floats to the surface, and why a rock thrown upwards falls back to the Earth. Each object was then a combination of all of these. A feather, lighter than a rock, must have more air than the rock, but less than the air itself. From this line of thinking arose "natural motion": motion that occurs due to the nature of the object. All other motion was violent; it had a separate cause. A brick falling to the ground would be natural, but a brick thrown through the air would be violent.

Aristotle concluded that heavier objects fall faster than light objects, and that this fall–rate is proportional to their weights: an object twice as heavy falls twice as fast. He also reasoned that the speed of progression through a medium was inversely proportional to the density of that medium. This reasoning implied that the speed of progression in the void would be infinite; thus he concluded that the very *existence* of a void was impossible.

> ... between any two movements there is a ratio (for they occupy time, and there is a ratio between any two times, so

[4] Greek philosophy is generally taken to begin with the work of Thales of Miletus (ca. 624 BC–ca. 546 BC), which is in modern–day Turkey.

> long as both are finite), but there is no ratio of void to full.

Elsewhere he wrote that, if a void were to exist, heavy objects would fall at the same rate as light ones. This statement should be understood in context, as he used this supposed equality of fall rates to then say by modus tollens that a void *cannot exist*. He further wrote that, in a void, there would be no reason for a body to stay in one place or move to another, and so motion would continue forever. It is often said, based on this statement, that he enunciated a principle of inertia, but this is only possible by a selective reading of his works.

Among the various physical questions pondered by ancient philosophers, the question of *why* an arrow continues to fly after it has left its bowstring was particularly perplexing. Aristotle (*ca.* 330 B.C.) reasoned that the arrow displaced the air in front of it, which rushed behind and then pushed the arrow forwards. The idea of a thing moving violently without some other thing pushing it along the way; moving without a mover, was entirely alien to Aristotelians. This fallacious separation of natural and violent motion would haunt physics for two thousand more years.

The progress towards a truer representation was slow and halting. Aristotle's worldview became ingrained upon both Western and Arabic science and theology. His prevalence in the latter of these fields impacted the progression of the former. Much of it became Church dogma. By raising his theology above and beyond criticism, by proxy it raised a protective wall around his physics.

The lengthy dominance of Aristotle is now difficult to imagine. Even into the early Renaissance entire contributions on physics from philosophers would consist solely of commentaries on Aristotle's works: two *millennia* after they were composed.

The 6th century Alexandrian philosopher, John Philoponus (*ca.* 490–*ca.* 570), wrote extensive critiques of Aristotelian physics (Philoponus 517), and it is here that the inklings of a modern approach to dynamics can be seen.

Philoponus found little satisfaction in Aristotle's approach to motion, indeed he also found little satisfaction in his other approaches. In his commentaries he demolished Aristotle's work on both natural and violent motion. For natural motion, Philoponus posited that an object has a natural rate of fall. Falling through a medium would hinder this natural rate:

> But a certain additional time is required because of the interference of the medium.

He introduced a natural fall rate in the void, and subtracted from this the effect of the resistance of the medium. This concept allowed him to nonsense the Aristotelian concept that the speeds at which objects fall at are in proportion to their weights. He did this with appeal to the same kind of experiment carried out in Renaissance Italy almost a millennium later[5]. The prior sentence should be read very carefully, as Philoponus did *not* suggest the equality of fall–rates in the void. In fact he concluded that this concept was wrong. His belief was that heavier objects *do* fall faster than do light ones in a void.

For violent motion, he asserted that when an object is moved, it is given a finite supply of forcing impetus[6]: a supply of force that, while it lasted, would explain the object's continuing motion:

> Rather it is necessary to assume that some incorporeal motive force is imparted by the projector to the projectile...

He denoted this *incorporeal motive enèrgeia*. This *enèrgeia* is exhausted over the course of an objects motion, which rests once this exhaustion is complete. This property was now *internal* to the body. He struck fairly close to some kind of rudimentary *concept* of kinetic energy. At the very least, he struck close to some concept which we can now relate to kinetic energy. A conceptual path can be traced from Philoponus to Maupertius, through Leibnitz and on to Young.

The conclusion of the sentence quoted above is:

> ... and that the air set in motion contributes either nothing at all or else very little to this motion of the projectile.

The strongest and most groundbreaking insight that Philoponus made was that a medium does *not* play a role in maintaining motion. It acts as a retarding force. This notion was in direct opposition to Aristotle, who required that the medium should *cause* the continuing motion. This paradigm shift that John Philoponus introduced allowed him to explain that motion in a void *was* possible. His lasting contribution is with these qualitative analyses. His quantitative explanations are without merit, although these analyses resonate through Galileo's dynamics.

[5] The comparison of the speeds of falling objects, carried out by Benedetti around 1553 (commonly atrributed to Galileo).

[6] Impetus theory, the precursor to the modern principle of inertia, can properly be attributed to Philoponus.

In the centuries that followed Philoponus, other philosophers followed in a staggering and haphazard progression towards Newton. It would be another millennium before Aristotelian motion would be disregarded once and for all. The reasons are various, but much of it is theological in nature. Philoponus' writings on Tritheism were declared anathema by the Church, which led to the neglect, condemnation, and ridicule of his writings. Zimmerman had the following to say (Sorabji 1987):

> His writings, then and later, enjoyed notoriety rather than authority.

The inferior works on mechanics from his contemporaries, such as Simplicius, were treated in a more favourable light.

In the following centuries, the development of dynamics was very slight. Although true, there is a pernicious modern idea that science stood still from the fall of the Western Roman Empire (476 A.D.) until the Renaissance. While the remark may hold water for the Early Middle Ages, it has no standing whatsoever with the High and Late Middle Ages.

Aristotle's views, or variations on these, were analysed further by the likes of the Andalusian–Arabs Avempace and Averröes[7] in the mid–13th century. They had little more than uncited rehashing and acidic remarks, respectively, for the work of Philoponus. The gratitude owed to these philosophers should not be understated. It is through their works that Philoponus' thoughts were preserved: his books were not published in Western Europe until the early 16th century. Averröes wrote such extensive treatises on Aristotelian physics and theology that he was nicknamed The Commentator by Thomas Aquinas. The intellectual stupor existed in the West because an Aristotelian theological worldview was dogma. Those studying mechanics were reticent to go further than simple reinterpretation of Aristotle, even when so much of it was clearly wrong.

The stimulus that reinvigorated the field can be traced to the Condemnations of 1277. In this year, Tempier, the Bishop of Paris, condemned various doctrines enveloping much of radical Aristoelianism and Averröeism, among others. This event is important because the condemnation of Aristotle's theology led philosophers to question the truth of the rest of his worldview. Deviating from dogma was then, and remained for centuries more, very dangerous for philosophers, but now Aristotle's physics were no longer protected. The importance of the Condemnations led to what Duhem (1917) called:

[7] Ibn Bājjah and Ibn Rushd in Anglicised Arabic.

> a large movement that liberated Christian thought from the shackles of Peripatetic and Neoplatonic philosophy and produced what the Renaissance archaically called the science of the 'Moderns.'

Soon after, in the early 14th century, the *Oxford Calculators*[8] explained, in a kinematic sense, the motion of objects under uniform acceleration. Importantly, these men did not concentrate solely on the qualitative description of motion. What was previously a murky description of motion became a quantitative derivation. They answered kinematic questions numerically. What is fantastic is that the notion of instantaneous speed was within their grasp, even without the strong grip afforded us by calculus. The mean–speed theorem dates from this period, and is attributed to William Heytesbury[9]. They were additionally responsible for separating motion itself from its causes: the separation of kinematics and kinetics. Bradwardine[10] also noted:

> All mixed bodies[11] of similar composition will move at equal speeds in a vacuum

The statement above shows that the Mertonians were well aware that objects of the same *composition* fall at the same rate, regardless of their mass. They could not use the concept of density, because they did not understand what it was. Instead, the fall–rates were explained in terms of the nonsense classical elements of Ancient Greece, but they *were* explained.

Within their work can be found thorough analyses of uniform and accelerated motion. What cannot be found is a conclusive connection between these mathematical analyses and the actual world. Deriving an equation describing accelerated motion is a long way from establishing that all objects fall according to this equation.

Their analytical approaches to motion were well received Europe–wide, and was quickly taken up by the Parisian schools. French priest, Jean Buridan (1300–1358), was by most accounts the giant of fourteenth century philosopy. He took these theories up with gusto, and expounded a theory

[8] The Oxford Calculators were a group of 14th century academics based at Merton College, Oxford, and included William Heytesbury, Thomas Bradwardine, Richard Swineshead and John Dumbleton.

[9] Bizarrely attributed to Galileo by many.

[10] The selfsame Bradwardine spoken of in Chaucer's Canterbury Tales.

[11] A mixed body is one that consists of two or more of the classical elements: fire, air, water and earth.

that can properly be described as an early and rudimentary concept of what we now call inertia.

He posited in a similar manner to Philoponus that the motion of an object was internal to it, and importantly recognised that this impetus does *not* dissipate through its own motion: that something *else* must act upon the object to slow its motion. His insights into the implications of this were more advanced than anything prior. In discussing a thrown projectile, he said that it would:

> ...continue to be moved as long as the impetus remained stronger than the resistance, and would be of infinite duration were it not diminished and corrupted by a contrary force resisting it or by something inclining it to a contrary motion.

To the typical reader, it is generally unexpected that a philosopher would have entertained the notion of infinite motion a full three centuries before Newton. His genius in descriptions of the qualitative properties was not matched by his genius in the quantitative.

Buridan's student, Nicolo Oresmè (*ca.* 1323–1382), developed geometrical descriptions of motion. More than that, he used geometry as a method of explaining the variations of *any* physical quantity. As great as this was, he had a poorer understanding of dynamics than his tutor, and treated impetus as something which decays with motion (Wallace 1981). Oresmè's work is a prime example of the stumbling advancement of dynamics: it was rare that any one person could advance in one area without a simultaneous regression in another.

Albert of Saxony (*ca.* 1316–1390), another student of Buridan, took impetus theory forwards in projectile motion. For an object propelled horizontally, he reasoned that the motion had three distinct periods. The first of these was purely horizontal, where the body moved by its own impetus. The second was a curve towards the ground, as gravity began to take effect. The third was a vertical drop, as gravity took over and impetus died. Although maintaining the distinction between natural and violent motion, Albert at least came closer to the true shape of projectile motion.

It is quite difficult to emphasise the true effect that the philosophers from the Oxford and Parisian schools had on mechanics, and on science in general. Mechanics had moved from indistinct qualities into defined quantities: if an object moves at this speed, how far does it go in this amount of time? If an object accelerates in this manner, what will its speed be after a given period? These questions were asked and answered.

Shortly after Giovannia di Casalè (d. *ca.* 1375) returned to Genoa from studying at Oxbridge, he developed a geometric approach (di Casalè 1346) similar to that of Oresmè. This work undoubtedly influenced the Venetian, Giambattista Benedetti, in his 1553 demonstration of the equality of fall–rates. The influence that Casali's geometric approach wielded is evident while reading Galileo's works on kinematics.

An important point is then evident: the field of kinematics had leapt ahead of dynamics. Truesdell (1968) speaks of the impact of the Calculators in the following glowing terms:

> In principle, the qualities of Greek physics were replaced, at least for motions, by the numerical quantities that have ruled Western science ever since.

While kinematics was becoming more and more capable of describing both uniform and accelerated motion, and was able to quantify these analytically, numerically and geometrically; philosophers remained unable to explain the *why* behind them. The causes of motion, now separate and distinct from kinematics, were not very much closer to being discovered. This situation changed very little until the late 16th century.

Galileo Galilei (1564–1642) sought these causative descriptions of motion: he was the first of the modern dynamicists. The Italian was well–read in the workings of both the Parisian and Mertonian schools. From these, he set out into the still poorly understood field of kinetics.

To move forward, he examined the most successful of the ancient sciences: Archimedes' hydrostatics. He took those principles as inspiration to examine the motion of a falling object. He utilised no mixed–body theory of matter. Instead, he treated bodies, and the media through which they travel, in terms of their densities[12].

Archimedes' propositions explain the forces of buoyancy in equilibrium: they detail where an object will rest in a body of water. Galileo extended these principles from static into dynamic concepts. Archimedes explained the behaviour of bodies and their natural positions of rest. Galileo took this notion and applied it to bodies in motion. His monumental postulation was that buoyancy, in addition to determining a body's position of rest, furthermore determines how *fast* a body will reach that position of rest. He used this force of buoyancy to try to explain why objects fell at the speed they did.

[12] or, rather, their specific gravity.

It is wrong to say that he devised a dynamical law based on static principles. His theorems are a generalisation of Archimedes' static principles, which are then derivable from Galileo's: the converse is untrue.

These notions were not wholly new. Instead of using a ratio of weight to resistance in order to explain motion, Galileo described it as a natural motion from which was subtracted the effect of the medium. Instead of having velocity determined by the ratio of a body's weight to the medium's resistance, it was to be determined by a natural value minus some part due to the resistance of the medium.

The approach, ingenious thought it was, led to no hoped for grand principle.

The comparison between Galileo and Avempace is commonly drawn, as Avempace had postulated the same kind of thing: discarding the Aristotelian ratio. Galileo was certainly aware of Avempace's work, through what Averröes wrote of it[13]. It is unfair to say that Avempace was the originator of this sort of analysis, as it predates him by hundreds of years. This theory again goes back to John Philoponus, who was also well known to Galileo. Additionally, Avempace did not postulate Galileo's explanations for the causes of motion (i.e., a dynamic buoyancy law).

A note should be made on his supposed discovery of the equality of fall–rates. Galileo did not make this discovery. The story is that in 1589 he dropped various cannon balls from the Leaning Tower of Pisa, and thus the world came to know that all objects fall at the same rate. The story is contemptibly wrong on several counts. Firstly, this experiment does not even *demonstrate* equal fall rates: it only shows that objects of the same *composition* fall at the same rate, independent of their weight. Secondly, in 1589, Galileo did *not* believe in the equality of fall–rates. His notes from this period (Galilei *ca.* 1602) state that objects of equal *density* fall at the same rate, but that denser objects fall faster than less dense ones:

> I say therefore that in a vacuum, heavier bodies would descend more rapidly than lighter ones, because the excess of the heavier bodies over the medium would be greater than the excess of the lighter ones.

That bodies of the same density fell at the same rate had been stated already by Bradwardine two hundred years before. Thirdly, the selfsame

[13] In his early notes, Galileo cites Averröes ahead of all, save Aquinas. See the essay Galileo and the Doctores Parisienses in (Wallace 1981).

experiment had already been performed by Giambattista Benedetti years before, and his work was known to Galileo.

It is difficult to ascertain when Galileo concluded that all objects fall at the same rate. He withheld publication on this subject for many years. The initial cause of his withholding was his own desire to bring the subject to a completion before revealing it. The later cause was the restrictions placed on him by the Inquisition. He knew of it by 1604, as he revealed it in correspondence with a confidant. In truth, he felt betrayed when a friend of his mistakenly revealed it to the world in the early 1630s, and only after this did he publish anything on the matter. It was not until Two New Sciences appeared in 1638, towards the close of his life, that he finally published what he knew.

For all Galileo's effort, he never satisfied himself with his explanations of the causes of motion. In *Dialogues Concerning Two New Sciences (Galileo 1638),* towards the close of his life, he sadly confessed to this failure. After listening to the thoughts on dynamics voiced by Simplicio and Sagredo, Salviati, proponent of Galileo's philosophy, makes the comment:

> Now, all these fantasies, and others too, ought to be examined; but it is really not worth while. At present it is the purpose of our Author merely to investigate and to demonstrate some of the properties of accelerated motion (whatever the cause of this acceleration may be)...

Here Galileo resigns himself to never finding what he sought. His characters instead progress through thorough discussions of the kinematics of motion alone: Salviati and Sagredo dragging Simplicio[14] by the coattails into modern science.

> ...we have decided to consider the phenomena of bodies falling with an acceleration such as actually occurs in nature and to make this definition of accelerated motion exhibit the essential features of observed accelerated motions.

Over the course of the rest of the book, Galileo sets forth his definitions of uniform and accelerated motion in lightning fast demonstrations. The topics of discussion then go through motions of various things, especially that of projectiles. This work sounded the death knell of Aristotle's physics.

[14] The name is a portmanteau of Simplicius, the classical Aristotelian, and the word for simpleton.

In discussing a body thrown upwards, then falling back downwards, Simplicio voices the two thousand year old distinction between natural and violent motion. Sagredo replies:

> ...this distinction between cases which you make [i.e., violent and natural] is superfluous or rather non existent.

Much is said about Newton unifying motion in the heavens and motion on Earth: that is, recognising that the laws apply equally so to the orbit of a massive planet as they do to the fall of a tiny apple. Very little is said about unifying natural and violent terrestrial motion, and yet it took two millennia of thought before the two were recognised as one and the same. The separation of the two had permeated Western science for two thousand years, and it was Galileo who demonstrated the insight to finally and permanently demolish this nonsense concept.

His dynamics were noteworthy and had a very large influence over his successors, but the true contribution of Galileo is in his kinematics, not in his dynamics. He could explain what he observed: uniformly accelerated motion, but he could not explain the causes behind it. While he failed, he set a great example for his successors: one that was well learnt and will never be forgotten. His dynamics were laden with no mystical indistinct properties. They were laden with rigorous definitions and analyses.

Aristotelian dynamics had been staggered by many deserved blows, but had kept standing, in various poses, for two thousand years. Galileo delivered the coup de grâce, putting it to its long overdue rest.

By the mid 17th century, dynamics was understood in the murkiest of ways. A myriad of problems, each requiring its own ingenious solution, was solvable almost solely by special cases. Much of this problem solving was needed before any general laws of dynamics could finally be grasped. Today we learn the principles, and then how to apply them. The developers of the field solved extraordinarily difficult problems, and lots of them, before any true governing principles were found. We learn the principles and then tackle problems, but the physicists had to tackle the problems before they could see the principles.

The giant of mechanics in the years leading up to Newton was the Dutchman, Christian Huygens (1629–1695). He was the first to explain oscillations of a finite pendulum, which he did so for a special case. His writings on solid body collisions had a monumental effect on the world. He observed that after two solid bodies collide, their collective speed may well be increased or decreased, but their collective momentum remains the same:

perhaps the first true expression of the conservation of momentum[15]. He furthermore recognised that in rigid body collisions, the centre of gravity of the system remains in uniform motion: a hugely penetrating notion.

1.1.2 Sir Isaac Newton, His Contemporaries and Successors

Sir Isaac Newton (1643–1728) made contributions to virtually every area of natural philosophy, mathematics, optics and astronomy. His monumental publication, *Philosophæ Naturalis Principia Mathematica (1687)*, usually called The Principia in short, was published in 1687. It is likely the most influential yet least read book in the field of classical mechanics. Its purpose was set forth in its preface:

> ... mechanics will be the science of motion resulting from any forces whatsoever, and of the forces required to produce any motion...

Newton set out to explain phenomena throughout the universe. What lay within was to apply everywhere, and to every process. The trajectory taken by a cannon ball was to be governed by the same laws which governed the orbits of the planets.

As the start of his work, he states his definitions of mass, momentum, inertia and forces, both through contact and at a distance (centripetal). He then states his laws:

First Law Every body perseveres in its state of rest, or of uniform motion in a right line, unless it be compelled to change that state by forces impressed upon it thereon.

Second Law The alteration of motion[16] is proportional to the motive force impressed; and is made in the direction of the right line in which that force is impressed.

Third Law To every action there is always opposed an equal reaction: or the mutual actions of two bodies upon each other are always equal, and directed to contrary parts.

[15] Descartes is often credited with this concept, but his notion of this was the bulk of an object times its scalar speed. His rationale was entirely different too.

[16] i.e. momentum, as per his Def. II

Books One and Two are titled *Of the Motion of Bodies*, being split into two exhaustive analyses. The third is titled *The System of the World*.

The first book analyses motions in a void. From his laws, he analyses a multitude of motions, such as elliptic, parabolic and hyperbolic orbits around some focus. He investigates the forces that maintain these, i.e. the centripetal forces. Universal gravitation is introduced. After showing how point masses behave in the void under gravitation, he demonstrates that finite bodies can be treated as such. Kepler's Laws follow directly. The first book organised and systematised principles, some of which were at least dimly understood before, but these principles had never been organised together into a system of analysis for application everywhere.

The second book sets out to explain motion on Earth, where motion does not occur in a void: he sought the details of motion in resisting media. It is here that Newton departs from his program of deducing physical behaviour based on his laws: he finds but little use for them. For example, in all his treatments of fluidic motion he finds no room to apply his principle of momentum. In contrast, he conjures ingenious hypotheses to explain a myriad of things ranging from projectile motions to the speed of sound in air. This book is a testament to Newton's towering stature as a mathematician and dynamicist. The second book of the Principia is almost entirely new. The scholium of the first section of it reads:

> But, yet, that the resistance of bodies is in the ratio of the velocity, is more a mathematical hypothesis than a physical one.

This sentiment is applicable to much of the hypotheses in the book. Today it is mostly forgotten. The book is dominated by hypothesis after hypothesis, with Newton displaying his flair for creative solutions: often precise, often an excellent approximation, but also often wrong and today of only historical value. There are veins of gold hidden within. His observation that fluidic resistance is proportional to the square of velocity can be found, as can the first description of internal fluidic friction:

> The resistance arising from the want of lubricity in the parts of a fluid is, cæteris paribus, proportional to the velocity with which the parts of the fluid are separated from each other.

That most of the results were incorrect cannot be a criticism of Newton either as a physicist or mathematician. The contribution of this book is immeasurable. For instance, it constitutes the beginning of fluid dynamics,

and studied many of its problems for the first time. From his efforts, his contemporaries and successors were gifted with a bridgehead from which to attack these subjects in earnest. A myriad of potential motions through fluids is contemplated. The book is the staging point for hydrodynamics. Newton contemplated which hullform might pass through the water with least resistance, introducing an optimisation problem that found application throughout the 19th century.

The third book set forth his solutions to problems in celestial dynamics, with great success. Kepler's Laws of Planetary Motion had resulted from Newton's own, and he performed exhaustive analyses of the Solar System.

The deficiencies in the Principia are little discussed. To the modern scholar, it is often impenetrable and confusing; the language of mathematics having evolved so much since then. A common remark made about the Principia is that Newton strangely resorts to geometrical methods instead of his own calculus. Newton does not use his notation of fluxions, but even as soon as we arrive at Lemma II of Book I, the notion of calculus is present, if in an unfamiliar form.

For rigid body mechanics, there is no treatment of rotation. Although Newton says that the spinning top: *"does not stop spinning except insofar as it is slowed by air."* there is no justification given. It appears directly after his statement of the First Law, but this law cannot tell us anything of the spinning top. Newton might have perceived that the top continues to spin, just as it would continue in linear motion if so impelled. He very well might have perceived that this is the case, but he did not demonstrate it, and it is not possible to explain the spinning top using what is within the Principia. There is certainly no treatment of angular momentum. The motion of a rigid body cannot be described by the methods given in the Principia.

There is no treatment of flexible bodies, such as the catenary curve or the vibrating string, nor is there any analysis of the finite body pendulum. No equations of motion appear for systems of more than two free masses, or one constrained. A prime example of the field's infancy is the three–body problem. Newton attempted to solve this problem, but the contents of the Principia are insufficient to do so. He devised insightful approximations and valid inequalities, but the three–body problem was insoluble from his principles. His talent in this area is evident, as his work would not be surpassed until the mid–18th century by the efforts of Euler and Lagrange.

That Newton did not solve all of mechanics' problems is not a criticism at all, but only part of a clear–headed appraisal of what he *did* do. His

achievements were monumental. He ought not to be credited with the completion of classical mechanics, but rather its beginnings.

In the century following The Principia's publication, the field of mechanics swelled immensely. For all the credit given to Newton, the world ought to be equally grateful to his contemporaries and successors, especially Leonhard Euler, the Bernoullis Jakob and John, and Joseph Lagrange. These are the men who synthesised what we now apply today.

Newton's Contemporaries and Successors

If The Principia contains no treatment of angular momentum, contrary to popular belief, then where and when did this law arise and who discovered it? The answer is difficult to ascertain, as the principle was applied for many years before it was recognised for what it was (For a comprehensive analysis, see *Whence the law of moment of momentum? in Truesdell 1968).*

The law of angular momentum is commonly treated as a consequence of linear momentum, but that is no more true than the common statement that Newton's First Law can be ascertained from his Second. This approach works for special cases only: it is not true in general. The Newtonian equations cannot contemplate deformable bodies or motion of a continuum without severe restriction. Angular momentum is a law of mechanics independent from any other. It took most of the 18th century for this to be realised.

In the Acta Eruditorum of 1686, Jakob Bernoulli (1654–1705) analysed the motion of a pendulum using the ancient law of the lever: i.e., by balancing the moments. By applying this static problem to the dynamic problem of the pendulum, he sought a new methodology for mechanics. His attempt at this stage was flawed, but was published in correct form in 1703 (Bernoulli 1703). His efforts led him to introduce many concepts which are now elementary, or even obvious, today.

By balancing the moments, the law of the lever is found. This static equilibrium condition was generalised into a dynamic equilibrium. Jakob Bernoulli wrote that the force of the lever can be regarded as equivalent to the acceleration per unit mass reversed in sign, thereby restoring a static condition. His was the earliest proper explanation of inertial force, and is a progenitor of what is now by convention called D'Alembert's Principle.

Jakob Bernoulli's statement of the moment of momentum can not be considered a consequence of applying Newton's Second Law. Its first appearance, flawed though it was, predates the publication of the Principia by a year. To emphasise: the law governing angular motion predates Newton's

law, which governs only linear motion. That said, it is only to be found and understood with great difficulty. The impenetrability of Jakob Bernoulli's work is evident, since it took many years before the genius within was recognised and developed by Euler.

Through analysing the catenary curve[17], it was Jakob Bernoulli who first recognised that solutions could be derived by balancing forces applied to infinitesimal portions of the cable, and furthermore that the selfsame solutions could be derived by balancing the moments acting on those infinitesimal portions: two essential principles of mechanics are equivalent for certain systems. This apparent equivalency caused the great physicists of the 18th century to seek, in vain, the single unifying principle through which all of mechanics could be analysed.

Using this work on the catenary as a springboard, Jakob Bernoulli vaulted into an analysis of elastic beams: the bending of finite bodies, which he published in the Acta Eruditorum of 1694. Here he recognised that the balancing of forces or moments alone was insufficient to the task. Between each infinitesimal stretch, there must be a contact force *and* moment.

In addition to these mammoth contributions, Jakob Bernoulli was the first to state how the motion of a constrained system can be analysed. Given the constraints, propose the forces which maintain these constraints. The motion of a system of constrained masses can then be analysed. Seemingly obvious today, the idea finds no ancestor before Jakob Bernoulli.

If it is typical to elevate some beyond their true achievements, it is equally typical to undermine those with achievements beyond measure. The laws, equations and principles named after Leonhard Euler (1707–1783) devastate Stigler's Law of Eponymy[18], and yet he is the very reason that the law applies virtually everywhere else. It is through Euler that much of dynamics was delivered to the modern world.

Between 1747 and 1750, Euler took his own works on constrained systems, and applied them to the three–body problem. In this work, he wrote:

> The foundation... is nothing else than the known principle of mechanics, $du = pdt$, ... we can see that this principle holds equally for each partial motion into which the true motion is thought of as reduced.

Euler is here saying that what had been found was an approach that applied to any dynamic process, and that it additionally applied to *every*

[17] The shape that a thin hanging cable assumes under its own weight.

[18] "No scientific discovery is named after its original discoverer."

part of that process. It was simply not understood prior to Euler's paper. In retrospect it seems too obvious to even mention. This retrospection emphasises the difficulty of analysing the history of science: today, it is thoroughly difficult *not* to see this principle as self–evident in Newton's writings: what is obvious now is supposed obvious then, but that is wrong.

In Euler's paper, *Discovery of a New Principle of Mechanics (Euler 1750),* he wrote down the following:

$$F_x = Ma_x, \quad F_y = Ma_y, \quad F_z = Ma_z.$$

Following his statement of the new principle, he derived the tensor of inertia by taking the moments about the centre of gravity. By these equations, Euler claimed, all mechanical problems could be solved. That we now call these equations Newton's Second Law is immaterial. In the words of Truesdell:

> ... they occur nowhere in the work of Newton or of anyone else prior to 1747. It is true that we, today, can easily read them into Newton's words, but we do so by hindsight.

Although Euler initially believed that the issue was resolved, he shortly came to realise his mistake. The principle of angular momentum lay hidden. The full classical equations would not be written down for another two decades.

The rotations of even a rigid body were problematic, let alone of a system of particles or continuum. That a rigid body could rotate ad infinitum was dimly perceived for almost a century before it was properly explained. As mentioned, Newton's spinning top is a key example, but we simply cannot admit stabs–in–the–dark. Throughout the early to mid 18th century, physicists had been unable to explain rotational motion in more than a single axis.

Euler contemplated the problem in the early 1730s, but did not approach it again for another decade. The driving force was his work on naval architecture in Scientia Navalis (Euler 1749). Here he was forced to deal with oscillations very different from the simple planar type. He hypothesised that each body has three orthogonal axes about which it may rotate.

The first rigorous treatment of these axes was by the Hungarian physicist, Ján Andrej Segner (1704–1777). He proved that free rotation is possible through a minimum of three individual axes, there being more than

three for special cases (spheres etc.). Euler recognised the strength of Segner's reasoning, and was the first to reason that these axes all had to pass through the centre of gravity.

1776 saw the birth of a foundation of classical mechanics. It was in this year that Euler published his First and Second Axioms (Euler 1776):

$$\begin{aligned} \mathbf{F} &= \dot{\mathbf{P}}, \quad \mathbf{P} = \mathbf{M}\mathbf{v} \\ \mathbf{L} &= \dot{\mathbf{H}}, \quad \mathbf{H} = \mathbf{I}\boldsymbol{\omega} \end{aligned}$$

At last, the road devised by Newton, and hewn by many, had been paved by Euler. The laws of vectorial mechanics were understood and formulated then just as they are today.

The Indirect Approach

Newton's approach takes force and momentum as its basis. It is often called the *direct approach*, or *vectorial dynamics*. D'Alembert wrote what is anything but a shining endorsement of the direct approach in his book *Treatise on Dynamics* in 1743:

> Why should we appeal to that principle used by everybody nowadays, that the accelerating or retarding force is proportional to the element [i.e. differential] of velocity, a principle resting only on that vague and obscure axiom that the effect is proportional to the cause? ... we shall be content to remark that the principle, be it true or be it dubious, be it clear or be it obscure, is useless to mechanics and ought therefore to be banished from it.

The lionisation of the Newtonian approach by the British certainly was not quite mirrored everywhere on the continent. In contrast to the direct approach, and with equal validity, the scalar quantities of energy and work can serve as a basis for an approach called the *indirect approach*, or *analytical dynamics (Williams Jr. 1996)*.

The history of analytical dynamics is just as cloudy and obscure as the development of Newton's Laws. Leibnitz (1647–1716) is the earliest true standard bearer for using energy and work as the bases for mechanical principles. He posited that through any process, a vis viva (living force) is preserved. This term he equated to mv^2 and so Leibnitz's living force is just twice the kinetic energy. He believed, and so did his contemporaries, that conservation of vis viva contradicted the Cartesian and Newtonian notion of

conservation of momentum. Leibnitz wished to use this vis viva, along with his dead force (potential energy), as the basic principles of mechanics. This "living" force irritated the delicate sensibilities of many, and with good reason. A living force seemed to invite the teleological and theological qualities of the ancient sciences to return from the dead.

One must question why Leibnitz objected so much to the Cartesians' and Newtonians' use of momentum. For them, landmark results were already inbound using the principle of momentum and its conservation. What was special about this vis viva, and why did velocity appear twice? These notions stem from Galileo's Two New Sciences.

In his final Dialogue (Galileo 1638), Galileo made key observations related to the indirect approach. Falling from a given height, a body acquires a velocity that is precisely the same velocity required to raise the body back to the given height. Since the square of the velocity acquired is proportional to the height, it seemed reasonable to surmise that v^2 has a link to some fundamental property of motion. Running along the same vein of gold, he noted that velocity acquired by a body rolling down an incline is only influenced by the height of the fall and not by the inclination itself: he recognised that the velocity was *independent* of the path.

Leibnitz considered many cases using his live and dead forces. Indeed, many problems can be solved by examining the energy quantities at key points. Instead of the Newtonian momentum, and its alteration through impressed forces, Leibnitz considered kinetic energy, and its alteration through the work done by impressed forces. The mathematics behind what lay ahead was undeveloped in his day, and the true leap forward for the indirect approach would have to wait many years from Leibnitz, until it found its home with Euler and Lagrange. Before the indirect method could come to fruition, the calculus of variations was required.

Along those lines, an interesting period in this development is the brachistochrone challenge of the late 17th century. Brachistochrone is a portmanteau of *brachistos* and *chronos*: Greek for shortest and time respectively. The problem is to take a bead on a frictionless wire, acted upon only by gravity, and to then determine the quickest possible route between two points A and B. It can be seen in Figure 1.1. The first version of the problem was posed by Galileo in Two New Sciences (Galileo 1638), but his solution was incorrect, mistakenly thinking that the solution was the arc of a circle. He at least recognised that it was not a straight line.

The first person to solve the problem was John Bernoulli. He posed this problem to the mathematicians of Europe as a challenge in the *Acta*

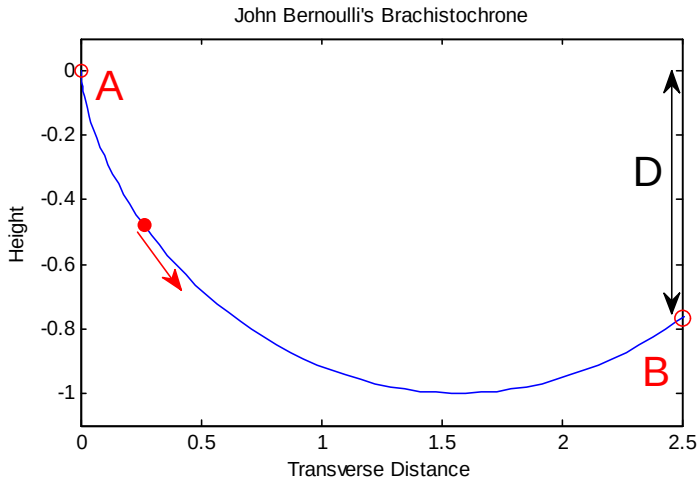

Figure 1.1: The brachistochrone problem posed by John Bernoulli.

Eruditorum of 1696.

In choosing the wording of his challenge, Bernoulli gave an unmistakable hint at *how* he had solved the problem. He invoked both Pascal and Fermat. Pascal had offered prizes for challenges on the cycloid four decades prior, while Fermat showed that light always takes the path of least time (Fermat's Principle). The solution to John Bernoulli's challenge was the former's curve, and his method was by applying Fermat's principle.

Solutions soon arrived from his elder brother Jakob, Leibniz, de L'Hôpital and an anonymous one from Newton[19]; all showing the solution to be the cycloid.

This challenge led to a clash between the fragile egos of the two Bernoullis. Following publication of the solutions to the brachistochrone problem in 1697, Jakob Bernoulli posed a more difficult version, again in the Acta Eruditorum. The first version sought the minimum time to a certain point. Jakob Bernoulli instead posed a problem to minimise the travel time to a vertical line. That is, to find out which of all the possible cycloids reaches the line first. The reposed problem is depicted in Figure 1.2.

This problem was quickly tackled by both Bernoullis, Leibniz and Euler. The answer to the problem is the cycloid which passes through the line at a right angle to it. It is not, however, the answer to the problem which makes

[19] Though anonymous, John Bernoulli realised who it was from, and famously remarked that the lion is known by its claw: *"tanquam ex ungue leonem."*

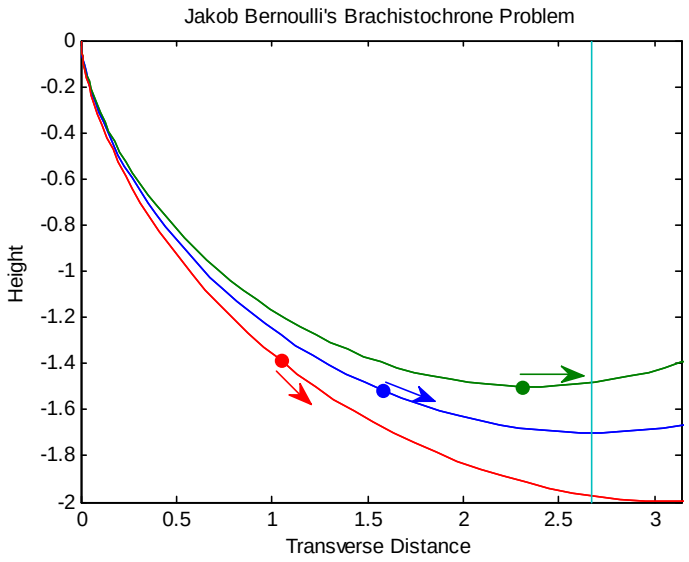

Figure 1.2: Jakob Bernoulli's Brachistochrone Problem.

this challenge especially noteworthy. The second version of the brachistochrone was obviously another minimum time problem, but now it was a problem to be solved by contemplating all possible paths. It was hardly the first optimisation problem to be contemplated, but it *was* the particular one which, in being solved, led to the development of the calculus of variations.

Over the next years these efforts led the Bernoullis in shamefully defamatory one–upmanship, as each tried to climb to the top of European mathematics at the expense of his sibling. The younger John Bernoulli outlived his elder brother. In the years of the early 18th Century, the calculus of variations was formalised and organised by the likes of John Bernoulli, D'Alembert and Euler.

It was during this timeframe that D'Alembert and Euler finally generalised Jakob Bernoulli's inertial force. They formalised the pre–existing principle and showed that the principle of virtual work applied equally to bodies in motion. Mechanics was then gifted with a single variational principle.

The furtherance of the attempts to use energy and work to ascertain physical principles is due to the work of the Frenchman, Pierre de Maupertius (1698–1759). He posited that in any and every process, an action

is minimised, with this action being defined according to the process. His perceptive qualities were remarkable. Most of his definitions of action found no use, but others did. For light, he posited in a 1744 paper that this action was the integral of the speed over the path taken. With this principle, he struck gold; deriving Snell's Law from an indirect approach. His genius here mirrors what John Bernoulli did in his brachistochrone solution. This principle of least action became ubiquitous throughout much of mechanics.

In the same year, Euler published his own results on the matter. He posited it in a far more general and accurate way. He applied the integral of the momentum of a body over its path travelled: the reduced action[20]. In the following years, he applied the same to static problems, taking variations of the potential energy. This method lead him to the classical result that a body, or a system of bodies at rest always lie at a minimum of potential energy.

The thrust in this direction was taken up by the French–Italian mathematician, Joseph Lagrange (1736–1813). A contemporary of Euler in his later years and common collaborator, the two formulated the Euler–Lagrange equation, bringing the formulation of the indirect method on by leaps and bounds. Lagrange was the true champion of this method throughout his Mècanique Analytique (Lagrange 1788). In addition, he recognised the usefulness of generalised coordinates, giving the method a towering strength: the invariance of the method to coordinate changes.

The future development of this field through Hamilton and Jacobi is well understood, and this historical review has already become drawn out.

1.2 The Beginnings of Naval Architecture

Naval architecture, like so many fields, predates history. Humans have constructed seagoing vessels for around 70,000 years, enabling the migration of the island communities throughout southeast Asia. By this route Australia was reached and settled 10,000 years before humans entered Europe. The largest ship of ancient times is Roman by design, and is now uninspiringly called *Caligula's Great Ship*[21]. Displacing 7400 tons; it is the heaviest wooden ship *ever* built. Measuring 104 m long; it was the longest wooden ship until it was surpassed 1800 years later by the 105m long French frigate,

[20] i.e., the action with kinetic energy alone.

[21] It is speculated that it carried the massive Vaticano obelisk from Heliopolis to Rome. Modern wooden ships of this size were hardly seaworthy. It was most likely a floating palace or temple, like Caligula's Nemi ships.

Rochambeau[22] (though this includes its 13 m ram.) The ancients were not lacking in ship–building knowhow. What they did know was hidden away as trade secrets, and their methods are unpreserved.

Once again, it is through Hellennic writings that we see the first analyses upon which naval architecture was founded. Discussion of the field commonly takes Archimedes (*ca.* 287 B.C.–*ca.* 212 B.C.) as the starting point, which this time is perfectly apt. In the 3rd century B.C. he formulated the law of hydrostatics which bears his name. The anecdote relating why Archimedes investigated buoyancy is found in the writings of Vitruvius (*ca.* 27 B.C.). Hiero II, king of Syracuse contracted some unknown party to build a crown using a weight of gold given him. Upon delivery of the crown, accusations were made that it had been alloyed with silver; thereby cheating the sovereign out of his gold. The crown weighed the correct amount, but Hiero had his friend Archimedes investigate the theft that he suspected but could not detect.

The discovery of the law, perhaps now more famous than the law itself, then followed. While pondering the problem, Archimedes settled into a bathtub, and noticed that the more he settled into the tub, the more water spilled over. From that he realised that he could measure the volume of an irregular object, and could therefore discover the specific density of any object; and thus tell the difference between a gold crown and an alloyed one. He then ran home, unclad, yelling eureka![23]

Using the correct masses of silver and gold, Archimedes showed that the crown was not made of pure gold. Vitruvius did not preserve the fate of the contractor.

The story is apocryphal: the earliest known version was written two hundred years after Archimedes' time. Anecdote aside, what Archimedes himself actually wrote has been preserved, and the most important propositions he made in *On Floating Bodies (Archimedes 2007)* are given here minus their proofs.

Proposition 3 Of solids those which, size for size, are of equal weight with a fluid will, if let down into the fluid, be immersed so that they do not project above the surface but do not sink lower

Proposition 4 A solid lighter than a fluid will, if immersed in it, not be completely submerged, but part of it will project above the surface.

[22] US built, and provisionally the USS Dunderberg, it was rejected and never commissioned into the US Navy.

[23] I have found it!

Proposition 5 Any solid lighter than a fluid will, if placed in the fluid, be so far immersed that the weight of the solid will be equal to the weight of the fluid displaced.

Proposition 6 If a solid lighter than a fluid be forcibly immersed in it, the solid will be driven upwards by a force equal to the difference between its weight and the weight of the fluid displaced.

Proposition 7 A solid heavier than a fluid will, if placed in it, descend to the bottom of the fluid, and the solid will, when weighed in the fluid, be lighter than its true weight by the weight of the fluid displaced.

These propositions explain the static behaviour of bodies partially or fully submerged. He developed these ideas in the second volume of *On Floating Bodies* by calculating the buoyancy of sections of certain paraboloids, likely as idealisations of ship hulls. Hero of Alexandria[24] advanced this work in the first century A.D. In the second book of his *Metrica* he demonstrated how to calculate the buoyancy of various irregular volumes (Cohen and Drabkin 1948). Hydrostatics essentially remained in this form for the next 1,500 years.

While dynamics and kinematics and other sciences developed greatly in the Middle Ages, hydrostatics found no outlet for advancement. Rather than a lack of interest in the field, it is indicative of the sheer success of Archimedes. That no one could improve on his work until the 16th century is evidence enough for this assertion.

The Flemish mathematician and engineer, Simon Stevin (*ca.* 1548–1620) is a progenitor of sorts for modern hydrostatics. He can be credited with a rudimentary explanation of hydrostatic pressure. Furthermore, he showed that the centre of gravity of a body and its centre of buoyancy must lie along the same vertical axis. Huygens followed that up with thoughts on shapes being naturally stable or unstable, this being done through analysing the buoyancy forces through 360 ° of rotation.

A variety of analyses took place in the following years. A comprehensive history of this topic can be found in (Ferreiro 2006).

In the realm of stability analyses, much of the earliest and most fundamental work was carried out by the Frenchman Pierre Bouguer (1698–1758). His work, Traitè du Navire (Bouguer 1746) contains extensive analyses of

[24] His many inventions include a holy water vending machine that would not look out of place in Asterix or The Flintstones.

all manner of topics in naval architecture. Among these we find the derivation of the metacentre of stability, with results given by experiment. He furthermore contemplates an extension of the metacentre to finite angles.

Euler, in his naval treatise, Scientia Navalis (Euler 1749), attacked the subject with his customary gusto. Applying infinitesimal calculus to a ship hull, and integrating the pressures gave Archimedes' law directly. From here he attacked the problem headon. He derived the equations describing the restoring moments in both roll and pitch, and then derived the heel and trim angles resulting from the sail. It is fair to say that Euler's work contains the superior theoretical results, while Bouguer's work contains the superior practical results. That is not to imply that either one floundered in the realm of the other.

The first work devoted solely to hydrodynamics was Daniel Bernoulli's work, Hydrodynamica (Bernoulli 1738). The fundamental basis for the book is the conservation of energy. D. Bernoulli asserted the equality between what he called the potential ascent and actual descent of a system. The first of these is the distance that the centre of gravity of a system can ascend if each component were to suddenly alter its velocity directly upwards until all parts were at rest. That is, if the whole kinetic energy of the system were converted to potential energy by immediate ascent, how far would the centre of gravity raise? His definition of the actual descent is the altitude that the centre of gravity would descend after all parts came to a rest. He credited this use of the conservation of energy to his father. These considerations hearken back to the approach of Huygens with the pendulum, and in inspiration back to Galileo.

The appearance of his son's work, and the consequent rise in his stature, motivated John Bernoulli to write his own treatise on hydrodynamics, entitled Hydraulica (Bernoulli 1743). In a shameful manoeuvre, he backdated this book purportedly showing his son to be a plagiariser. That aside, his work was a mark of true genius, and left more of a mark than did Hydrodynamica. In contrast to his son's approach, he used the Newtonian principles and calculus, as they were understood at that stage. It appears to be the first application of Newtonian principles to the continuum, in this case fluid motion through pipes. Within this work is also the crude appearances of internal pressure and a general representation of the Bernoulli equation.

It is again to Euler that we owe the largest debt of gratitude. While D'Alembert conceived the first field description of motion in his work of 1752, it was Euler who described it using partial differential equations. In 1752 he published a paper replete with concepts that are still applied today.

He analysed the infinitesimal tetrahedron, which led to

$$\frac{\partial u}{\partial x} + \frac{\partial v}{\partial y} + \frac{\partial w}{\partial z} = 0:$$

the equation of continuity. Among the various other concepts he introduced both velocity and acceleration potentials, with the Laplace equation applied. Bernoulli's equation is derived for unsteady irrotational motions.

Three years later, the ideas had matured fantastically. The concept of pressure, dimly applied in the past, was explained as a field acting on some closed boundary, with equal action external and internal to this boundary. Using his axioms, the hydrodynamic equations describing ideal fluids are derived.

1.3 History of Manoeuvring

Serious investigation into manoeuvring characteristics of ships began over one century ago, with analyses of the turning performance of warships (White 1877). The main motivation, as for many fields, was military. For a good summary of the history of manoeuvring, see the work by Clarke (2003).

In a modern sense, the mathematical modelling of a ship can be said to have begun with the work by Davidson and Schiff (1946), in which equations describing linear steering dynamics were derived, incorporating the interactions between sway and yaw. The model derived in the paper is recognisable today.

In the work by Nomoto *et al.* (1957), the steering equations derived by Davidson were reformed such that the steering dynamics of the yaw mode could be analysed in isolation, through either a first or second order transfer function. Even today, this simple and thoroughly effective model is used within a multitude of guidance and control system design papers.

The method of analysing the yaw behaviour independent of other modes was further developed in Norrbin's (1963) work. This approach maintained the same structure as Nomoto's first order representation, and added a nonlinear component to the first order transfer function. The form of this nonlinearity was a time invariant polynomial function of the yaw rate. These functions are commonly referred to as *static nonlinearities* or *manoeuvring characteristics*.

The second order representation was extended to include similar nonlinearities in the work by Bech and Wagner Smith (1969). This paper also

introduces the now familiar *Bech's reverse spiral manoeuvre* which shows how the parameters of the nonlinearities can be found from time–series analyses.

A significant development arrived with Abkowitz's (1964) work, in which an entirely new approach was applied to explain the forces acting on a ship. Abkowitz applied Taylor–series expansions to the hydrodynamic forces about a forward cruise speed. These expansion models give an unlimited number of parameters, and can model forces to an arbitrary degree of precision, at the expense of a large number of coefficients. Abkowitz presented both linear and nonlinear equations of motion in the three degrees of freedom of most interest to manoeuvring problems: namely surge, sway and yaw. This work constitutes the beginning of nonlinear analyses of multiple degrees of freedom manoeuvring problems, and opened the door to a vast field, introducing a multitude of problems to be tackled. A variety of publications have dealt with how to calculate, estimate or identify the coefficients of these models (e.g. Abkowitz 1975, Abkowitz 1980, Hwang 1980, Källström and Åström 1981).

In the work by Fedayevsky and Sobolev (1963), another new type of model was derived. This manoeuvring model, instead of being based upon a series expansion, characterised the hydrodynamic forces in terms of modulus–quadratic equations, which were seen to be empirically accurate and of low order.

The differences between the series and modulus approaches are quite fundamental, and the different coefficients are in general irreconcilable.

The series models were further developed in the work by Son and Nomoto (1982), in which the Abkowitz model was extended to include roll, enabling a more complete analysis of the forces acting on a ship.

The modulus models were developed as follows. In the work by Norrbin (1970), another model was derived, this time modelling the hydrodynamic forces in terms of nonlinear quadratic and quartic terms for even functions, and quadratic modulus models for odd terms. This model was made more manageable in the work by Blanke (1981). The most important parts of Norrbin's model were retained, and physical reasoning used to simplify some of the more unwieldy terms.

Further developments were made by Christensen and Blanke (1986), in which a linear–time varying model was derived. This model added a roll mode, and removed the surge equation by incorporating the forward speed as a time–varying parameter in the other modes. This approach allows for quick and yet accurate analysis to be made of the roll–mode, making

it especially suited for use in rudder roll damping and fin roll damping problems.

Takashina (1986) developed a method for describing the forces acting on a manoeuvring ship in terms of Fourier series analyses. These Fourier series were expanded about the angle between the ship's total velocity and the encounter angle with the current velocity. This apprach results in a mixture of odd functions and modulus terms. The model has demonstrated good accuracy across a wide range of sideslip angles (Tanaka 1995) for certain manoeuvres, although the model has no inertial coupling terms, and as such suffers in the modelling of complex manoeuvres.

Several models have been developed that apply cross–flow drag formulations in order to explain the sway and yaw forces on a ship. Obokata *et al.* (1981) developed a model based on a sectional cross–flow drag formulation, which was expanded and tested to demonstrate its capability (Obokata and Sasaki 1982, Obokata 1987). Hooft (1994) mixed sectional cross–flow drag theory with the low aspect ratio lift and drag theory of Jones (1946) to derive a more comprehensive model of the hydrodynamic forces acting during manoeuvring.

There are many related papers which draw on the approach by Hooft of combining various formulations to derive a more comprehensive model (Leite *et al.* 1998, Beukelman and Journee 2001, Karasuno and Igarashi 1990). Leite *et al.* (1998) utilised Fourier series in the same fashion as Takashina, and merged these with low aspect ratio wing properties and the linear theory of Clarke *et al.* (1983). Experimental verification of this work can be seen in the work by Aranha *et al.* (2001).

Comparative analyses of many of the model types described within this introduction have also been carried out (e.g. Matsuura *et al.* 2000, Simos *et al.* 2002).

The basis for a large number of models is the work of the Mathematical Modelling Group. The work of this group can be found in (MMG 1977*a*, MMG 1977*b*, MMG 1977*c*, MMG 1977*d*, MMG 1980), and also in papers such as (Inoue *et al.* 1981, Kijima *et al.* 1990*b*, Kijima *et al.* 1990*a*).

The simulation and control of ships and other seagoing vehicles was influenced greatly by the work of Fossen (1994, 2002*a*). In these publications, the field of robotics was related to the marine field (Craig 1989), enabling a crossover from each formerly independent field.

Energy based approaches to hydrodynamics can be seen, for example, in Milne-Thomson (1968). The application of Kirchhoff's law to aid in solving the equations of motion in a moving and rotating frame of reference can be

seen in Meirovitch and Kwak (1989).

Time–domain formulations of the equations of motion for ships began to be analysed in the 1950s. The work by Cummins (1962) is an invaluable historical review of the early development of these time–domain relations. Not only that, it is the main citation for modern time–domain formulations. Cummins formulated the equations of motion as convolutions of the history of velocities. Ogilvie (1964) related Cummins' formulations to the classical equations, increasing their utility and enabling them to be tied to conventional hydrodynamic codes. Analyses of the functional form of the equations can be seen, for example, in (Bishop and Price 1981, Bishop *et al.* 1984). Recent works on the unification of manoeuvring and seakeeping can be seen in (Bailey *et al.* 1997, Fossen 2005).

1.4 Thesis Organisation

The thesis is organised as follows:

Chapter 2 sets up the mathematical framework for analysing the dynamics of ships. The first section analyses the kinematic aspects of motion. The second section introduces the kinetic portion of dynamics by writing down the Kirchhoff Equations, and applying them to a regular rigid body.

Chapter 3 starts by deriving the conventional low–frequency equations of motion for ships. This chapter contributes by generalising this low–frequency approach. The new formulation is valid for arbitrary motion, is derived. It is developed by taking a convolution formulation of the added–mass matrix, and applying Kirchhoff's Equations.

Chapter 4 contains the derivation of a novel four degree of freedom manoeuvring model. It is developed from conventional low aspect–ratio aerodynamics. Several different physical processes are analysed. The forces are typically treated in the flow axes, and converted to the body–fixed frame. Circulatory lift and drag are dealt with in this manner. Nonlinear lift and drag (cross–flow drag) are included. A roll model is included, with emphasis on how the roll angle influences the circulatory lift and drag forces. The final result is a model structure suitable for analysis over a wide range of operating conditions.

Chapter 5 collates the results from Chapters 3 and 4, and sets down the finished models.

Chapter 6 uses experimental data to establish the viability of the low–frequency manoeuvring model that was derived in earlier chapters. This work validates and verifies the model. A set of planar motion mechanism tests were used as the datasource for this task. The model is verified by performing a regression analysis on the PMM data at one speed. It is then verified by showing that it can accurately replicate a dataset at a wholly different speed. This same approach is taken with an existing commercial model, and comparisons drawn between the two.

Chapter 7 uses full–scale data from a high speed trimaran test, and fits the manoeuvring model to it. This work serves as an additional validation test.

1.4.1 Publications

The following publications are directly connected with the work presented in this thesis:

1. Ross, A., T. Perez and T. I. Fossen. Clarification of the Low–Frequency Modelling Concept for Marine Craft. *Proc. of the IFAC MCMC'06*, Lisbon, Portugal, September 20–22, 2006.

2. Ross, A., T. Perez and T. I. Fossen. A Novel Maneuvering Model Based on Low–Aspect Ratio Lift Theory and Lagrangian Mechanics. *Proc. of the IFAC CAMS'07*, Bol Croatia, September 19–21, 2007.

3. Perez, T., T. Mak, T. Armstrong, A. Ross and Thor I. Fossen. Validation of a 4DOF Manoeuvring Model of a High–speed Vehicle–Passenger Trimaran. *Proc. of Ninth International Conference on Fast Sea Transportation FAST2007*, Shanghai, China.

4. Ross, A., T. Perez and T. I. Fossen. Relating Lagrangian Ship Models to Classical Manoeuvring Theory. *Accepted for publication in Journal of Ship Research*, 2008.

Part I

Development of the Ship Model

Chapter 2

Dynamics

The English word dynamic spawns from the Ancient Greek noun $\delta\upsilon\nu\alpha\mu\iota\varsigma$, meaning strength or power. This field of science deals with the motion of bodies, and is subdivided into two main sections of analysis: kinematics and kinetics. Kinematics studies the geometry of motion, but without regard for any causes of that motion. Kinetics studies the forces acting on a body, and the motions resulting from these. This chapter mirrors the subdivision of dynamics: the first part states the mathematics behind motion, and the second part derives the equations of motion for rigid bodies.

2.1 Kinematics

The treatment of the geometry of motion is called kinematics. The word comes from the Greek verb, $\kappa\iota\nu\varepsilon\iota\nu$, *to move*. The field deals *purely* with motion itself with no regard for its causes.

To deal with the geometry of motion, one must first specify *what* the motion is relative to. Several frames of reference are necessary for an adequate treatise on ship motion, and so a description of these follows.

2.1.1 Frames of Reference

The equations of motion can be formed in an arbitrary frame of reference. Various frames exist, and some are natural choices for certain problems and unnatural choices for certain others. Descriptions shall be made of several of these, according to the standards defined by the ANSI/AIAA (1992).

Earth Centred Inertial

The Earth Centred Inertial (ECI) frame, or $\{i\}$–frame of reference, has its origin coincident with the centre of the Earth, but it does *not* rotate with it. It is given by $\{i\} \triangleq (o_i, \overrightarrow{x_i}, \overrightarrow{y_i}, \overrightarrow{z_i})$. The components are defined relative to two planes; defined below.

Definition 2.1 *Ecliptic plane: the plane coincident with the ellipse traced out by the orbit of the geometric centre of the Earth around the barycentre of the Solar System.*

Definition 2.2 *Equatorial plane: the plane that is normal to the axis of rotation of the Earth, and that intersects the geometric centre of the Earth.*

The components of the $\{i\}$–frame are then defined as follows: o_i is fixed at the intersection of the ecliptic plane with the axis of rotation of the Earth; $\overrightarrow{z_i}$ points through the North Celestial Pole; $\overrightarrow{x_i}$ points in the direction of the vernal equinox; finally $\overrightarrow{y_i}$ is fixed relative to the other two ordinal directions to give a right–hand frame of reference. In words: $\overrightarrow{x_i}$ and $\overrightarrow{y_i}$ form a plane in line with the equator, while $\overrightarrow{z_i}$ points "northwards." It is depicted in Figure 2.1.

This frame of reference still moves in relation to the fixed stars, as the Earth's orbit varies over time. The precession of the Earth's orbit means that over the course of roughly 26,000 years, $\overrightarrow{z_i}$ traces out a cone with a half–angle of around $23.5\,^\circ$ (Herman 1995). Additionally, nutation and polar motions perturb the Earth's orbit to smaller degrees, with the latter being difficult to predict far in advance. Closer approximations to inertial frames are possible, such as the International Celestial Reference Frame (ICRF), which is used in studying planetary motion, spacecraft dynamics, and other problems on similar scales.

Earth Centred Earth Fixed

The Earth Centred Earth Fixed (ECEF) frame, or $\{e\}$–frame, is shown in Figure 2.2.

The frame is given by $\{e\} \triangleq (o_e, \overrightarrow{x_e}, \overrightarrow{y_e}, \overrightarrow{z_e})$. It has its origin coincident with the ECI–frame, and $\overrightarrow{z_e} \equiv \overrightarrow{z_i}$. Its distinguishing feature is that it rotates around the $\overrightarrow{z_i}$ axis with the rotational velocity of the Earth: $\omega^i_{z_e} = 7.2921e^{-5}$ rad/ s. That means that any location on the Earth's surface is time–invariant in this frame.

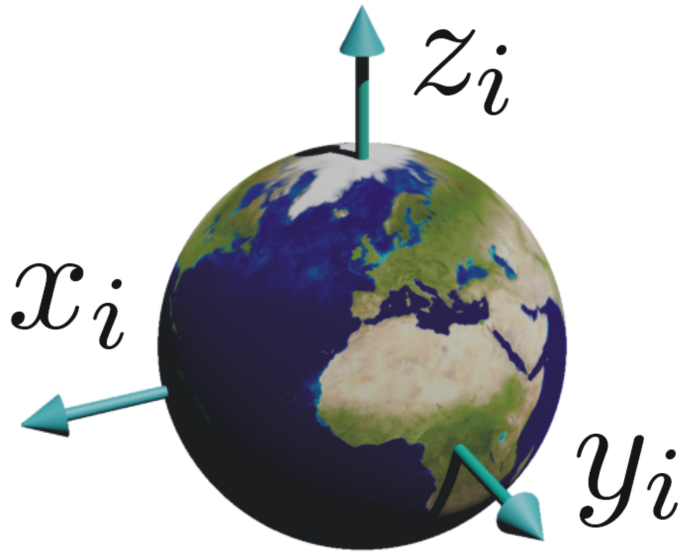

Figure 2.1: The Earth-Centred Inertial Frame

The $\overrightarrow{x_e}$ axis points directly from the centre of the Earth through the intersection of the prime meridian and the equator (i.e. $0\,^\circ N$, $0\,^\circ E$), while the $\overrightarrow{y_e}$ axis is set to give a right–handed frame, and so points directly towards the location $0\,^\circ N$, $90\,^\circ E$.

The frame's position relative to the $\{i\}$–frame is shown in Figure 2.3.

North–East–Down

A North–East–Down (NED) or $\{n\}$–frame is defined relative to the World Geodetic System (World Geodetic System 1984). The WGS–84 is in turn defined relative to the ECEF–frame, and is a reference ellipsoid that approximates the surface of the Earth.

An NED–frame can be defined relative to any point on the WGS, excluding either celestial pole. The reference frame is given by $\{n\} \triangleq (o_n, \overrightarrow{x_n}, \overrightarrow{y_n}, \overrightarrow{z_n})$, where $\overrightarrow{x_n}$ is in the direction of the geodesic pointing towards the Northern Celestial Pole; $\overrightarrow{z_n}$ is directly towards the origin of the ECEF–frame, and finally $\overrightarrow{y_n}$ is formed to give a right–handed frame, which gives an eastward pointing $\overrightarrow{y_n}$.

Since the rotation of the earth is so slow, relative to the accelerations and rotations a manoeuvring ship experiences, its effects can be neglected

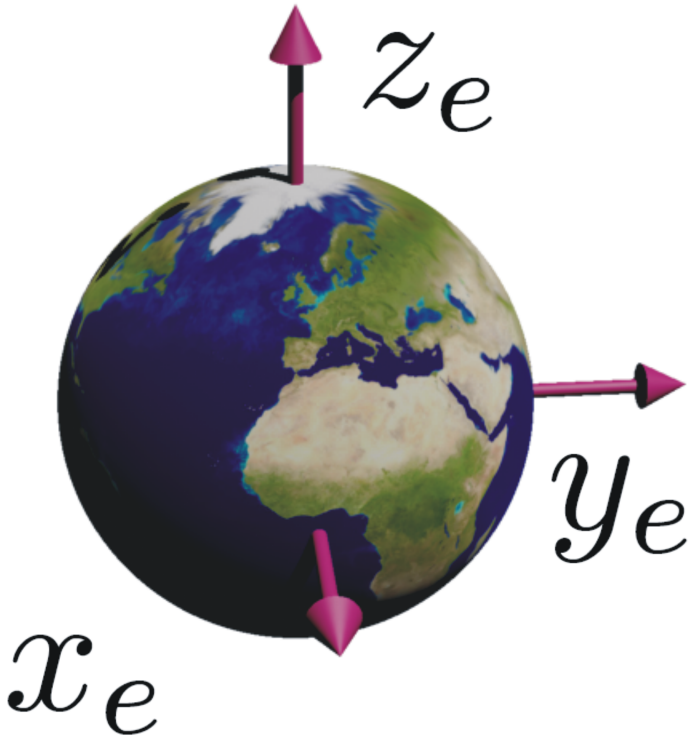

Figure 2.2: The Earth Centred Earth Fixed frame

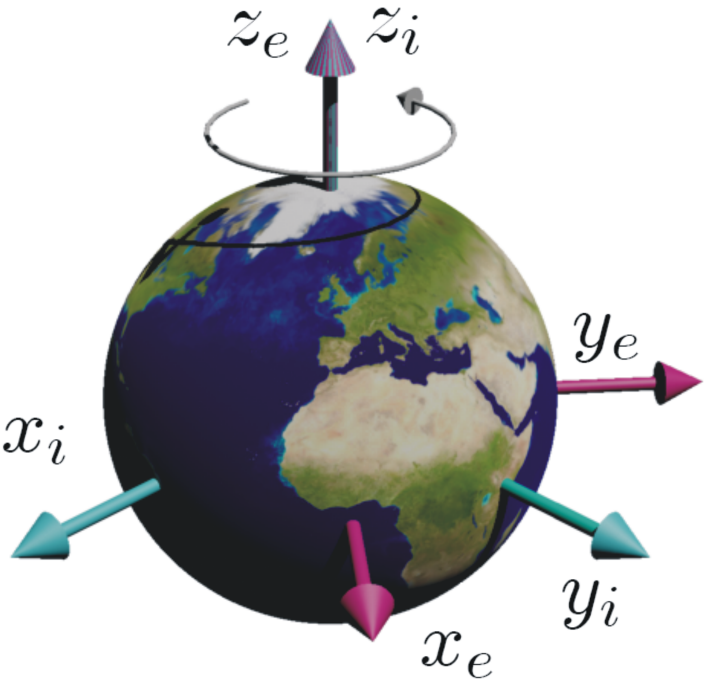

Figure 2.3: The relationship between the ECI and ECEF frames

for the purposes of ship modelling and control. For this reason, the $\{n\}$ frame is assumed to be sufficiently inertial throughout this thesis.

Body–fixed

A body–fixed frame, or $\{b\}$–frame, given by $\{b\} \triangleq (o_b, \overrightarrow{x_b}, \overrightarrow{y_b}, \overrightarrow{z_b})$, is a frame which translates and rotates with a body of interest. The frame is typically fixed at a useful point on the body. This point might be, for instance, at the centre of gravity, or collocated with the origin of an inertial measurement unit (IMU).

In ships, and in this thesis, it is conventional to set: $\overrightarrow{x_b}$ towards the bow of the ship; $\overrightarrow{y_b}$ towards starboard; and $\overrightarrow{z_b}$ to give a right–handed frame, which entails a "downward" pointing $\overrightarrow{z_b}$.

The $\{b\}$–frame moves and rotates with respect to the NED–frame, and so the coordinates describing the relative position of the former to the latter are vital. The generalised position vector of the body–fixed frame relative to the NED–frame is given by the vector $\boldsymbol{\eta}$, where:

$$\boldsymbol{\eta} \triangleq [n, e, d, \phi, \theta, \psi]^\top \in \mathbb{R}^3 \times \mathbf{S}^3. \tag{2.1}$$

This vector is commonly sectioned into the translational and rotational components as:

$$\mathbf{p}^n \triangleq [n, e, d]^\top \in \mathbb{R}^3 \tag{2.2}$$

$$\boldsymbol{\theta} \triangleq [\phi, \theta, \psi]^\top \in \mathbf{S}^3, \tag{2.3}$$

where (n, e, d) is the vector of positions north, east, and down respectively, and (ϕ, θ, ψ) signifies the roll, pitch, and yaw angles respectively.

Additionally, the body–fixed velocities: the velocities of the body–fixed frame *relative* to the $\{n\}$–frame but *expressed* in the $\{b\}$–frame. are commonly utilised:

$$\boldsymbol{\nu} \triangleq [u, v, w, p, q, r]^\top \in \mathbb{R}^6, \tag{2.4}$$

where the components (u, v, w, p, q, r) are the velocities in surge, sway, heave, roll, pitch and yaw respectively. These can be sectioned into linear and rotational velocities: $\boldsymbol{\nu}_1 \triangleq [u, v, w]$ and $\boldsymbol{\nu}_2 \triangleq [p, q, r]$.

The velocities are depicted in Figure 2.4. The red vector shows the surge velocity, u; the green vector shows the sway velocity v; the green vector shows the heave velocity w; and the grey vector $\boldsymbol{\nu}_1$ depicts the linear velocity vector.

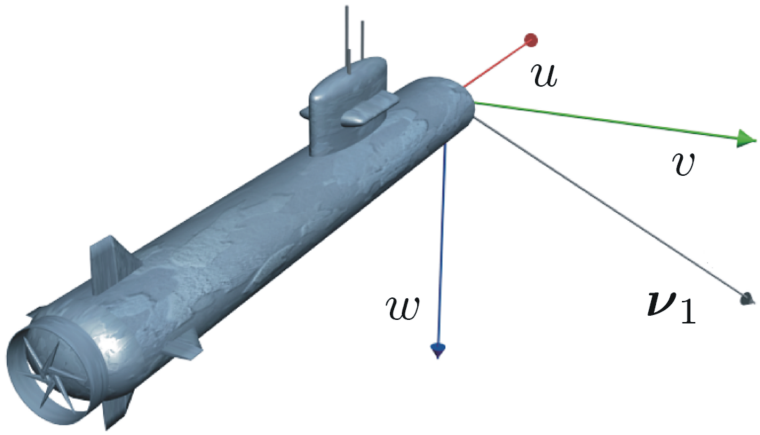

Figure 2.4: Linear velocities u, v, and w.

Flow Axes

The flow axes, or $\{f\}$–frame can be defined by the velocity of a body through a fluid. This axis system is also commonly used in aerodynamics, in which they are named wind–axes. The angle that a body moves through a fluid at is vitally important in calculating both the direction and magnitude of forces that arise due to this motion. The axes are $\{f\} \triangleq (o_f, \overrightarrow{x_f}, \overrightarrow{y_f}, \overrightarrow{z_f})$. The origin, o_f can in principle be set anywhere, but it makes sense to collocate it with o_b. The longitudinal vector $\overrightarrow{x_f}$ points directly along the body–fixed linear velocity vector $\boldsymbol{\nu}_1$. The $\overrightarrow{z_f}$ vector acts acts along the $\overrightarrow{z_b}$–axis, rotated about the $\overrightarrow{y_b}$–axis by the angle–of–attack, α. The $\overrightarrow{y_f}$ vector is set to form a right–handed frame: it points along the $\overrightarrow{y_b}$–axis, rotated about $\overrightarrow{z_b}$ by the sideslip angle, β. The angle of attack and angle of sideslip are shown in Figures 2.5 and 2.6 respectively.

The transformations between frames will be dealt with in the coming section.

2.1.2 Transformations between frames

The field of kinematics deals with the motion of an object in a geometric fashion: there is not treatment of the *causes* of this motion. Dealing with multiple reference frames is fundamental. Many forces are naturally calculated in one frame of reference. For example, gravity naturally acts in the

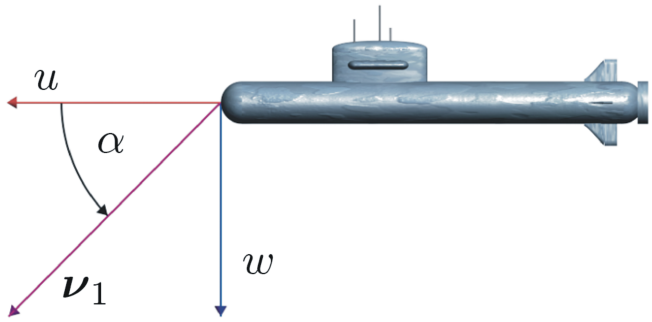

Figure 2.5: Angle of attack, α.

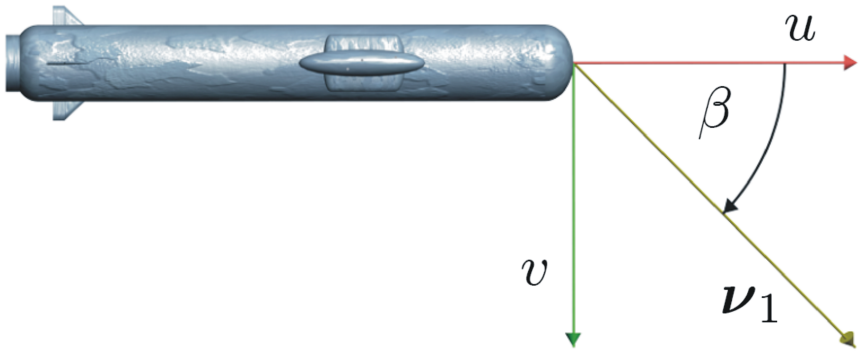

Figure 2.6: Angle of Sideslip, β.

$z-$direction of the $\{n\}$–frame. Alternatively, it acts precisely in the opposite direction of $\mathbf{r}^i$ (i.e., exactly in reverse to the position vector relative to the centre of the Earth). Considering gravity in the body–fixed frame, however, presents us with no help at all. Similarly, considering a lift force in the flow axes gives an immediately apparent direction and calculable magnitude for the force. Considering it in the NED frame offers no such possibility. These facts entail much changing from one frame to another. This task is done through the following matrix transformations.

Transformation between $\{n\}$ and $\{b\}$

- $\{n\} \triangleq (o_n, \overrightarrow{x_n}, \overrightarrow{y_n}, \overrightarrow{z_n})$
- $\{b\} \triangleq (o_b, \overrightarrow{x_b}, \overrightarrow{y_b}, \overrightarrow{z_b})$

Linear Velocity Transformation The notation used to rotate a vector from one frame to another is given by:

$$\mathbf{r}^y = \mathbf{R}_x^y \mathbf{r}^x, \tag{2.5}$$

where $\mathbf{R}_x^y$ is a rotation matrix: the subscript denoting which frame is the source, and the superscript denoting which frame is the destination. The matrix above rotates the vector $\mathbf{r}$ from frame $\{x\}$ to frame $\{y\}$. By definition, every rotation matrix is a member of the *special orthogonal group* (i.e., the group of orthogonal matrices with $det = +1$). For three–dimensional rotations

$$\mathbf{R}_x^y \in SO(3) \quad \forall \{x\}, \{y\} \tag{2.6}$$

$$\Rightarrow (\mathbf{R}_x^y)^{-1} = (\mathbf{R}_x^y)^\top = \mathbf{R}_y^x. \tag{2.7}$$

The orientation of one frame, $\{y\}$, relative to another, $\{x\}$, can be described through three separate rotations, by Euler's Theorem on Rotation (Fossen 2002*a*). Each consecutive rotation is *simple* (i.e., each rotation is performed about one axis at a time). The order in which these rotations are carried out is not fixed.

Since three rotations are sufficient to describe an arbitrary orientation in three dimensions, there are 27 possible orders in which these rotations can take place. The necessary condition on these twenty seven is that consecutive rotations cannot take place around the same axis (i.e., roll–roll–pitch can not work, while roll–pitch–roll is fine). There are 12 of the 27 which satisfy this condition.

The one used almost universally in marine control and also aeronautics and aerospace engineering is described here. The convention in rotating *from* the $\{b\}$–frame *to* the $\{n\}$–frame is to rotate about x, then y then z. This approach is sometimes called the *123 convention*, but it is **not** the x–convention (which is roll, then pitch, then roll again). The *123 convention* is:

1. A rotation, ϕ, about the x–axis of the $\{b\}$–frame: $\mathbf{R}_x(\phi)$
2. A rotation, θ, about the y–axis of the intermediate frame: $\mathbf{R}_y(\theta)$
3. A rotation, ϕ, about the z–axis of the second intermediate frame: $\mathbf{R}_z(\psi)$

The resulting rotation matrix is then:

$$\begin{aligned} \mathbf{R}_b^n(\boldsymbol{\theta}) &= \mathbf{R}_z(\psi)\mathbf{R}_y(\theta)\mathbf{R}_x(\phi) && (2.8)\\ \Rightarrow \mathbf{R}_b^n(\boldsymbol{\theta})^{-1} &= (\mathbf{R}_z(\psi)\mathbf{R}_y(\theta)\mathbf{R}_x(\phi))^\top \\ \Rightarrow \mathbf{R}_n^b(\boldsymbol{\theta}) &= \mathbf{R}_x(\phi)^\top \mathbf{R}_y(\theta)^\top \mathbf{R}_z(\psi)^\top && (2.9) \end{aligned}$$

A rotation by the angle ϕ about the x–axis is:

$$\mathbf{R}_x(\phi) = \begin{bmatrix} 1 & 0 & 0 \\ 0 & \cos\phi & -\sin\phi \\ 0 & \sin\phi & \cos\phi \end{bmatrix}. \quad (2.10)$$

A rotation by the angle θ about the y–axis is:

$$\mathbf{R}_y(\theta) = \begin{bmatrix} \cos\theta & 0 & \sin\theta \\ 0 & 1 & 0 \\ -\sin\theta & 0 & \cos\theta \end{bmatrix}. \quad (2.11)$$

A rotation by the angle ψ about the z–axis is:

$$\mathbf{R}_z(\psi) = \begin{bmatrix} 1 & 0 & 0 \\ 0 & \cos\phi & -\sin\phi \\ 0 & \sin\phi & \cos\phi \end{bmatrix}. \quad (2.12)$$

These rotations give the solution for (2.8) and (2.9) as:

$$\mathbf{R}_b^n(\boldsymbol{\theta}) = \begin{bmatrix} c_\psi c_\theta & s_\phi c_\theta & -s_\theta \\ c_\psi s_\theta s_\phi - s_\psi c_\phi & c_\psi c_\phi + s_\phi s_\theta s_\psi & c_\theta s_\phi \\ s_\psi s_\phi + c_\psi c_\phi s_\theta & s_\psi c_\phi s_\theta - c_\psi s_\phi & c_\theta c_\phi \end{bmatrix} \quad (2.13)$$

$$\mathbf{R}_n^b(\boldsymbol{\theta}) = \mathbf{R}_b^n(\boldsymbol{\theta})^\top = \begin{bmatrix} c_\psi c_\theta & c_\psi s_\theta s_\phi - s_\psi c_\phi & s_\psi s_\phi + c_\psi c_\phi s_\theta \\ s_\phi c_\theta & c_\psi c_\phi + s_\phi s_\theta s_\psi & s_\psi c_\phi s_\theta - c_\psi s_\phi \\ -s_\theta & c_\theta s_\phi & c_\theta c_\phi \end{bmatrix} \quad (2.14)$$

with:

$$s. \triangleq \sin(\cdot) \tag{2.15}$$

$$c. \triangleq \cos(\cdot) \tag{2.16}$$

Remark 2.1 *The angles ϕ, θ and ψ are typically called* ***the*** *Euler–angles. It is a longstanding convention in aerospace and marine engineering, and will not be changed in this thesis. That said, the convention is generally not accepted in mathematics and physics (e.g. Goldstein* et al. *1953, Lifshitz and Landau 1982, Arfken 1985, Weisstein 2008). The angles, as special cases of Euler–angles, ought to be more precisely named either the* Tait–Bryan *angles (Kelvin and Tait 1896) or the* Cardano *angles.*

The matrices in (2.13) and (2.14) allow for the transformation of any linear quantity, such as force or velocity, from one frame of reference to another. To transform the angular velocities from one to another requires additional analysis.

Angular Velocity Transformation Given the body–fixed angular velocities $\boldsymbol{\nu}_2 = [p, q, r]^\top$, we wish to calculate the time–rate of change of the Euler Angles, $[\phi, \theta, \psi]^\top$. As with linear velocity, the integral of the body–fixed angular velocity, $\int \boldsymbol{\nu}_2 d\tau$, is has no physical interpretation here. The rate of change of the Euler–angles can, however, be derived from a transformation matrix $\mathbf{T}_\theta(\boldsymbol{\theta})$ applied to these velocities:

$$\dot{\boldsymbol{\theta}} = \mathbf{T}_\theta(\boldsymbol{\theta})\,\boldsymbol{\nu}_2. \tag{2.17}$$

This transformation can be derived as (Fossen 2002*a*, Perez and Fossen 2007):

$$\boldsymbol{\nu}_2 = \begin{bmatrix}\dot{\phi}\\0\\0\end{bmatrix} + \mathbf{R}_x(\phi)^\top \begin{bmatrix}0\\\dot{\theta}\\0\end{bmatrix} + \mathbf{R}_x(\phi)^\top \mathbf{R}_y(\theta)^\top \begin{bmatrix}0\\0\\\dot{\psi}\end{bmatrix} \triangleq \mathbf{T}_\theta(\boldsymbol{\theta})^{-1}\,\dot{\boldsymbol{\theta}}. \tag{2.18}$$

Using (2.10)–(2.12) gives:

$$\mathbf{T}_\theta(\boldsymbol{\theta})^{-1} = \begin{bmatrix}1 & 0 & -s_\theta\\0 & c_\phi & c_\theta s_\phi\\0 & -s_\phi & c_\theta s_\phi\end{bmatrix} \tag{2.19}$$

$$\Rightarrow \mathbf{T}_\theta(\boldsymbol{\theta}) = \begin{bmatrix}1 & s_\phi t_\theta & c_\phi t_\theta\\0 & c_\phi & -s_\phi\\0 & -s_\phi/c_\theta & c_\theta/c_\theta\end{bmatrix}, \quad \theta \neq \pm\pi/2. \tag{2.20}$$

Complete Transformation The transformation matrix from the $\{b\}$– frame to the $\{n\}$– frame is then given by:

$$\mathbf{J}(\boldsymbol{\theta}) \triangleq \begin{bmatrix} \mathbf{R}_b^n(\boldsymbol{\theta}) & 0 \\ 0 & \mathbf{T}_\theta(\boldsymbol{\theta}) \end{bmatrix} \tag{2.21}$$

$$\Rightarrow \dot{\boldsymbol{\eta}} = \mathbf{J}(\boldsymbol{\theta})\boldsymbol{\nu}. \tag{2.22}$$

Transformation Between $\{f\}$ and $\{b\}$

- $\{b\} \triangleq (o_b, \overrightarrow{x_b}, \overrightarrow{y_b}, \overrightarrow{z_b})$
- $\{f\} \triangleq (o_f, \overrightarrow{x_f}, \overrightarrow{y_f}, \overrightarrow{z_f})$

Many forces are most easily interpreted in the flow axes. The drag force by definition acts precisely in the opposite direction of $\overrightarrow{x_f}$. The lift force acts precisely in the opposite direction of $\overrightarrow{z_f}$. The rotation matrices to transform between $\{b\}$ and $\{f\}$ are are given by:

$$\mathbf{R}_b^f = \begin{bmatrix} \cos\beta\cos\alpha & \sin\beta & \cos\beta\sin\alpha \\ -\sin\beta\cos\alpha & \cos\beta & -\sin\beta\sin\alpha \\ -\sin\alpha & 0 & \cos\alpha \end{bmatrix} \tag{2.23}$$

$$\mathbf{R}_f^b = \begin{bmatrix} \cos\beta\cos\alpha & -\sin\beta\cos\alpha & -\sin\alpha \\ \sin\beta & \cos\beta & 0 \\ \cos\beta\sin\alpha & -\sin\beta\sin\alpha & \cos\alpha \end{bmatrix}, \tag{2.24}$$

where:

$$\alpha \triangleq \arctan\frac{w}{u} \tag{2.25}$$

$$\beta \triangleq \arctan\frac{v}{u}. \tag{2.26}$$

Note that if heave is neglected, these relations are equivalent to:

$$\alpha \equiv 0 \tag{2.27}$$

$$\beta \equiv \arctan\frac{v}{u} \equiv \arcsin\frac{v}{U} \equiv \arccos\frac{u}{U}. \tag{2.28}$$

2.2 Kinetics

The word kinetics is also of Greek origin, stemming from the word $\kappa\iota\nu\eta\sigma\iota\zeta$, which means the act of moving. This field deals with the forces and moments acting on objects, and explains the accelerations caused by these.

Once complete, the accelerations can be combined with the kinematics studied in Section 2.1. This combination gives a set of differential equations; the solution of which completes the problem of motion analysis.

There are a number of approaches through which equations of motion can be derived. The first and most easily recognised is through Newton's Second Law $F = ma$ (for fixed mass). A second is through an energy based approach, referred to as the Euler–Lagrange equation. The latter approach is used within this thesis.

Newton's Laws describe motion in an inertial reference frame. The E–L equations do not share this restriction: they possess frame–indifference. This property means that the law applied is the same regardless of which reference frame is chosen. This symmetry exemplifies Dirac's belief that physical laws should possess a mathematical beauty (see the final essay in Truesdell 1988).

The distinction between Newtonian and Lagrangian mechanics can be understood by noting where one *begins*. To form the equations of motion with Newtonian mechanics, one begins by defining a mass. The force acting on this mass is directly proportional to the product of mass and acceleration:

$$F = ma. \tag{2.29}$$

Conversely, in the Euler–Lagrange approach, the first step is to state the Lagrangian to be:

$$L \triangleq T^* \left(\dot{\boldsymbol{\xi}}, \boldsymbol{\xi}, t \right) - P \left(\boldsymbol{\xi} \right), \tag{2.30}$$

where T^* and P are the kinetic coenergy and potential energy respectively[1]. The Euler–Lagrange equation is (e.g. Naidu 2003):

$$\frac{d}{dt} \left(\frac{\partial L}{\partial \dot{\boldsymbol{\xi}}} \right) - \frac{\partial L}{\partial \boldsymbol{\xi}} = \mathbf{J}^{-T} \left(\boldsymbol{\xi} \right) \boldsymbol{\tau}, \tag{2.31}$$

where $\boldsymbol{\xi}$ is a generalised coordinate system[2].

In principle, *any* such coordinate system can be used in this formulation: there is no need to constrain $\boldsymbol{\xi} = \boldsymbol{\eta}$. Although it is valid, there is no benefit to setting $\boldsymbol{\xi} = \int \boldsymbol{\nu} dt$, since this integral has no real meaning here (although in other fields, the distance travelled along each axis might be of interest).

This approach relates the forces acting on an object to the time–rate–of–change of the energy, and by doing so gives differential equations describing

[1] The kinetic coenergy and kinetic energy are identical throughout this thesis.

[2] The term *generalised coordinate* first appears in (Kelvin and Tait 1896).

the motion itself. It is this mathematical framework in which the analyses of motion will be placed in this thesis.

2.2.1 Kirchhoff's Equations of Motion

Kirchhoff's (1869) equations are a set of relations used to obtain the equations of motion from the derivatives of the kinetic energy of a system; they are a special case of the Euler–Lagrange equations. The derived equations also give the Coriolis–centripetal forces, which arise in non–inertial frames. Derivations in the marine field can be seen, for example, in (Milne-Thomson 1968, Fossen 2002*a*). The derivations are included in Appendix A.

$$\frac{d}{dt}\left(\frac{\partial T}{\partial \boldsymbol{\nu}_1}\right) + \mathbf{S}\left(\boldsymbol{\nu}_2\right)\frac{\partial T}{\partial \boldsymbol{\nu}_1} = \boldsymbol{\tau}_1 \tag{2.32}$$

$$\frac{d}{dt}\left(\frac{\partial T}{\partial \boldsymbol{\nu}_2}\right) + \mathbf{S}\left(\boldsymbol{\nu}_2\right)\frac{\partial T}{\partial \boldsymbol{\nu}_2} + \mathbf{S}\left(\boldsymbol{\nu}_1\right)\frac{\partial T}{\partial \boldsymbol{\nu}_1} = \boldsymbol{\tau}_2. \tag{2.33}$$

Applicability of Kirchhoff's Equations

Being a special case of the E–L equations, Kirchhoff's equations share the limitations of the most typical Euler–Lagrange formulation. Note that not *all* E–L formulations necessarily share the following requirements.

Holonomic The system must be holonomic: the number of generalised coordinates must be equal to the degrees–of–freedom of the system. Note that this property the use of a quaternion approach, or any other chart on $SO\left(3\right)$ with more than three parameters, as there are too many generalised coordinates.

Time–invariant The system can not have any time–varying constraints. A fixed–mass criterion is then placed on the rigid body. For example, a rocket losing mass continuously is not explainable using the formulation given by (2.32)–(2.33). The reason for this is that the work–energy relation used in the derivation is no longer applicable, as it no longer takes into account the energy lost in the mass exiting the system. In these kinds of problems additional terms are necessary to account for the reaction forces from any loss (or gain) in mass. Such a reaction force is typically referred to as Metchersky's force (Pesce 2003, Pesce and Tannuri 2006).

2.2.2 Rigid Body Equations of Motion

To develop the rigid body equations of motion from (2.32)–(2.33), we first specify the system we are interested in. Given a rigid body, its mass matrix can be formed as (Fossen 1994, Fossen 2002*a*):

$$\mathbf{M}_{RB} = \begin{bmatrix} m\mathbf{I}_{3\times 3} & -m\mathbf{S}\left(\mathbf{r}_g^b\right) \\ m\mathbf{S}\left(\mathbf{r}_g^b\right) & \mathbf{I}_0 \end{bmatrix} \in \mathbb{R}^{6\times 6}, \tag{2.34}$$

where $\mathbf{r}_g^b$ is the location of o_b: the origin of body fixed frame relative to the centre–of–gravity of the ship. The mass matrix has the following properties:

Property 2.1 $\dot{\mathbf{M}}_{RB} = 0$.

Property 2.2 $\mathbf{M}_{RB} = \left(\mathbf{M}_{RB}\right)^\top > 0$.

The body–fixed frame is defined relative to the NED frame, which is assumed to be inertial. Motion of the rigid body is then described wholly by six independent coordinates. As the admissible motion of the body is also in six degrees of freedom, the system is holonomic.

The kinetic energy of this system is given by:

$$T_{RB} = \frac{1}{2}\boldsymbol{\nu}^\top \mathbf{M}_{RB}\boldsymbol{\nu}. \tag{2.35}$$

For convenience, the equations are solved at the centre of gravity (i.e., $\mathbf{r}_g^b = \mathbf{0}$). Furthermore, port–starboard symmetry is assumed. The full set of equations is given in Appendix B.1.

The kinetic energy given by (2.35) is time–invariant, and we are treating a holonomic system, satisfying the requirements given in Section 2.2.1, so Kirchhoff's Equations apply. They are solved as

$$\frac{d}{dt}\left(\frac{\partial T_{RB}}{\partial \boldsymbol{\nu}_1}\right) + \mathbf{S}\left(\boldsymbol{\nu}_2\right)\frac{\partial T_{RB}}{\partial \boldsymbol{\nu}_1} = \begin{bmatrix} m\dot{u} - mvr + mqw \\ m\dot{v} + mur - mpw \\ m\dot{w} - mqu + mpq \end{bmatrix} \tag{2.36}$$

$$\begin{aligned} \frac{d}{dt}\left(\frac{\partial T_{RB}}{\partial \boldsymbol{\nu}_2}\right) + \mathbf{S}\left(\boldsymbol{\nu}_2\right)\frac{\partial T_{RB}}{\partial \boldsymbol{\nu}_2} & \\ + \mathbf{S}\left(\boldsymbol{\nu}_1\right)\frac{\partial T_{RB}}{\partial \boldsymbol{\nu}_1} &= \begin{bmatrix} I_x\dot{p} + \left(I_z - I_y\right)pr + I_{xz}pq \\ I_y\dot{q} + \left(I_x - I_z\right)pr - I_{xz}\left(p^2 + q^2\right) \\ I_z\dot{r} + \left(I_y - I_x\right)pq - I_{xz}qr \end{bmatrix}. \end{aligned} \tag{2.37}$$

They can be formulated into:

$$\mathbf{M}_{RB}\dot{\boldsymbol{\nu}} + \mathbf{C}_{RB}(\boldsymbol{\nu})\,\boldsymbol{\nu} = \boldsymbol{\tau}_{RB}, \tag{2.38}$$

where:

$$\mathbf{M}_{RB} \triangleq \begin{bmatrix} m & 0 & 0 & 0 & 0 & 0 \\ 0 & m & 0 & 0 & 0 & 0 \\ 0 & 0 & m & 0 & 0 & 0 \\ 0 & 0 & 0 & I_x & 0 & I_{xz} \\ 0 & 0 & 0 & 0 & I_y & 0 \\ 0 & 0 & 0 & I_{xz} & 0 & I_z \end{bmatrix} \tag{2.39}$$

$$\mathbf{C}_{RB}(\boldsymbol{\nu}) \triangleq \begin{bmatrix} 0 & 0 & 0 & 0 & mw & -mv \\ 0 & 0 & 0 & -mw & 0 & mu \\ 0 & 0 & 0 & mv & -mu & 0 \\ 0 & mw & -mv & 0 & I_{xz}p + I_z r & -I_y q \\ -mw & 0 & mu & -I_{xz}p - I_z r & 0 & I_x p + I_{xz} r \\ mv & -mu & 0 & I_y q & -I_x p - I_{xz} r & 0 \end{bmatrix}. \tag{2.40}$$

Note the properties $\mathbf{M}_{RB} \equiv \mathbf{M}_{RB}^{\top}$ and $\mathbf{C}_{RB}(\boldsymbol{\nu}) \equiv -\mathbf{C}_{RB}^{\top}(\boldsymbol{\nu})$.

Using (2.38), and adding the transformation from the $\{b\}$–frame to the $\{n\}$–frame (see Section 2.1.2) gives us the final form for the rigid body equations of motion:

$$\dot{\boldsymbol{\eta}} = \mathbf{J}(\boldsymbol{\theta})\,\boldsymbol{\nu} \tag{2.41}$$

$$\mathbf{M}_{RB}\dot{\boldsymbol{\nu}} + \mathbf{C}_{RB}(\boldsymbol{\nu})\,\boldsymbol{\nu} = \boldsymbol{\tau}_{RB}. \tag{2.42}$$

Properties of Kirchhoff's Equations

$$\overbrace{\frac{d}{dt}\left(\frac{\partial T}{\partial \boldsymbol{\nu}_1}\right)}^{\text{mass–terms}} + \overbrace{\mathbf{S}(\boldsymbol{\nu}_2)\frac{\partial T}{\partial \boldsymbol{\nu}_1}}^{\text{Coriolis–centrip.}} = \boldsymbol{\tau}_1 \tag{2.43}$$

$$\underbrace{\frac{d}{dt}\left(\frac{\partial T}{\partial \boldsymbol{\nu}_2}\right)}_{\text{inertia–terms}} + \underbrace{\mathbf{S}(\boldsymbol{\nu}_2)\frac{\partial T}{\partial \boldsymbol{\nu}_2} + \mathbf{S}(\boldsymbol{\nu}_1)\frac{\partial T}{\partial \boldsymbol{\nu}_1}}_{\text{Coriolis–centripetal moments}} = \boldsymbol{\tau}_2. \tag{2.44}$$

For a constant rigid body mass matrix, $\mathbf{M}_{RB}$, the Kirchhoff Equations can always be partitioned into the form (Sagatun and Fossen 1991, Fossen 1994, Fossen 2002*a*):

$$\mathbf{M}_{RB}\dot{\boldsymbol{\nu}} + \mathbf{C}_{RB}(\boldsymbol{\nu})\boldsymbol{\nu} = \boldsymbol{\tau}_{RB},$$

which has the following properties:

Property 2.3 $\dot{\mathbf{M}}_{RB} = \mathbf{0}$.

Property 2.4 $\mathbf{M}_{RB} = (\mathbf{M}_{RB})^{\top} > 0$.

These first two properties follow immediately from the definition of the system.

Property 2.5 $\mathbf{C}_{RB}(\boldsymbol{\nu}) = -\mathbf{C}_{RB}(\boldsymbol{\nu})^{\top}$.

Proof. This property was proved in (Sagatun and Fossen 1991), which is repeated here. The Coriolis–centripetal terms in (2.43)–(2.44) are:

$$\mathbf{C}_{RB}(\boldsymbol{\nu})\boldsymbol{\nu} = \begin{bmatrix} \mathbf{S}(\boldsymbol{\nu}_2)\frac{\partial T}{\partial \boldsymbol{\nu}_1} \\ \mathbf{S}(\boldsymbol{\nu}_2)\frac{\partial T}{\partial \boldsymbol{\nu}_2} + \mathbf{S}(\boldsymbol{\nu}_1)\left(\frac{\partial T}{\partial \boldsymbol{\nu}_1}\right) \end{bmatrix}. \tag{2.45}$$

By the properties of the cross–product, $\mathbf{S}(a)\,b = -\mathbf{S}(b)\,a$, and so the above can be rewritten:

$$\begin{aligned} \mathbf{C}_{RB}(\boldsymbol{\nu})\boldsymbol{\nu} &= \begin{bmatrix} -\mathbf{S}\left(\frac{\partial T}{\partial \boldsymbol{\nu}_1}\right)\boldsymbol{\nu}_2 \\ -\mathbf{S}\left(\frac{\partial T}{\partial \boldsymbol{\nu}_1}\right)\boldsymbol{\nu}_1 - \mathbf{S}\left(\frac{\partial T}{\partial \boldsymbol{\nu}_2}\right)\boldsymbol{\nu}_2 \end{bmatrix} && (2.46) \\ &= \begin{bmatrix} 0 & -\mathbf{S}\left(\frac{\partial T}{\partial \boldsymbol{\nu}_1}\right) \\ -\mathbf{S}\left(\frac{\partial T}{\partial \boldsymbol{\nu}_1}\right) & -\mathbf{S}\left(\frac{\partial T}{\partial \boldsymbol{\nu}_2}\right) \end{bmatrix} \begin{bmatrix} \boldsymbol{\nu}_1 \\ \boldsymbol{\nu}_2 \end{bmatrix}. && (2.47) \end{aligned}$$

Since $\mathbf{S}(\mathbf{a}) = -\mathbf{S}(\mathbf{a})^{\top}\ \forall \mathbf{a}$, the skew–symmetry of $\mathbf{C}(\boldsymbol{\nu})$ is trivial. ■

This skew symmetry of the Coriolis–centripetal matrix, $\mathbf{C}_{RB}(\boldsymbol{\nu})$, offers physical insight. This term performs no actual work on the system: the forces are fictive and only appear from the usage of a non–inertial frame–of–reference. This is true regardless of the formulation of the kinetic energy.

Property 2.6 $\boldsymbol{\nu}^{\top}\left(\dot{\mathbf{M}}_{RB} - 2\mathbf{C}(\boldsymbol{\nu})\right)\boldsymbol{\nu} = 0$.

Proof. $\dot{\mathbf{M}}_{RB} = \mathbf{0}$, so the only term required to analyse is $\boldsymbol{\nu}^\top \mathbf{C}(\boldsymbol{\nu})\boldsymbol{\nu}$**:**

$$\begin{aligned}
\boldsymbol{\nu}^\top \mathbf{C}(\boldsymbol{\nu})\boldsymbol{\nu} &= a \\
\left(\boldsymbol{\nu}^\top \mathbf{C}(\boldsymbol{\nu})\boldsymbol{\nu}\right)^\top &= a \\
\boldsymbol{\nu}^\top \mathbf{C}(\boldsymbol{\nu})^\top \boldsymbol{\nu} &= a \\
\boldsymbol{\nu}^\top \left(\mathbf{C}(\boldsymbol{\nu}) + \mathbf{C}(\boldsymbol{\nu})^\top\right)\boldsymbol{\nu} &= 2a \\
\Rightarrow a &= 0,
\end{aligned}$$

where the skew–symmetry of $\mathbf{C}(\boldsymbol{\nu})$ has been exploited. ■

We can compare and contrast Kirchhoff's Equations with Newton's Second Law:

$$\mathbf{M}(\boldsymbol{\eta})\ddot{\boldsymbol{\eta}} = \boldsymbol{\tau}^\eta. \tag{2.48}$$

$\mathbf{M}(\boldsymbol{\eta})$ is the rigid body mass matrix defined in the $\{n\}$–frame: the mass distribution therefore varies as the body rotates; and $\boldsymbol{\tau}^\eta$ is the generalised force in the inertial frame. This equation is by necessity applied in an inertial frame. If we were to rotate these terms into the body fixed frame, substitute a constant mass matrix, and then compensate for the time–varying parts, we would find the Kirchhoff equations. It is aesthetically pleasing to think of the mass and inertia terms of the Kirchhoff equations as being applications of Newton's Second Law:

$$\mathbf{M}_{RB}\dot{\boldsymbol{\nu}} + \mathbf{C}_{RB}(\boldsymbol{\nu})\boldsymbol{\nu} = \boldsymbol{\tau}_{RB}. \tag{2.49}$$

The first part, $\mathbf{M}_{RB}\dot{\boldsymbol{\nu}}$, can be considered to be Newton's Second Law: the next part, $\mathbf{C}_{RB}(\boldsymbol{\nu})\boldsymbol{\nu}$, can be considered to be a correction of the first to compensate for the fact that the equation is being solved in a non–inertial frame of reference.

The mathematical basis for deriving the equations of motion for a vessel have now been set down, and so this task can now be contemplated.

Chapter 3

Equation of Motion for Ships

The rigid body equations of motion given by (2.41)–(2.42) are insufficient to model a body moving through water. During this motion, kinetic energy is imparted to the fluid which it would otherwise not have, and so this energy must be included as part of the formulation of the equations of motion. Of the pressure induced forces acting on a ship, some are proportional to the acceleration through the fluid. These are denoted *added–mass*, *virtual mass*, or sometimes *added–inertia*. These forces oppose the change in speed of the vessel. In the equations of motion, they are grouped alongside the rigid–body mass.

The solution is to use the energy of this mass in applying the Kirchhoff equations. It is not sufficient to derive the equations of motion using the rigid–body mass, and then insert the added–mass pressure force as an external force. That is, it is fundamentally unsatisfactory to write that:

$$\mathbf{M}_{RB}\dot{\boldsymbol{\nu}} + \mathbf{C}_{RB}\left(\boldsymbol{\nu}\right)\boldsymbol{\nu} = -\mathbf{M}_{A}\dot{\boldsymbol{\nu}} + \boldsymbol{\tau}. \tag{3.1}$$

In formulating the equations of motion, it is also necessary to account for the Coriolis–centripetal forces that arise due to the added–mass forces. However, before the proper form can be derived, it is necessary to give the form of the hydrodynamic added mass.

The coefficients describing the added mass can be written according to the notation of Bailey *et al.* (1997) as:

$$F_a\left(\omega\right), \text{ with} \tag{3.2}$$

$$F \in \{X, Y, Z, K, M, N\} \tag{3.3}$$

$$a \in \{\dot{u}, \dot{v}, \dot{w}, \dot{p}, \dot{q}, \dot{r}, u, v, w, p, q, r, n, e, d\}, \tag{3.4}$$

where ω is the frequency of oscillation. At any given frequency, $F_a(\omega) = \frac{\partial F}{\partial a}(\omega)\, a$, which is typically called an oscillatory derivative. The inertial pressure forces are those corresponding to $\dot{u}$, $\dot{v}$ etc. These can be grouped into matrix form as:

$$\mathbf{M}_A(\omega) = -\begin{bmatrix} X_{\dot{u}}(\omega) & X_{\dot{v}}(\omega) & X_{\dot{w}}(\omega) & X_{\dot{p}}(\omega) & X_{\dot{q}}(\omega) & X_{\dot{r}}(\omega) \\ Y_{\dot{u}}(\omega) & Y_{\dot{v}}(\omega) & Y_{\dot{w}}(\omega) & Y_{\dot{p}}(\omega) & Y_{\dot{q}}(\omega) & Y_{\dot{r}}(\omega) \\ Z_{\dot{u}}(\omega) & Z_{\dot{v}}(\omega) & Z_{\dot{w}}(\omega) & Z_{\dot{p}}(\omega) & Z_{\dot{q}}(\omega) & Z_{\dot{r}}(\omega) \\ K_{\dot{u}}(\omega) & K_{\dot{v}}(\omega) & K_{\dot{w}}(\omega) & K_{\dot{p}}(\omega) & K_{\dot{q}}(\omega) & K_{\dot{r}}(\omega) \\ M_{\dot{u}}(\omega) & M_{\dot{v}}(\omega) & M_{\dot{w}}(\omega) & M_{\dot{p}}(\omega) & M_{\dot{q}}(\omega) & M_{\dot{r}}(\omega) \\ N_{\dot{u}}(\omega) & N_{\dot{v}}(\omega) & N_{\dot{w}}(\omega) & N_{\dot{p}}(\omega) & N_{\dot{q}}(\omega) & N_{\dot{r}}(\omega) \end{bmatrix}. \tag{3.5}$$

At low frequency, these are typically referred to as the hydrodynamic derivatives (e.g. Bailey *et al.* 1997, Journée and Massie 2001, Fossen 1994, Fossen 2002*a*). This frequency is often said to be zero–frequency, but that makes little sense while discussing the oscillatory modes in heave, roll and pitch (Ross *et al.* 2006).

We make the definitions:

$$\mathbf{M}_A^0 \triangleq \mathbf{M}_A(\omega = 0) \tag{3.6}$$

$$\mathbf{M}_A^\infty \triangleq \mathbf{M}_A(\omega = \infty), \tag{3.7}$$

with the associated matrix components:

$$\mathbf{M}_A^0 = -\begin{bmatrix} X_{\dot{u}}^0 & X_{\dot{v}}^0 & X_{\dot{w}}^0 & X_{\dot{p}}^0 & X_{\dot{q}}^0 & X_{\dot{r}}^0 \\ Y_{\dot{u}}^0 & Y_{\dot{v}}^0 & Y_{\dot{w}}^0 & Y_{\dot{p}}^0 & Y_{\dot{q}}^0 & Y_{\dot{r}}^0 \\ Z_{\dot{u}}^0 & Z_{\dot{v}}^0 & Z_{\dot{w}}^0 & Z_{\dot{p}}^0 & Z_{\dot{q}}^0 & Z_{\dot{r}}^0 \\ K_{\dot{u}}^0 & K_{\dot{v}}^0 & K_{\dot{w}}^0 & K_{\dot{p}}^0 & K_{\dot{q}}^0 & K_{\dot{r}}^0 \\ M_{\dot{u}}^0 & M_{\dot{v}}^0 & M_{\dot{w}}^0 & M_{\dot{p}}^0 & M_{\dot{q}}^0 & M_{\dot{r}}^0 \\ N_{\dot{u}}^0 & N_{\dot{v}}^0 & N_{\dot{w}}^0 & N_{\dot{p}}^0 & N_{\dot{q}}^0 & N_{\dot{r}}^0 \end{bmatrix} \tag{3.8}$$

$$\mathbf{M}_A^\infty = -\begin{bmatrix} X_{\dot{u}}^\infty & X_{\dot{v}}^\infty & X_{\dot{w}}^\infty & X_{\dot{p}}^\infty & X_{\dot{q}}^\infty & X_{\dot{r}}^\infty \\ Y_{\dot{u}}^\infty & Y_{\dot{v}}^\infty & Y_{\dot{w}}^\infty & Y_{\dot{p}}^\infty & Y_{\dot{q}}^\infty & Y_{\dot{r}}^\infty \\ Z_{\dot{u}}^\infty & Z_{\dot{v}}^\infty & Z_{\dot{w}}^\infty & Z_{\dot{p}}^\infty & Z_{\dot{q}}^\infty & Z_{\dot{r}}^\infty \\ K_{\dot{u}}^\infty & K_{\dot{v}}^\infty & K_{\dot{w}}^\infty & K_{\dot{p}}^\infty & K_{\dot{q}}^\infty & K_{\dot{r}}^\infty \\ M_{\dot{u}}^\infty & M_{\dot{v}}^\infty & M_{\dot{w}}^\infty & M_{\dot{p}}^\infty & M_{\dot{q}}^\infty & M_{\dot{r}}^\infty \\ N_{\dot{u}}^\infty & N_{\dot{v}}^\infty & N_{\dot{w}}^\infty & N_{\dot{p}}^\infty & N_{\dot{q}}^\infty & N_{\dot{r}}^\infty \end{bmatrix}, \tag{3.9}$$

where the superscript 0 or ∞ implies that the coefficient is defined at low–frequency or infinite frequency respectively. No assumption of symmetry is made on $\mathbf{M}_A^0$. Newman (1977) showed symmetry at zero speed in an ideal

fluid, but also that symmetry is no longer guaranteed at forward speed. At infinite frequency, symmetry is assured regardless of forward speed.

This section proceeds by first re–deriving the equations of motion valid at low–frequency, and then by deriving them for arbitrary motion. The former is valid for manoeuvring in calm water, while the latter is valid for manoeuvring in waves. Prior to the derivation, some discussion of the applicability of the Kirchhoff equations is necessary.

The rigid body system, as reasoned in Chapter 2.2, is holonomic and time–invariant. Its use in the Kirchhoff equations is satisfactory.

In the fluid, there are infinite degrees of freedom. The added–mass coefficients relate the six body fixed velocities of the rigid body to the energy imparted to the fluid. As such there are six generalised coordinates, but infinite admissible variations, and therefore the fluid system is not holonomic. Even though the system fails to meet this criterion, it can still be treated as a conventional Lagrangian system. The proof is given in (Lamb 1932, Birkhoff 1960). Discussion of the validity of applying the EL equations to the added–mass system can be found in (Sagatun and Fossen 1991, Sagatun 1992, Wichlund *et al.* 1995).

3.1 Equations of motion for Low–Frequency Added Mass

This section repeats the results from (Imlay 1961, Sagatun and Fossen 1991, Sagatun 1992, Fossen 1994, Fossen 2002*b*).

Motion in calm water is typically at very low–frequency. The kinetic energy of the total system is:

$$T = \frac{1}{2}\boldsymbol{\nu}^\top \mathbf{M}\boldsymbol{\nu}, \tag{3.10}$$

where $\mathbf{M} = \mathbf{M}_{RB} + \mathbf{M}_A^0$, with these defined being according to equations (2.39) and (3.8).

It is important to note that *only* the symmetric parts of $\mathbf{M}_A^0$ are relevant. The skew–symmetric parts can have no influence whatsoever on the kinetic energy of the system, by observing the simple relation:

$$\begin{aligned} \mathbf{K} &= -\mathbf{K}^\top \\ \Rightarrow \mathbf{x}^\top \mathbf{K}\mathbf{x} &= \mathbf{0} \quad \forall \mathbf{x}. \end{aligned} \tag{3.11}$$

Therefore, using the relation (Fossen 2002*b*):

$$\mathbf{M}_A^0 \equiv \frac{1}{2}\underbrace{\left(\mathbf{M}_A^0 + \left(\mathbf{M}_A^0\right)^\top\right)}_{\text{symmetric}} + \frac{1}{2}\underbrace{\left(\mathbf{M}_A^0 - \left(\mathbf{M}_A^0\right)^\top\right)}_{\text{skew–symmetric}}, \tag{3.12}$$

we make the definition

$$\bar{\mathbf{M}}_A^0 \triangleq \frac{1}{2}\left(\mathbf{M}_A^0 + \left(\mathbf{M}_A^0\right)^\top\right). \tag{3.13}$$

Note that

$$T_A = \frac{1}{2}\boldsymbol{\nu}^\top \mathbf{M}_A^0 \boldsymbol{\nu} \equiv \frac{1}{2}\boldsymbol{\nu}^\top \bar{\mathbf{M}}_A^0 \boldsymbol{\nu} \quad \forall \boldsymbol{\nu}, \tag{3.14}$$

and so we can exclusively apply the symmetric part of the added–mass matrix. Although this property is noticed, even if it were not, the Kirchhoff equations symmetrise the inertial forces in their very application.

Kirchhoff's equations can be applied as follows:

$$\frac{d}{dt}\left(\frac{\partial T}{\partial \boldsymbol{\nu}_1}\right) + \mathbf{S}\left(\boldsymbol{\nu}_2\right)\frac{\partial T}{\partial \boldsymbol{\nu}_1} = \boldsymbol{\tau}_1 \tag{3.15}$$

$$\frac{d}{dt}\left(\frac{\partial T}{\partial \boldsymbol{\nu}_2}\right) + \mathbf{S}\left(\boldsymbol{\nu}_2\right)\frac{\partial T}{\partial \boldsymbol{\nu}_2} + \mathbf{S}\left(\boldsymbol{\nu}_1\right)\frac{\partial T}{\partial \boldsymbol{\nu}_1} = \boldsymbol{\tau}_2. \tag{3.16}$$

If we segregate the energy of the system into two components: that of the rigid body mass, and that of the added–mass, i.e. $T = T_{RB} + T_A$, then the forces *on* the rigid body due to added–mass can then be written as:

$$\boldsymbol{\tau}_{a1} = -\frac{d}{dt}\left(\frac{\partial T_A}{\partial \boldsymbol{\nu}_1}\right) - \mathbf{S}\left(\boldsymbol{\nu}_2\right)\frac{\partial T_A}{\partial \boldsymbol{\nu}_1} \tag{3.17}$$

$$\boldsymbol{\tau}_{a2} = -\frac{d}{dt}\left(\frac{\partial T_A}{\partial \boldsymbol{\nu}_2}\right) - \mathbf{S}\left(\boldsymbol{\nu}_2\right)\frac{\partial T_A}{\partial \boldsymbol{\nu}_2} - \mathbf{S}\left(\boldsymbol{\nu}_1\right)\frac{\partial T_A}{\partial \boldsymbol{\nu}_1}. \tag{3.18}$$

In component form these forces and moments are:

$$X_A = -\frac{d}{dt}\frac{\partial T_A}{\partial u} + r\frac{\partial T_A}{\partial v} - q\frac{\partial T_A}{\partial w} \tag{3.19}$$

$$Y_A = -\frac{d}{dt}\frac{\partial T_A}{\partial v} + p\frac{\partial T_A}{\partial w} - r\frac{\partial T_A}{\partial u} \tag{3.20}$$

$$Z_A = -\frac{d}{dt}\frac{\partial T_A}{\partial w} + q\frac{\partial T_A}{\partial u} - p\frac{\partial T_A}{\partial v} \tag{3.21}$$

$$K_A = -\frac{d}{dt}\frac{\partial T_A}{\partial p} + w\frac{\partial T_A}{\partial v} - v\frac{\partial T_A}{\partial w} + r\frac{\partial T_A}{\partial q} - q\frac{\partial T_A}{\partial r} \tag{3.22}$$

$$M_A = -\frac{d}{dt}\frac{\partial T_A}{\partial q} + u\frac{\partial T_A}{\partial w} - w\frac{\partial T_A}{\partial u} + p\frac{\partial T_A}{\partial r} - r\frac{\partial T_A}{\partial p} \tag{3.23}$$

$$N_A = \underbrace{-\frac{d}{dt}\frac{\partial T_A}{\partial r}}_{\text{Added mass}} + \underbrace{v\frac{\partial T_A}{\partial u} - u\frac{\partial T_A}{\partial v} + q\frac{\partial T_A}{\partial p} - p\frac{\partial T_A}{\partial q}}_{\text{Coriolis–centripetal}}. \tag{3.24}$$

For a constant mass, these forces can always be parameterised (Fossen 1994, Fossen 2002*a*) according to:

$$\begin{bmatrix} \boldsymbol{\tau}_{a1} \\ \boldsymbol{\tau}_{a2} \end{bmatrix} = -\bar{\mathbf{M}}_A^0 \dot{\boldsymbol{\nu}} - \mathbf{C}_A^0(\boldsymbol{\nu})\boldsymbol{\nu}. \tag{3.25}$$

The equations of motion are:

$$\dot{\boldsymbol{\eta}} = \mathbf{J}(\boldsymbol{\theta})\boldsymbol{\nu} \tag{3.26}$$

$$\left(\mathbf{M}_{RB} + \bar{\mathbf{M}}_A^0\right)\dot{\boldsymbol{\nu}} + \left(\mathbf{C}_{RB}(\boldsymbol{\nu}) + \mathbf{C}_A^0(\boldsymbol{\nu})\right)\boldsymbol{\nu} = \boldsymbol{\tau}^b, \tag{3.27}$$

where τ^b is the generalised force resolved in the $\{b\}$–frame acting on $\mathbf{M}_{RB}$ and $\bar{\mathbf{M}}_A^0$.

3.1.1 Dynamic Properties

which has the following properties:

Property 3.1 $\left(\mathbf{M}_{RB} + \bar{\mathbf{M}}_A^0\right) = \left(\mathbf{M}_{RB} + \bar{\mathbf{M}}_A^0\right)^\top > 0.$

Property 3.2 $\dot{\mathbf{M}}_{RB} = \dot{\bar{\mathbf{M}}}_A^0 = \mathbf{0}.$

Property 3.3 $\mathbf{C}(\boldsymbol{\nu}) = -\mathbf{C}(\boldsymbol{\nu})^\top.$

Proof. This proof is identical to that given in Section 2.2.2. ■

Property 3.4 $\boldsymbol{\nu}^\top \left(\dot{\mathbf{M}}_{RB} + \dot{\overset{\cdot}{\mathbf{M}}}{}^{0}_{A} - 2\mathbf{C}\left(\boldsymbol{\nu}\right) \right) \boldsymbol{\nu} = 0.$

Proof. $\dot{\mathbf{M}}_{RB} = \dot{\overset{\cdot}{\mathbf{M}}}{}^{0}_{A} = \mathbf{0}$, and the rest of the proof is identical to that given in Section 2.2.2. ■

3.1.2 4–DOF Example

Take a typical example of a port–starboard symmetric ship. The analysis is for surge, sway, roll and yaw; typically detailed enough for most manoeuvring problems. The added mass is of the following form:

$$\mathbf{M}_A^0 = -\begin{bmatrix} X_{\dot{u}}^0 & 0 & 0 & 0 \\ 0 & Y_{\dot{v}}^0 & Y_{\dot{p}}^0 & Y_{\dot{r}}^0 \\ 0 & K_{\dot{v}}^0 & K_{\dot{p}}^0 & K_{\dot{r}}^0 \\ 0 & N_{\dot{v}}^0 & N_{\dot{p}}^0 & N_{\dot{r}}^0 \end{bmatrix}. \tag{3.28}$$

The added mass forces acting on the rigid body mass are described by

$$-\frac{d}{dt}\frac{\partial T_A}{\partial \boldsymbol{\nu}} = -\frac{d}{dt}\frac{\partial}{\partial \boldsymbol{\nu}}\frac{1}{2}\boldsymbol{\nu}^\top \bar{\mathbf{M}}_A^0 \boldsymbol{\nu} \tag{3.29}$$

$$= -\bar{\mathbf{M}}_A^0 \dot{\boldsymbol{\nu}}, \tag{3.30}$$

with $\boldsymbol{\nu} = [u, v, p, r]^\top$.

The symbolic solution for the Coriolis–centripetal forces acting on the rigid–body mass is:

$$X_c = -Y_{\dot{v}}^0 vr - \frac{1}{2}\left(N_{\dot{v}}^0 + Y_{\dot{r}}^0\right) r^2 - \frac{1}{2}\left(Y_{\dot{p}}^0 + K_{\dot{v}}^0\right) pr \tag{3.31}$$

$$Y_c = X_{\dot{u}}^0 ur \tag{3.32}$$

$$K_c = 0 \tag{3.33}$$

$$N_c = \left(Y_{\dot{v}}^0 - X_{\dot{u}}^0\right) uv + \frac{1}{2}\left(Y_{\dot{r}}^0 + N_{\dot{v}}^0\right) ur + \frac{1}{2}\left(Y_{\dot{p}}^0 + K_{\dot{v}}^0\right) pu. \tag{3.34}$$

Since we have $\begin{bmatrix} X_c & Y_c & K_c & N_c \end{bmatrix}^\top = -\mathbf{C}_A\left(\boldsymbol{\nu}\right)\boldsymbol{\nu}$, the matrix form is given by:

$$\mathbf{C}_A\left(\boldsymbol{\nu}\right) = \begin{bmatrix} 0 & 0 & 0 & Y_{\dot{v}}^0 v + \frac{1}{2}\left(N_{\dot{v}}^0 + Y_{\dot{r}}^0\right) r + \frac{1}{2}\left(Y_{\dot{p}}^0 + K_{\dot{v}}^0\right) p \\ 0 & 0 & 0 & -X_{\dot{u}}^0 u \\ 0 & 0 & 0 & 0 \\ -Y_{\dot{v}}^0 v - \frac{1}{2}\left(N_{\dot{v}}^0 + Y_{\dot{r}}^0\right) r - \frac{1}{2}\left(Y_{\dot{p}}^0 + K_{\dot{v}}^0\right) p & X_{\dot{u}}^0 u & 0 & 0 \end{bmatrix}. \tag{3.35}$$

Under the additional assumption of a symmetric added mass, this matrix is:

$$\mathbf{C}_A(\boldsymbol{\nu}) = \begin{bmatrix} 0 & 0 & 0 & Y^0_{\dot{v}}v + Y^0_{\dot{r}}r + Y^0_{\dot{p}}p \\ 0 & 0 & 0 & -X^0_{\dot{u}}u \\ 0 & 0 & 0 & 0 \\ -Y^0_{\dot{v}}v - Y^0_{\dot{r}}r - Y^0_{\dot{p}}p & X^0_{\dot{u}}u & 0 & 0 \end{bmatrix}, \tag{3.36}$$

where $N^0_{\dot{v}}/Y^0_{\dot{r}}$ and $Y^0_{\dot{p}}/K^0_{\dot{v}}$ are interchangeable.

3.2 Equations of motion with Fluid Memory Effects

This section proceeds to apply the Kirchhoff formulation to a time–domain model with fluid memory effects. The end result is a new formulation of the equations of motion, valid under arbitrary motion.

Section 3.1 showed the structure of the equations of motion for the case of zero frequency motion, but this tells us little of how they ought to look if the added–mass matrix is frequency dependent. Consider a simple example of undamped surge motion:

$$\left(m - X_{\dot{u}}(\omega)\right)\dot{u} = X. \tag{3.37}$$

This equation has the rough appearance of a differential equation, but this is not so. It is limited by the fact that both the motion and excitation must be at the frequency ω (Tick 1959). Such a pseudo–differential equation is entirely unable to cope with random or transient motions and excitations. Using inverse Fourier transforms, it is trivial to derive a time–domain equivalent which has the following structure:

$$m\dot{u} - \left(X^C_{\dot{u}} * \dot{u}\right)(t) = X(t), \tag{3.38}$$

where $X^C_{\dot{u}} = \mathcal{F}^{-1}[X_{\dot{u}}(\omega)]$ and $X(t) = \mathcal{F}^{-1}[X]$. This formulation is valid under arbitrary motion, without any limitations on frequency of either the motion or excitation. Under this structure, arbitrary forces are perfectly acceptable. This versatility allows nonlinear damping and the like to be included on the right hand side of the equation as excitation forces. Even with this result it is still unclear how the complete equations of motion ought to look. A long line of research exists on time–domain formulations (e.g. Cummins 1962, Ogilvie 1964, Bishop *et al.* 1984, Bailey *et al.* 1997,

Fossen 2005, Perez and Fossen 2007). The approach in this chapter derives a new structure for the equations of motion by using the kinetic energy of the fluid as the basis. This formulation is inherently defined in the body fixed frame, in contrast with formulations in which the model is tied to a steady forward speed or to oscillatory motion about some equilibrium axes.

The kinetic energy of the added–mass in the frequency domain is:

$$T_A(\omega) = \frac{1}{2}\boldsymbol{\nu}^\top(\omega)\,\mathbf{M}_A(\omega)\,\boldsymbol{\nu}(\omega) \tag{3.39}$$

By application of the Convolution Theorem for unitary Fourier transforms (e.g. Bracewell 1999), we can write that:

$$T_A(t) = \frac{1}{2}\sqrt{2\pi}\mathcal{F}^{-1}[\mathcal{F}[\boldsymbol{\nu}^\top(t)]\mathcal{F}[\mathbf{M}_A(t)]\mathcal{F}[\boldsymbol{\nu}(t)]] \tag{3.40}$$

$$= \sqrt{\frac{\pi}{2}}\left(\boldsymbol{\nu}^\top * \mathbf{M}_A * \boldsymbol{\nu}\right)(t) \tag{3.41}$$

The impulse response of the added mass is found from the inverse Fourier transform as follows:

$$\begin{aligned}\mathbf{M}_A(t) &= \frac{1}{\sqrt{2\pi}}\int_{-\infty}^{\infty}\mathbf{M}_A(\omega)\exp(i\omega t)\,d\omega \qquad (3.42)\\ &= \frac{1}{\sqrt{2\pi}}\int_{-\infty}^{\infty}(\mathbf{M}_A(\omega)-\mathbf{M}_A^\infty)\exp(i\omega t)\,d\omega\\ &\qquad +\frac{1}{\sqrt{2\pi}}\int_{-\infty}^{\infty}\mathbf{M}_A^\infty\exp(i\omega t)\,d\omega\\ &= \frac{1}{\sqrt{2\pi}}\int_{-\infty}^{\infty}(\mathbf{M}_A(\omega)-\mathbf{M}_A^\infty)\exp(i\omega t)\,d\omega\\ &\qquad +\frac{1}{\sqrt{2\pi}}\mathbf{M}_A^\infty\boldsymbol{\delta}(t)\\ \mathbf{M}_A(t) &= \frac{1}{\sqrt{2\pi}}\int_{-\infty}^{\infty}(\mathbf{M}_A(\omega)-\mathbf{M}_A^\infty)\exp(i\omega t)\,d\omega\\ &\qquad +\frac{1}{\sqrt{2\pi}}\mathbf{M}_A^\infty. \qquad (3.43)\end{aligned}$$

Let us separate the convolution part of the impulse response from the constant infinite frequency contribution by defining:

$$\mathbf{M}_A^*(t) \triangleq \int_{-\infty}^{\infty}(\mathbf{M}_A(\omega)-\mathbf{M}_A^\infty)\exp(i\omega t)\,d\omega \tag{3.44}$$

$$\Rightarrow \mathbf{M}_A(t) = \frac{1}{\sqrt{2\pi}}\mathbf{M}_A^*(t) + \frac{1}{\sqrt{2\pi}}\mathbf{M}_A^\infty, \tag{3.45}$$

and to furthermore define the components of $\mathbf{M}_A^*(t)$ to be:

$$\mathbf{M}_A^*(t) = -\begin{bmatrix} X_{\dot{u}}^*(t) & X_{\dot{v}}^*(t) & X_{\dot{w}}^*(t) & X_{\dot{p}}^*(t) & X_{\dot{q}}^*(t) & X_{\dot{r}}^*(t) \\ Y_{\dot{u}}^*(t) & Y_{\dot{v}}^*(t) & Y_{\dot{w}}^*(t) & Y_{\dot{p}}^*(t) & Y_{\dot{q}}^*(t) & Y_{\dot{r}}^*(t) \\ Z_{\dot{u}}^*(t) & Z_{\dot{v}}^*(t) & Z_{\dot{w}}^*(t) & Z_{\dot{p}}^*(t) & Z_{\dot{q}}^*(t) & Z_{\dot{r}}^*(t) \\ K_{\dot{u}}^*(t) & K_{\dot{v}}^*(t) & K_{\dot{w}}^*(t) & K_{\dot{p}}^*(t) & K_{\dot{q}}^*(t) & K_{\dot{r}}^*(t) \\ M_{\dot{u}}^*(t) & M_{\dot{v}}^*(t) & M_{\dot{w}}^*(t) & M_{\dot{p}}^*(t) & M_{\dot{q}}^*(t) & M_{\dot{r}}^*(t) \\ N_{\dot{u}}^*(t) & N_{\dot{v}}^*(t) & N_{\dot{w}}^*(t) & N_{\dot{p}}^*(t) & N_{\dot{q}}^*(t) & N_{\dot{r}}^*(t) \end{bmatrix}. \quad (3.46)$$

The following properties are assumed:

Property 3.5 $\mathbf{M}_A^*(t)$ *is absolutely convergent.*

Property 3.6 $\mathbf{M}_A^\infty = (\mathbf{M}_A^\infty)^\top$. *This symmetry is shown in (Newman 1977, Journée and Massie 2001).*

Using the same approach as in Section 3.1.2, the symmetric components are applied, and the skew–symmetric portions are discarded by defining:

$$\mathbf{M}_A^*(t) \triangleq \frac{1}{2}\left(\mathbf{M}_A^*(t) + \mathbf{M}_A^*(t)^\top\right) + \frac{1}{2}\left(\mathbf{M}_A^*(t) - \mathbf{M}_A^*(t)^\top\right) \quad (3.47)$$

$$\bar{\mathbf{M}}_A^*(t) \triangleq \frac{1}{2}\left(\mathbf{M}_A^*(t) + \mathbf{M}_A^*(t)^\top\right) \quad (3.48)$$

$$\Rightarrow T_A = \frac{1}{2}\boldsymbol{\nu}^\top \mathbf{M}_A^\infty \boldsymbol{\nu} + \sqrt{\frac{\pi}{2}}\left(\boldsymbol{\nu}^\top * \bar{\mathbf{M}}_A^* * \boldsymbol{\nu}\right)(t) \quad (3.49)$$

The total kinetic energy is then

$$\begin{aligned} T &= T_{RB} + T_A \\ &= \frac{1}{2}\boldsymbol{\nu}^\top (\mathbf{M}_{RB} + \mathbf{M}_A^\infty)\boldsymbol{\nu} + \sqrt{\frac{\pi}{2}}\left(\boldsymbol{\nu}^\top * \bar{\mathbf{M}}_A^* * \boldsymbol{\nu}\right)(t). \end{aligned} \quad (3.50)$$

Whether this system is treatable using Kirchhoff's Equations must now be dealt with. As in Section 3.1, the fluid system is not holonomic. Equally so, the same reasoning holds and the system can be treated as if it were a conventional Lagrangian system. The system appears to have an explicit time–dependence, as the impulse response function for the added–mass is convolved with time. The momentum of the system is defined by:

$$\left(\bar{\mathbf{M}}_A^* * \boldsymbol{\nu}\right)(t) = \int_{-\infty}^{\infty} \bar{\mathbf{M}}_A^*(\tau)\,\boldsymbol{\nu}(t-\tau)\,d\tau, \quad (3.51)$$

and so the added–mass kernel does not appear as a function of time. Rather, the kinetic energy is a bilinear function of the body–fixed velocities, and so the time–invariance holds. The Kirchhoff equations can then be applied:

$$\boldsymbol{\tau}_{a1} = -\frac{d}{dt}\left(\frac{\partial T_A}{\partial \boldsymbol{\nu}_1}\right) - \mathbf{S}\left(\boldsymbol{\nu}_2\right)\frac{\partial T_A}{\partial \boldsymbol{\nu}_1} \tag{3.52}$$

$$\boldsymbol{\tau}_{a2} = -\frac{d}{dt}\left(\frac{\partial T_A}{\partial \boldsymbol{\nu}_2}\right) - \mathbf{S}\left(\boldsymbol{\nu}_2\right)\frac{\partial T_A}{\partial \boldsymbol{\nu}_2} - \mathbf{S}\left(\boldsymbol{\nu}_1\right)\frac{\partial T_A}{\partial \boldsymbol{\nu}_1}. \tag{3.53}$$

We first note the rule for differentiating convolutions:

$$\frac{d}{dt}\left(x * y\right)(t) = \left(\dot{x} * y\right)(t) = \left(x * \dot{y}\right)(t). \tag{3.54}$$

The inertial terms are then given by:

$$\frac{d}{dt}\left(\frac{\partial T_A}{\partial \boldsymbol{\nu}}\right) = \frac{d}{dt}\left(\frac{\partial}{\partial \boldsymbol{\nu}}\frac{1}{2}\boldsymbol{\nu}^\top \mathbf{M}_A^\infty \boldsymbol{\nu} + \frac{1}{2}\left(\boldsymbol{\nu}^\top * \bar{\mathbf{M}}_A^* * \boldsymbol{\nu}\right)(t)\right) \tag{3.55}$$

$$= \frac{d}{dt}\left(\left(\bar{\mathbf{M}}_A^* * \boldsymbol{\nu}\right)(t) + \mathbf{M}_A^\infty \boldsymbol{\nu}\right) \tag{3.56}$$

$$\frac{d}{dt}\left(\frac{\partial T_A}{\partial \boldsymbol{\nu}}\right) = \left(\bar{\mathbf{M}}_A^* * \dot{\boldsymbol{\nu}}\right)(t) + \mathbf{M}_A^\infty \dot{\boldsymbol{\nu}}. \tag{3.57}$$

An example derivation will be given first, before writing down the final structure of the equations of motion.

3.2.1 Derivation Example

Beginning with the matrix of added–mass coefficients:

$$\mathbf{M}_A\left(\omega\right) = -\begin{bmatrix} X_{\dot{u}}\left(\omega\right) & 0 & 0 & 0 \\ 0 & Y_{\dot{v}}\left(\omega\right) & Y_{\dot{p}}\left(\omega\right) & Y_{\dot{r}}\left(\omega\right) \\ 0 & K_{\dot{v}}\left(\omega\right) & K_{\dot{p}}\left(\omega\right) & K_{\dot{r}}\left(\omega\right) \\ 0 & N_{\dot{v}}\left(\omega\right) & N_{\dot{p}}\left(\omega\right) & N_{\dot{r}}\left(\omega\right) \end{bmatrix}, \tag{3.58}$$

the time domain equivalents are given by:

$$\mathbf{M}_A(t) = \sqrt{\frac{1}{2\pi}}\mathbf{M}_A^*(t) + \sqrt{\frac{1}{2\pi}}\mathbf{M}_A^\infty \tag{3.59}$$

$$\mathbf{M}_A^*(t) = -\begin{bmatrix} X_{\dot{u}}^*(t) & 0 & 0 & 0 \\ 0 & Y_{\dot{v}}^*(t) & Y_{\dot{p}}^*(t) & Y_{\dot{r}}^*(t) \\ 0 & K_{\dot{v}}^*(t) & K_{\dot{p}}^*(t) & K_{\dot{r}}^*(t) \\ 0 & N_{\dot{v}}^*(t) & N_{\dot{p}}^*(t) & N_{\dot{r}}^*(t) \end{bmatrix} \tag{3.60}$$

$$\mathbf{M}_A^\infty = -\begin{bmatrix} X_{\dot{u}}^\infty & 0 & 0 & 0 \\ 0 & Y_{\dot{v}}^\infty & Y_{\dot{p}}^\infty & Y_{\dot{r}}^\infty \\ 0 & K_{\dot{v}}^\infty & K_{\dot{p}}^\infty & K_{\dot{r}}^\infty \\ 0 & N_{\dot{v}}^\infty & N_{\dot{p}}^\infty & N_{\dot{r}}^\infty \end{bmatrix} \tag{3.61}$$

$$\bar{\mathbf{M}}_A^*(t) = \frac{1}{2}\left(\mathbf{M}_A^*(t) + \mathbf{M}_A^*(t)^\top\right). \tag{3.62}$$

Since surge is decoupled from other modes; the simplest part to analyse is the inertial force in surge, and the Coriolis–centripetal force in sway. The added–mass force acting on the rigid body in surge is:

$$\begin{aligned} X_i &= -\frac{d}{dt}\frac{\partial}{\partial u}T_A \qquad (3.63)\\ &= -\frac{d}{dt}\frac{\partial}{\partial u}\left(-\frac{1}{2}\left(u * X_{\dot{u}}^* * u\right)(t) - \frac{1}{2}X_{\dot{u}}^\infty u^2\right) \\ &= \frac{d}{dt}\left(\frac{1}{2}\left(X_{\dot{u}}^* * u\right)(t) + \frac{1}{2}\left(u * X_{\dot{u}}^*\right)(t) + X_{\dot{u}}^\infty u\right) \\ &= \frac{d}{dt}\left(\left(X_{\dot{u}}^* * u\right)(t) + X_{\dot{u}}^\infty u\right) \\ X_i &= \left(X_{\dot{u}}^* * \dot{u}\right)(t) + X_{\dot{u}}^\infty \dot{u}. \qquad (3.64) \end{aligned}$$

The Coriolis–centripetal force in sway is given by:

$$\begin{aligned} Y_c &= -r\frac{\partial}{\partial u}T_A \qquad (3.65)\\ &= \left(X_{\dot{u}}^* * u\right)(t)\, r + X_{\dot{u}}^\infty u r. \qquad (3.66) \end{aligned}$$

Equations (3.64) and (3.66) can be examined at two important limiting cases; at infinite and at zero (low) frequency. The behaviour in these two cases should be consistent with what is expected. At high frequency, we should expect the entire behaviour to be governed by the infinite frequency

behaviour. At low frequency, the behaviour out to replicate that derived in Section 3.1.

High–Frequency To describe the high–frequency behaviour, take equation (3.66). We set $u = u_0 \cos(\omega t)$, and take the limiting case as $\omega \to \infty$:

$$Y_c = r \lim_{\omega \to \infty} \int_{-\infty}^{\infty} X_{\dot{u}}^*(t-\tau)\, u(\tau)\, d\tau + X_{\dot{u}}^{\infty} ur \tag{3.67}$$

$$= r u_0 . \lim_{\omega \to \infty} \int_{-\infty}^{\infty} X_{\dot{u}}^*(t-\tau) \cos(\omega\tau)\, d\tau + X_{\dot{u}}^{\infty} ur. \tag{3.68}$$

Since the components of $\bar{\mathbf{M}}_A^*(t)$ are absolutely convergent by assumption, we can apply the Riemann–Lebesgue Lemma (Gradshteyn and Ryzhik 2000), giving the following:

$$\lim_{\omega \to \infty} \int_{-\infty}^{\infty} X_{\dot{u}}^*(t-\tau) \cos(\omega\tau)\, d\tau = 0. \tag{3.69}$$

The Coriolis–centripetal force in sway at infinite frequency is given by

$$Y_c = (X_{\dot{u}}^* * u)(t)\, r + X_{\dot{u}}^{\infty} ur \tag{3.70}$$

$$= X_{\dot{u}}^{\infty} ur, \tag{3.71}$$

and so the high–frequency behaviour is consistent.

Low–frequency At low–frequency, the inertial surge behaviour is governed by:

$$u_0 . \lim_{\omega \to 0} \int_{-\infty}^{\infty} X_{\dot{u}}^*(t-\tau) \cos(\omega\tau)\, d\tau \tag{3.72}$$

$$\simeq u_0 . \lim_{\omega \to 0} \int_{-\infty}^{\infty} X_{\dot{u}}^*(t-\tau)\, d\tau \tag{3.73}$$

$$= u_0 \int_{-\infty}^{\infty} X_{\dot{u}}^*(\tau)\, d\tau. \tag{3.74}$$

This integral is the final value of the step response of $X_{\dot{u}}^*(\tau)$, which is given by:

$$\int_{-\infty}^{\infty} X_{\dot{u}}^*(\tau)\, d\tau = X_{\dot{u}}^0 - X_{\dot{u}}^{\infty}, \tag{3.75}$$

which gives the Coriolis–centripetal force:

$$\begin{aligned} Y_c &= \left(X^*_{\dot{u}} * u\right)(t)\, r + X^{\infty}_{\dot{u}} ur && (3.76)\\ &= \left(X^0_{\dot{u}} - X^{\infty}_{\dot{u}}\right) ur + X^{\infty}_{\dot{u}} ur && (3.77)\\ Y_c &= X^0_{\dot{u}} ur. && (3.78) \end{aligned}$$

Arbitrary Frequency The surge equation is now analysed at an arbitrary frequency to investigate whether standard behaviour can be replicated.

The inertial force in surge can be described as:

$$\begin{aligned} \left(m - X^{\infty}_{\dot{u}}\right)\dot{u} - \left(X^*_{\dot{u}} * \dot{u}\right)(t) &= X_i && (3.79)\\ \mathcal{F}[\left(m - X^{\infty}_{\dot{u}}\right)\dot{u} - \left(X^*_{\dot{u}} * \dot{u}\right)(t)] &= \mathcal{F}[X_i] && (3.80)\\ \left(m - X^{\infty}_{\dot{u}}\right)\dot{u}(\omega) - \left(X_{\dot{u}}(\omega) - X^{\infty}_{\dot{u}}\right)\dot{u}(\omega) &= X_i(\omega) && (3.81)\\ \left(m - X_{\dot{u}}(\omega)\right)\dot{u}(\omega) &= X_i(\omega), && (3.82) \end{aligned}$$

where the relation

$$\begin{aligned} \mathcal{F}[\left(X^*_{\dot{u}} * \dot{u}\right)(t)] &= \sqrt{2\pi}\mathcal{F}[\left(X^*_{\dot{u}}\right)(t)]\mathcal{F}[\dot{u}(t)] && (3.83)\\ &= \left(X_{\dot{u}}(\omega) - X^{\infty}_{\dot{u}}\right)\dot{u}(\omega) && (3.84) \end{aligned}$$

has been applied.

These examples demonstrate that the new formulation corresponds correctly with known cases.

3.2.2 4–DOF Solution

The solution for the Coriolis–centripetal forces in four degrees of freedom is:

$$\begin{aligned} X_c &= -\left(Y_{\dot{v}} * v\right)(t)\, r - \left(Y_{\dot{p}} * p\right)(t)\, r - \left(Y_{\dot{r}} * r\right)(t)\, r \\ &\quad - Y^{\infty}_{\dot{v}} vr - \frac{1}{2}\left(Y^{\infty}_{\dot{p}} + K^{\infty}_{\dot{v}}\right) pr - \frac{1}{2}\left(N^{\infty}_{\dot{v}} + Y^{\infty}_{\dot{r}}\right) r^2 && (3.85)\\ Y_c &= X^{\infty}_{\dot{u}} ur + \left(X^*_{\dot{u}} * u\right)(t)\, r && (3.86)\\ K_c &= 0 && (3.87)\\ N_c &= -\left(X_{\dot{u}} * u\right)(t)\, v + \left(Y_{\dot{v}} * v\right)(t)\, u + \left(Y_{\dot{p}} * p\right)(t)\, u + \left(Y_{\dot{r}} * r\right)(t)\, u \\ &\quad + \left(Y^{\infty}_{\dot{v}} - X^{\infty}_{\dot{u}}\right) uv + \frac{1}{2}\left(Y^{\infty}_{\dot{p}} + K^{\infty}_{\dot{v}}\right) pu + \frac{1}{2}\left(Y^{\infty}_{\dot{r}} + N^{\infty}_{\dot{v}}\right) ru. && (3.88) \end{aligned}$$

In matrix form these are:

$$\mathbf{C}_A^{\infty}(\boldsymbol{\nu}) = \begin{bmatrix} 0 & 0 \\ 0 & 0 \\ 0 & 0 \\ -Y_{\dot{v}}^{\infty} v - \frac{1}{2}\left(N_{\dot{v}}^{\infty} + Y_{\dot{r}}^{\infty}\right) r & \\ -\frac{1}{2}\left(Y_{\dot{p}}^{\infty} + K_{\dot{v}}^{\infty}\right) p & X_{\dot{u}}^{\infty} u \end{bmatrix} \begin{bmatrix} 0 & Y_{\dot{v}}^{\infty} v + \frac{1}{2}\left(N_{\dot{v}}^{\infty} + Y_{\dot{r}}^{\infty}\right) r \\ & + \frac{1}{2}\left(Y_{\dot{p}}^{\infty} + K_{\dot{v}}^{\infty}\right) p \\ 0 & -X_{\dot{u}}^{\infty} u \\ 0 & 0 \\ 0 & 0 \end{bmatrix} \tag{3.89}$$

$$\mathbf{C}_A^{*}(\boldsymbol{\nu}) = \begin{bmatrix} 0 & 0 \\ 0 & 0 \\ 0 & 0 \\ -\left(Y_{\dot{v}} * v\right)(t) & \\ -\left(Y_{\dot{p}} * p\right)(t) & \left(X_{\dot{u}}^{*} * u\right)(t) \\ -\left(Y_{\dot{r}} * r\right)(t) & \end{bmatrix} \begin{bmatrix} 0 & \left(Y_{\dot{v}} * v\right)(t) + \left(Y_{\dot{p}} * p\right)(t) \\ & + \left(Y_{\dot{r}} * r\right)(t) \\ 0 & -\left(X_{\dot{u}}^{*} * u\right)(t) \\ 0 & 0 \\ 0 & 0 \end{bmatrix}. \tag{3.90}$$

Note that both are skew–symmetric, and possess a very familiar form. The difference is that the matrix shown in (3.90) has convolution integrals in place of static multiplications. The final form for the model is then:

$$\dot{\boldsymbol{\eta}} = \mathbf{J}(\boldsymbol{\theta})\,\boldsymbol{\nu} \tag{3.91}$$

$$\mathbf{M}\dot{\boldsymbol{\nu}} + \left(\bar{\mathbf{M}}_A^{*} * \dot{\boldsymbol{\nu}}\right)(t) + \mathbf{C}(\boldsymbol{\nu})\,\boldsymbol{\nu} = \boldsymbol{\tau}^{b}, \tag{3.92}$$

where $\mathbf{M} = \mathbf{M}_{RB} + \mathbf{M}_A^{\infty}$ and $\mathbf{C}(\boldsymbol{\nu}) = \mathbf{C}_{RB}(\boldsymbol{\nu}) + \mathbf{C}_A^{\infty}(\boldsymbol{\nu}) + \mathbf{C}_A^{*}(\boldsymbol{\nu})$. At low frequency, these equations match (3.26)–(3.27). At high frequency they behave solely according to the infinite frequency behaviour.

The full six DOF matrices of the this model are given in Appendix B.3.

Note that the equations are not trivially implementable, as $\dot{\boldsymbol{\nu}}$ appears inside of a convolution integral. However, it is easily recognisable that

$$\left(\bar{\mathbf{M}}_A^{*} * \dot{\boldsymbol{\nu}}\right)(t) \equiv \left(\dot{\bar{\mathbf{M}}}_A^{*} * \boldsymbol{\nu}\right)(t), \tag{3.93}$$

and so an equivalent formulation is:

$$\dot{\boldsymbol{\eta}} = \mathbf{J}(\boldsymbol{\theta})\boldsymbol{\nu} \tag{3.94}$$

$$\mathbf{M}\dot{\boldsymbol{\nu}} + \left(\dot{\tilde{\mathbf{M}}}_A^* * \boldsymbol{\nu}\right)(t) + \mathbf{C}(\boldsymbol{\nu})\boldsymbol{\nu} = \boldsymbol{\tau}^b. \tag{3.95}$$

3.2.3 Dynamic Properties

Property 3.7 $\mathbf{M} = \mathbf{M}^\top > 0$.

Property 3.8 $\dot{\mathbf{M}} = \mathbf{0}$.

Property 3.9 $\mathbf{C}(\boldsymbol{\nu}) = -\mathbf{C}(\boldsymbol{\nu})^\top$.

Proof. This property is independent of the actual formulation of the kinetic energy, and so its proof is identical to that given in Section 2.2.2. ■

Property 3.10 $\boldsymbol{\nu}^\top \left(\dot{\mathbf{M}} - 2\mathbf{C}(\boldsymbol{\nu})\right)\boldsymbol{\nu} = 0$.

Proof. This proof is identical to that given in Section 2.2.2. ■

3.3 Added "Mass" and "Destabilising" Coriolis–centripetal Forces

It is worthwhile to take a few sentences to clarify the behaviour of the equations of motion as formulated up to this point. The added–mass is purely a pressure–induced force that arises proportional to the accelerations of the ship. So in this sense it behaves in a like manner to conventional rigid body mass; its energy content is an inherent part of the equations of motion. That said, it certainly cannot be a mass of water that moves *with* the ship, as the term might be interpreted to suggest. This idea is obviously not true on at least three counts.

Firstly, it cannot be true since the *whole* fluid moves, to some degree, as the ship moves through it.

Secondly, the added mass is different, in general, for each degree of freedom. If there were a mass of water *attached* to the ship, then this mass would apply equally in surge, sway and heave. In a rigid body setting, the notion of an object weighing a certain amount if pushed in one direction, yet another amount if pushed in a different direction is entirely ridiculous. The fact that it *is* the case for added mass demonstrates that it is not a true mass of water.

Thirdly, by Newton's First Law, a body in constant straight line motion will continue in this state unless an external unbalanced force acts upon it.

Let us take the case of low–frequency surge, sway and yaw motion. For simplicity's sake, we have assumed a diagonal mass and added–mass, and neglect damping entirely. This example allows us to look solely at the low frequency added mass and Coriolis–centripetal terms which arise, without altering any of the fundamental properties of the system.

$$\begin{aligned}
\left(m - X^0_{\dot{u}}\right)\dot{u} + \left(Y^0_{\dot{v}} - m\right)vr &= X && (3.96)\\
\left(m - Y_{\dot{v}}\right)\dot{v} + \left(m - X^0_{\dot{u}}\right)ur &= Y && (3.97)\\
\underbrace{\left(I_z - N^0_{\dot{r}}\right)\dot{r}}_{\text{inertial}} - \underbrace{\left(Y^0_{\dot{v}} - X^0_{\dot{u}}\right)uv}_{\text{Coriolis–centripetal}} &= N. && (3.98)
\end{aligned}$$

If the body begins in steady motion, then $\dot{\boldsymbol{\nu}} = \mathbf{0}$. Milne-Thomson (1968) described some motions in this manner in Chapter 18. He used the term *directions of permanent translation* to denote those directions in which a body will continue to travel uniformly, in the sense of Newton's First Law. At $t = t_0$, in an unforced condition, we have:

$$\dot{r} = \frac{1}{\left(I_z - N^0_{\dot{r}}\right)} \underbrace{\left(Y^0_{\dot{v}} - X^0_{\dot{u}}\right)uv}_{\text{Munk moment}}. \tag{3.99}$$

This yaw moment is called the Munk moment (Munk 1936). It arises solely from the Coriolis–centripetal effects of the added–mass. Note that the only two directions of permanent translation are firstly when $u \neq 0$ and $v \equiv 0$, and secondly when $u \equiv 0$ and $v \neq 0$: uniform surge motion and uniform sway motion respectively. For all other steady motions, even though no external unbalanced force acts on the ship, a rotation is induced. If the added mass *were* a mass, it would violate Newton's First Law (one must note that the added mass force *is* an unbalanced external force). For the case of any mass, *every* potential direction is a direction of permanent translation.

A special case exists for the case when the body in question is circular about the z–axis, for example a cylinder or sphere. In this case, since $X_{\dot{u}} \equiv Y_{\dot{v}}$, every direction is also direction of permanent translation. For every other shape, hence all ships, there are only two.

A simulation of the equations of motion given in (3.96)–(3.98) is shown in Figure 3.1. The parameters were arbitrarily set to:

Parameter	Value
m	$100\,\mathrm{kg}$
$X^0_{\dot{u}}$	$-10\,\mathrm{kg}$
$Y^0_{\dot{v}}$	$-100\,\mathrm{kg}$
I_z	$1000\,\mathrm{kg.\,m^2}$
$N_{\dot{r}}$	$-1000\,\mathrm{kg.\,m^2}$
u_0	$2\,\mathrm{m/\,s}$
v_0	$2\,\mathrm{m/\,s}$
r_0	$0\,\mathrm{rad/\,s}$

Parameters used in Figure 3.1

Note the stable periodic motion of the body. Note also that the kinetic energy is constant over the whole simulation. The notion that the Munk–moment is destabilising is imprecise and confusing. It is certainly not destabilising in the sense of an uncontrolled growth of energy; it has precisely no influence whatsoever on the energy of the system.

It is often written that the Munk–moment impels a ship to a perpendicular orientation toward the flow. This sentiment contains some truth but is not wholly correct. The pure, isolated effect of the Munk–moment is shown in Figure 3.1, and it cannot be reasoned that the body moves towards a perpendicular orientation. Neither $(u, v) = (0, v_0)$ nor $(u, v) = (u_0, 0)$ are asymptotically stable equilibrium points. Any disturbance will remain and will not decay. What *is* true is that a small deviation in sideslip from either $(u, v) = (u_0, 0)$ or $(u, v) = (0, v_0)$ will periodically grow and decay. It is in this sense that the Munk–moment is destabilising. The body will always be stable within some neighbourhood whose size is governed by the unchanging kinetic energy of the system.

3.4 Structure of the Equations of Motion

The emphasis in this chapter has been on deriving the behaviour of the added–mass in the body–fixed frame. The equations of motion described in Section 3.2 are more complex than is usual. The derivation has led to a situation in which the added–mass and also the Coriolis–centripetal forces are modelled by convolution integrals. This formulations contrasts heavily with others, in which there is typically a single convolution integral describing a mixture of potential damping and inertial behaviour (Cummins 1962, Ogilvie 1964, Bailey *et al.* 1997, Fossen 2005).

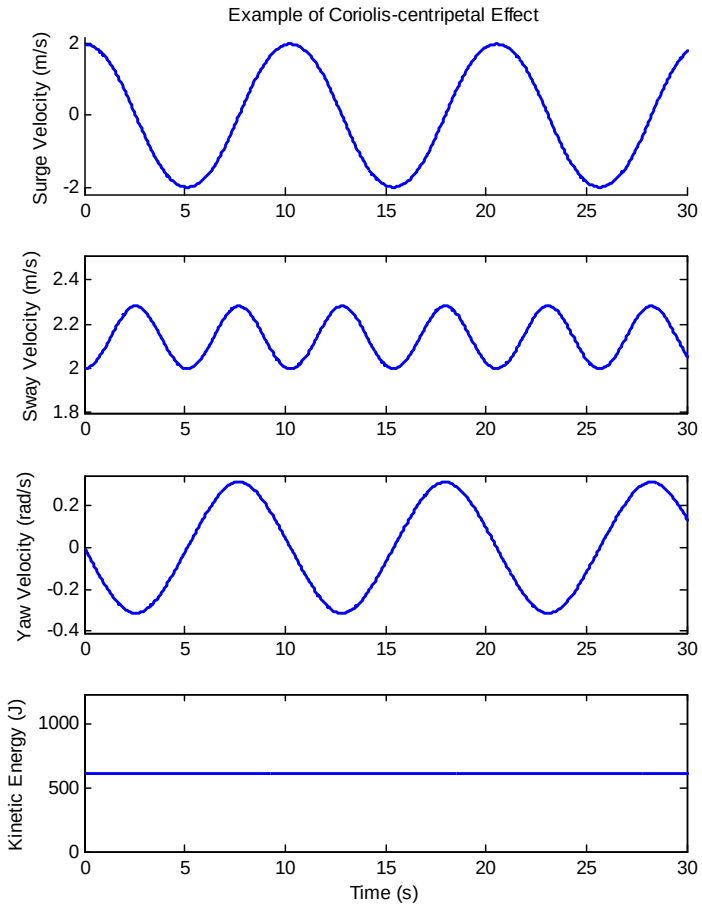

Figure 3.1: The effects of Coriolis–centripetal Forces on an arbitrary body.

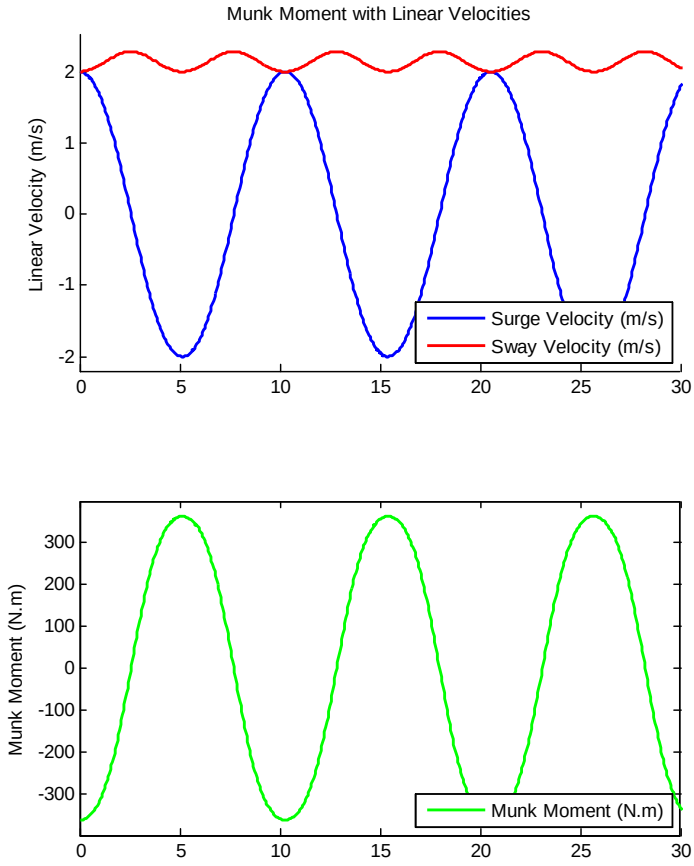

Figure 3.2: The linear velocities and the Munk–moment arising from these.

Although control theory is usually applied to a simplified model–structure, it is claimed here that the formulations in this chapter are more suitable, even though they are more complex. Taking cue from the work of Sørensen (Sørensen 2005*a*, Sørensen 2005*b*, Smogeli 2006, Refsnes 2008), the suitable way to model a system is to design both a process plant model (PPM) and a control plant model (CPM). The first of these is an accurate model designed for simulation and testing, while the second is a simplified structure that is suitable for tasks like control and observer design. These designs are then tested using the PPM. The claim that the new equations of motion are suited for control system design ought to give rise to suspicion, and requires justification.

The basis for a large portion of control theory is Lyapunov analysis (e.g. Khalil 2002, Krstic *et al.* 1995, Slotine and Li 1991). Such analysis will typically begin by specifying a Lyapunov function closely related to the kinetic energy, if not the kinetic energy itself. Passivity theory (e.g. van der Schaft 1999, Egeland and Gravdahl 2002) is itself a fundamentally energy inspired field. Ortega *et al.* (2001) describe it as an "energy shaping approach", describing the control methodology thusly:

> The control problem can then be recast as finding a dynamical system and an interconnection pattern such that the overall energy function takes the desired form.

If the energy is concealed within a mixed mass–damping convolution integral, then there is no clear total energy function. It is unclear if such an analysis outlined by Ortega is even possible. If the energy were to be calculated using solely $1/2\boldsymbol{\nu}^\top \mathbf{M}_A^\infty \boldsymbol{\nu}$, a crucial error would be made, as this contradicts both equations (3.39) and (3.50), which both describes the energy correctly. Any analysis based on this would be misguided.

There are therefore three approaches which ought to be avoided, for the reasons given so far in this chapter.

1. Grouping the Coriolis–centripetal terms within the damping matrix, as is typical in the low–frequency model. This grouping can often be seen written as $\mathbf{N}(\boldsymbol{\nu}) = \mathbf{C}(\boldsymbol{\nu}) + \mathbf{D}(\boldsymbol{\nu})$. In this approach the skew–symmetry of the $\mathbf{C}(\boldsymbol{\nu})$ matrix is concealed, and therefore unexploitable. Controllers.

2. If the Coriolis–centripetal forces are linearised, their skew–symmetry is broken, violating a fundamental property of those forces: that they perform no work on the system.

3. Grouping the added–mass convolution inside a mixed potential damping–inertia convolution. Again, by hiding energy, this at the very least hampers any approach related to energy shaping or balance. Methods built around approximations will then typically be more conservative than necessary.

Chapter 4

Forces

There are a multitude of physical processes that act on a manoeuvring ship. An outline of the various forces is given here.

Inertial Pressure Forces Typically called *added mass*, these are pressure forces that act in proportion to acceleration through the fluid. These forces have been comprehensively dealt with in Chapter 3.

Potential Damping Similarly, these are pressure generated damping forces. They are also typically referred to as *pressure*, *profile or form* drag. Essentially, as a body passes through a fluid, pressure increases in front of this motion, and decreases behind, giving a net force which opposes motion.

Friction This is a damping force which is generated as the viscous fluid interacts with the hull as it passes underneath and around it, e.g. skin friction.

Vortex Shedding This is commonly referred to as *interference drag*. It arises due to the shedding of vortex sheets at sharp edges.

Lifting Forces Hydrodynamic lift forces arise from two physical mechanisms. The first is due to the linear circulation of water around the hull. The second is a nonlinear effect, commonly called cross–flow drag, which acts from a momentum transfer from the body to the fluid. This secondary effect is closely linked to vortex shedding.

Restoring Forces These forces arise from buoyancy, which is a result of the displacement of the water around the ship. The force due to gravity is conventionally grouped alongside these forces.

Current Forces The ship's body–fixed velocity is generally defined relative to the fixed seafloor. The sea itself also moves relative to this fixed point, and the differences between them arise as current forces.

Control Forces These forces are from control surfaces such as rudders, fins or interceptors, and propulsive forces such as from a propeller or waterjet

Wind Forces Wind is defined as the rough motion of air over the Earth's surface. This motion induces considerable forces on the superstructure of a manoeuvring ship.

The methods by which the hydrodynamic forces may be modelled are various. They range from a purely mathematical approach, through to a purely empirical approach, through to a purely computational approach. Each has its merits and none is without its weaknesses. This thesis combines the first with the second. The equations of motion are derived analytically, while the actions of the other forces are dealt with using a combination of mathematics and empiricism.

Of the forces listed above, this thesis contemplates the first six, and neglects the last three. As a qualifier on this statement, although potential damping is contemplated, it is done so in a limited way. The potential damping in calm water is dealt with, but not the damping in waves. Although the current forces are ignored, they can be included as relative velocities (Fossen 2002*a*, Refsnes 2008).

The organisation of this chapter is as follows:

1. The structure of the circulatory lift and drag forces acting on a ship are derived.
2. The crossflow principle is applied to explain the effects of nonlinear lift and drag.
3. The effects of roll on circulation are derived, appearing as additional circulatory lift and drag.
4. An empirical roll model is added.

4.1 Damping Forces

Damping forces constitute the most awkward and ill–defined of the forces acting on a ship. The drive of the rest of this chapter is to arrive at a

model *structure* which can best describe the damping forces acting on a vessel. The goal is not to arrive at numbers for this structure, but rather to find a firm physical footing upon which experimental data might rest. This marks a definite divergence from the approach to this point. This change in methodology needs some justification.

For a body moving along the free surface of a fluid, we can generally write a generic force as:

$$F = \frac{1}{2}\rho U^2 S C_F,$$

where F is the force; ρ is the fluid density; S is the wetted surface area; and C_F is a non–dimensional coefficient. Although of a simple form, this equation is deceptive:

Wetted Surface The wetted surface varies with the velocity of the ship. The wave profile along the vessel is heavily dependent on forward speed, the mass distribution and the geometry of the vessel. This value then cannot be taken to be constant across the speed range.

Speed In a manoeuvring ship, the speed U varies across the length of the body. For surge, sway and yaw, the local speed is given by $U(x) = \sqrt{u^2 + (v + xr)^2}$. It is inappropriate to use only the speed at a single location.

Force Coefficient The coefficient is *itself* an unknown function of other non–dimensional parameters, such as the Reynold's Number, Froude Number, or sideslip angle.

The indeterminacy of all of these makes the modelling of damping exceedingly difficult. It is for this reason that the drive is to arrive at the structure itself, rather than specific numbers. Given this approach, two key approaches guide the following work:

- The linear superposition of damping forces on top of the equations of motion is valid. This means that lift, drag, crossflow drag as well as other forces can be investigated independently. Each investigation then gives an additional set of terms to be included as forces acting on the right hand side of the equations of motion.

- Deriving the structure of the forces is sufficient. This is done with the intention of using experiment to enumerate this derived structure.

The rest of this chapter will deal with lift and drag forces in four degrees of freedom: surge, sway, roll, and yaw. These are of most importance in manoeuvring ships, and the other degrees of freedom can typically be neglected (Blanke 1981).

4.2 Circulatory Lift and Drag

A ship can be modelled as a low aspect ratio wing (Blanke 1981, Hooft 1994, Leite *et al.* 1998). Note that the discussion of lift and drag here entail forces in the horizontal plane, and do not refer to lifting in the sense of lifting a body out of the water (e.g. Faltinsen 2006*a*).

The lift and drag can be characterised by two coefficients: namely the lift and drag coefficient respectively.

These forces act in the flow axes: the former acting perpendicular to the direction of motion, and the latter acting parallel and directly opposite to the direction of motion. The forces from these can be written as:

$$L = \frac{1}{2}\rho U^2 S C_L(\beta, \mathrm{Re}) \tag{4.1}$$

$$D = \frac{1}{2}\rho U^2 S C_D(\beta, \mathrm{Re}), \tag{4.2}$$

where L is lift, D is drag, ρ is the water density, U is the total speed, S is a characteristic area such as L_{pp}^2, C_L is the nondimensional lift coefficient, C_D is the nondimensional drag coefficient, β is the sideslip angle, and finally Re is the Reynold's number.

Since these forces are resolved in the flow axes, they must be converted to the body fixed frame before being added. This is done using the transformation:

$$\begin{bmatrix} X_{LD} \\ Y_{LD} \end{bmatrix} = \begin{bmatrix} -\cos\beta & \sin\beta \\ -\sin\beta & -\cos\beta \end{bmatrix} \begin{bmatrix} D \\ L \end{bmatrix}. \tag{4.3}$$

The lift and drag forces, and the sideslip angle, β, are depicted in Figure 4.1.

The moments arising from lift and drag are then derived as:

$$\begin{bmatrix} K_{LD} \\ N_{LD} \end{bmatrix} = \begin{bmatrix} z_{cp} \\ x_{cp} \end{bmatrix} .Y_{LD}, \tag{4.4}$$

where (x_{cp}, z_{cp}) defines the location of the centre of pressure.

The approach taken within this chapter is to formulate the local lift and drag forces: the speed is local: $U(x) = \sqrt{u^2 + (v + xr)^2}$. Note that

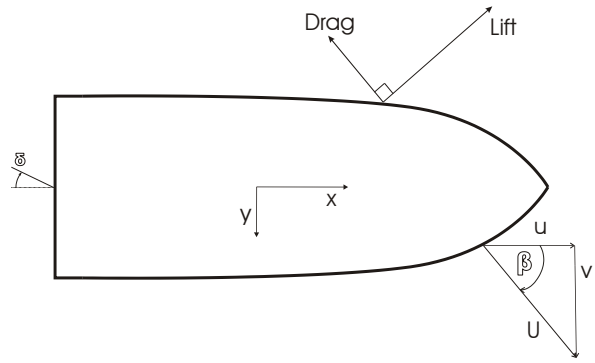

Figure 4.1: Lift and Drag Forces on a Ship

this local speed is also used in the calculation of the sideslip angles. It is elementary to show that $\beta = \arctan v/u = \arccos u/U = \arcsin v/U$. The localised lift and drag is then integrated over the length of the ship to give the structure for a set of three–dimensional coefficients.

4.2.1 Lift

The lift coefficient is modelled as proportional to the sine of the sideslip angle (Lewis 1989*b*):

$$C_L = C_{L\beta} \sin \beta, \tag{4.5}$$

where $C_{L\beta}$ is a constant of proportionality.

Treating this force as a function of longitudinal position, i.e. applying the local speed $U(x) = \sqrt{u^2 + (v + xr)^2}$ gives us:

$$\begin{aligned} C_L(x) &= C_{L\beta} \sin \beta(x) && (4.6) \\ &= C_{L\beta} \frac{v + xr}{U(x)}. && (4.7) \end{aligned}$$

Applying this to the lift equation given by (4.1) then gives:

$$\begin{aligned} L(x) &= \frac{1}{2} \rho U(x)^2 S C_L(x) && (4.8) \\ &= \frac{1}{2} \rho U(x) S C_{L\beta} (v + xr). && (4.9) \end{aligned}$$

This lift force is then resolved in the longitudinal direction, using equation (4.3) as:

$$\begin{aligned} X_L(x) &= L(x)\sin\beta(x) && (4.10)\\ &= L(x)\frac{v}{U(x)} \\ &= \frac{1}{2}\rho S C_{L\beta}(v+xr)^2. && (4.11)\end{aligned}$$

If this is integrated this over the length of the ship, the total longitudinal force is:

$$X_L = X_{vv}v^2 + X_{rv}rv + X_{rr}r^2 \tag{4.12}$$

Similarly, the lift force resolved in the transverse direction can be calculated as:

$$\begin{aligned} Y_L(x) &= -L(x)\cos\beta(x) && (4.13)\\ &= -L(x)\frac{u}{U(x)} \\ &= -\frac{1}{2}\rho S C_{L\beta}(uv+uxr) && (4.14)\end{aligned}$$

Integrating over the length then gives:

$$Y_L = Y_{uv}uv + Y_{ur}ur \tag{4.15}$$

4.2.2 Drag

A drag force acts precisely in opposition to the motion of the ship. As such, it is a purely dissipative term. There are several ways in which drag forces may be modelled. Linear modelling is necessary and sufficient at very low speeds, whereas at medium to high speed operation, higher order terms become necessary.

The drag coefficient is conventionally modelled as a quadratic function of sideslip, with a zero angle drag coefficient (Hoerner and Borst 1975) as:

$$C_D = C_{D0} + C_{D\beta\beta}\sin^2\beta, \tag{4.16}$$

where C_{D0} is a dimensionless drag coefficient at 0° angle of sideslip, and $C_{D\beta\beta}$ describes the induced drag proportional to $\sin^2\beta$. In pure surge motion (i.e. without sideslip), the drag force arising from C_{D0} can be

considered to be the same as the ITTC drag formula (Lewis 1989*a*):

$$X_{ITTC} = -\frac{1}{2}\rho S\left(1+k\right)\left(C_f+\Delta C_f\right)|u|\,u \tag{4.17}$$

$$\Rightarrow C_{D0} \equiv \left(1+k\right)\left(C_f+\Delta C_f\right), \tag{4.18}$$

where k is a correction term that can be set according to Hoerner (1965), S is the wetted surface area, C_f is the flat plate friction from the ITTC–1957 line, and ΔC_f is a hull roughness parameter.

The structure that the drag coefficient takes from this point forward is similar to that in equation (4.16), with a term that we propose acts linearly with the total speed, U (which agrees with the results seen in Berg and Utnes 1978, Skjetne *et al.* 2004, Ayaz *et al.* 2006). Sectionally, the drag coefficient is then given by:

$$C_D\left(x\right) = C_{D0} + C_{DU}U\left(x\right) + C_{D\beta\beta}\sin^2\beta\left(x\right) \tag{4.19}$$

$$= C_{D0} + C_{DU}U\left(x\right) + C_{D\beta\beta}\left(\frac{v+xr}{U\left(x\right)}\right)^2. \tag{4.20}$$

This is a slight abuse of notation, as the equation is seemingly no longer dimensionally correct. The drag coefficient C_{DU} actually varies linearly with the *Reynold's number*, but we do not include the constant length and viscosity for brevity: these are hidden within C_{DU}, which has dimensions TIME/LENGTH. The sectional drag force is then:

$$D\left(x\right) = \frac{1}{2}\rho SU\left(x\right)^2 C_D\left(\mathrm{Re},\beta\right) \tag{4.21}$$

$$= \frac{1}{2}\rho SU\left(x\right)^2\left(C_{D0} + C_{DU}U\left(x\right) + C_{D\beta\beta}\left(\frac{v+xr}{U\left(x\right)}\right)^2\right)$$

$$= \frac{1}{2}\rho S\left(U\left(x\right)^2 C_{D0} + U\left(x\right)^3 C_{DU} + C_{D\beta\beta}\left(v+xr\right)^2\right) \tag{4.22}$$

This force acts in the longitudinal direction as:

$$\begin{aligned} X_D(x) &= -D(x)\cos\beta(x) \qquad (4.23)\\ &= -D(x)\frac{u}{U(x)}\\ &= -\frac{1}{2}\rho S\left(C_{D0}U(x)u + U(x)^2 uC_{Du} + C_{D\beta\beta}\frac{u}{U(x)}(v+xr)^2\right)\\ &\cong -\frac{1}{2}\rho S\left(\begin{array}{c} C_{D0}u^2 + C_{DU}u^3 + C_{DU}uv^2 + C_{DU}ux^2r^2\\ +2C_{DU}xrvu + C_{D\beta\beta}\left(v^2 + x^2r^2 + 2xvr\right)\end{array}\right)\\ \Rightarrow X_D &= X_{uu}u^2 + X_{uuu}u^3 + X_{vv}v^2 + X_{rr}r^2 + X_{vr}vr + X_{uvv}uv^2\\ &\quad +X_{rvu}rvu + X_{urr}ur^2. \qquad (4.24)\end{aligned}$$

In the sway direction, this force is resolved as:

$$\begin{aligned} Y_D(x) &= -D(x)\sin\beta(x)\\ &= -D(x)\frac{v+xr}{U(x)}\\ &= -\frac{1}{2}\rho S\left(\begin{array}{c} C_{D0}(uv+uxr) + U(x)^2 C_{DU}(v+xr)\\ +C_{D\beta\beta}\frac{1}{U(x)}(v+xr)^3\end{array}\right) \qquad (4.25)\end{aligned}$$

Since for most high speed manoeuvring problems $U(x) \gg (v+xr)^3$, which is equivalent to the assumption of a small angle of sideslip, we discard the terms corresponding to $C_{D\beta\beta}$. The assumption is reasonably good for slow speed, high β operation too, since the sideforce will be dominated by the lower order terms, such as $C_{D0}uv$. Under the stated assumption, the sectional sideforce is then:

$$\begin{aligned} Y_D(x) &\cong -\frac{1}{2}\rho S\left(C_{D0}(uv+uxr)\right.\\ &\quad \left.+C_{DU}\left(u^2xr + u^2v + (v+xr)^3\right)\right) \qquad (4.26)\\ \Rightarrow Y_D &= Y_{uv}uv + Y_{ur}ur + Y_{uur}u^2r + Y_{uuv}u^2v + Y_{vvv}v^3 + Y_{rrr}r^3\\ &\quad +Y_{rrv}r^2v + Y_{vvr}v^2r. \qquad (4.27)\end{aligned}$$

4.2.3 Total Forces from Lift and Drag

We can then summate the lift and drag forces in their relevant degrees of freedom.

The total surge and sway forces that arise from lift and drag are then:

$$\begin{aligned} X_{LD} &= X_L + X_D && (4.28)\\ &= X_{uu}u^2 + X_{uuu}u^3 + X_{vv}v^2 + X_{rr}r^2 + X_{vr}vr + X_{uvv}uv^2 \\ &\quad + X_{rvu}rvu + X_{urr}ur^2 && (4.29)\\ Y_{LD} &= Y_L + Y_D && (4.30)\\ &= Y_{uv}uv + Y_{ur}ur + Y_{uur}u^2r + Y_{uuv}u^2v + Y_{vvv}v^3 + Y_{rrr}r^3 \\ &\quad + Y_{rrv}r^2v + Y_{vvr}v^2r. && (4.31) \end{aligned}$$

The sway force induces a rolling and yawing moment according to:

$$\begin{aligned} K_{LD} &= Y_{LD}.z_{cp} = K_{uv}uv + K_{ur}ur + K_{uur}u^2r + K_{uuv}u^2v + K_{vvv}v^3 \\ &\quad + K_{rrr}r^3 + K_{rrv}r^2v + K_{vvr}v^2r && (4.32)\\ N_{LD} &= Y_{LD}.x_{cp} = N_{uv}uv + N_{ur}ur + N_{uur}u^2r + N_{uuv}u^2v + N_{vvv}v^3 \\ &\quad + N_{rrr}r^3 + N_{rrv}r^2v + N_{vvr}v^2r. && (4.33) \end{aligned}$$

4.2.4 Low–speed Drag

If low speed operations are to be considered, then the drag force should be augmented with a linear component that dominates near $u = 0$ m/s. Without a linear component, exponential convergence is not present, and the system is not physically correct. This linear drag decays with velocity, to reflect the observed results that at higher speeds, the drag is dominated by higher order effects. This is somewhat similar to the situation in aerodynamics, in which induced drag dominates at low airspeed, decaying as the velocity grows, until the contribution from profile drag becomes prevalent at higher speeds (e.g. Lewis 1989*b*). Such a term can be added as:

$$D_l = D_U \exp(-aU)\, U, \tag{4.34}$$

where a is set to give a transition between linear and nonlinear regimes: $a \approxeq \frac{1}{2}$ achieves this, although this is nothing more than a convenient value. Note that the drag force should be implemented directly, instead of forming a drag coefficient, as the coefficient would be singular at zero speed:

$$\begin{aligned} C_{Dl} &= \frac{D_U \exp(-aU)\, U}{\frac{1}{2}\rho U^2 S} && (4.35)\\ &= \frac{1}{U}\frac{2}{\rho S} D_U \exp(-aU)\,. && (4.36) \end{aligned}$$

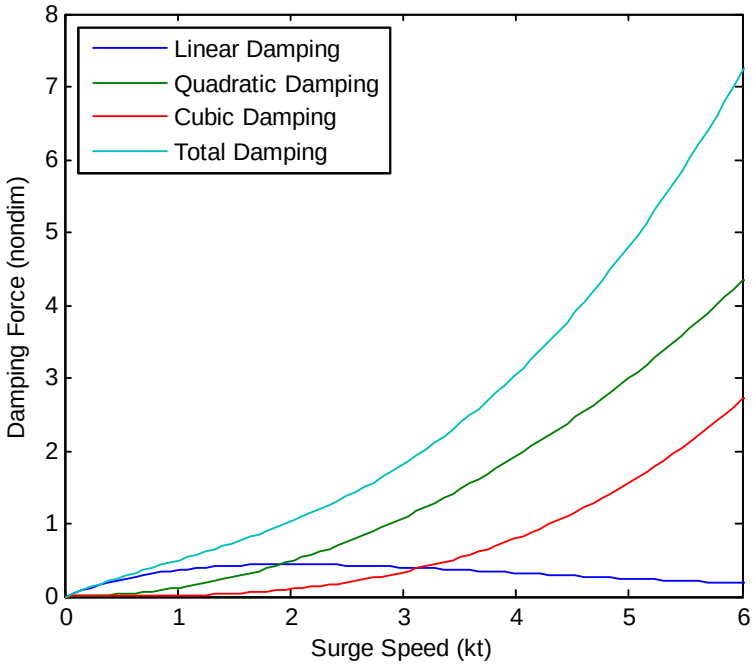

Figure 4.2: An example of the linear damping decaying with velocity.

The linear drag component with the singular coefficient at zero speed agrees with the results published by Hoerner (1965) for drag coefficients at very low Reynold's numbers, in which the drag coefficient is found to be proportional to Re^{-1}.

4.3 Non–linear Lift (Cross–Flow Drag)

The lift and drag forces described in Section 4.2 describe the lift and drag forces that arise from circulatory effects. However, since the ship hull is being treated as a low aspect–ratio wing, it is necessary to include an additional non–linear lift component, with an associated induced drag term.

An interesting way to see this is that, were an infinitely long ship to be present, there could certainly be no circulation: there would be neither a leading nor a trailing edge, and therefore nothing for the water to circulate about (Hoerner and Borst 1975).

Even in this situation there is a component of lift present that arises from the deflection of water and the imparting of momentum onto this water. Hoerner and Borst (1975) stated that this comes from the presence of a pair vortex sheets around the lateral edges of a wing. In a ship, this corresponds to the presence of a single vortex sheet that curls vertically around the bottom of the hull. This is depicted in Figure 4.3. It is common to reason that these vortices curl horizontally at the bow and the stern, but this is not correct; as has already been stated, crossflow drag is present in an infinitely long ship.

The form that this nonlinear component takes is

$$\Delta C_L = k^{'} C_{nl} \sin^2 \beta \cos \beta. \tag{4.37}$$

where $k^{'}$ is a form coefficient. This equation is somewhat similar to 34th Proposition within Newton's Principia, usually referred to as *Newton's Sine–Squared Law*, although this should not be taken to imply that this lift force arises from the impact and subsequent uniform deflection of water particles on the hull. The induced drag that arises from this is

$$\Delta C_D = k^{'} C_{nl} \sin^3 \beta. \tag{4.38}$$

For our purposes, it does not serve any purpose to resolve these forces in the flow axes any more. The initial assumption in the cross–flow drag principle is that the nonlinear lift and drag arise due to transverse flow across the hull or wing, and therefore it makes no sense to derive the non-linear lift and drag in equations (4.37) and (4.38), as the force that these are calculated from is already in the body fixed frame. We instead invoke the cross–flow drag principle directly.

The cross–flow drag principle assumes that the viscous drag is a function solely of the fluid velocity athwartships (i.e., the sway velocity across the hull, v). Given this, the sectional cross–flow drag coefficients can be used to calculate the sway, yaw and roll forces acting on the ship. Explanations of this principle can be found, for example, in the work by Faltinsen (1990), Beukelman and Journee (2001) or Golding *et al.* (2006).

The sectional cross–flow force acting on a ship can be written as:

$$Y_{cf} = \frac{1}{2} \rho \int_0^{L_{pp}} U(x)^2 C_{cf}(x) T(x) \, dx. \tag{4.39}$$

The cross–flow drag coefficient $C_{cf}(x)$ is typically given one of two forms: both asymmetric about the sideslip angle β. The first (e.g. Faltinsen

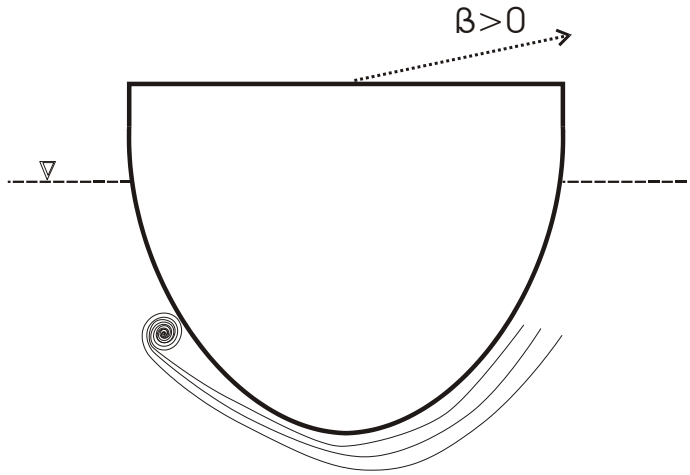

Figure 4.3: Nonlinear Flow Underneath Hull

2006*b*, Beukelman and Journee 2001) is of the form $C_{cf}(x) = C_{cf} \sin\beta(x) |\sin\beta(x)|$, the second form, from Hoerner and Borst (1975) is $C_{cf}(x) = C_{cf} \sin^3\beta(x)$.
We apply the first model, using $\beta(x) = \arcsin\frac{v+xr}{U(x)}$ to get:

$$Y_{cf} = \frac{1}{2}\rho \int_0^{L_{pp}} U(x)^2 C_{cf} \sin\beta(x) |\sin\beta(x)| T(x)\, dx \tag{4.40}$$

$$= \frac{1}{2}\rho C_{cf} \int_0^{L_{pp}} (v + xr) |v + xr| T(x)\, dx, \tag{4.41}$$

with corresponding moments in roll and yaw:

$$K_{cf} = \frac{1}{2}\rho C_{cf} \int_0^{L_{pp}} z_{cp}(x) (v + xr) |v + xr| T(x)\, dx \tag{4.42}$$

$$N_{cf} = \frac{1}{2}\rho C_{cf} \int_0^{L_{pp}} x (v + xr) |v + xr| T(x)\, dx, \tag{4.43}$$

where $z_{cp}(x)$ is the vertical centre of pressure as a function of longitudinal position.

4.3.1 Approximation of Cross–flow Drag

From the work of Norrbin (1971), it is known that the cross–flow drag described in equations (4.41)–(4.43) can be approximated using quadratic damping terms in modulus form, and written as:

$$Y_{cf} \cong Y_{|v|v}\,|v|\,v + Y_{|r|v}\,|r|\,v + Y_{|v|r}\,|v|\,r + Y_{|r|r}\,|r|\,r \quad (4.44)$$

$$K_{cf} \cong K_{|v|v}\,|v|\,v + K_{|r|v}\,|r|\,v + K_{|v|r}\,|v|\,r + K_{|r|r}\,|r|\,r \quad (4.45)$$

$$N_{cf} \cong N_{|v|v}\,|v|\,v + N_{|r|v}\,|r| + N_{|v|r}\,|v|\,r + N_{|r|r}\,|r|\,r. \quad (4.46)$$

This approximation is commonly used. Its accuracy varies from excellent to very poor. The errors are actually asymmetric about the sideslip angle. The surface shown in Figure 4.4 shows a representation of the error as a function of both the sway and yaw velocities. When both v and $x.r$ have the same sign, there is no error. When they differ in sign, an error arises.

The numbers in Figure 4.4 are only representative of the structure of the errors. A value of zero means that there is no difference between the full formulation and its approximation. The green areas then represent the well modelled portions of the cross–flow drag. The key point is that there will always be two quadrants with errors. The location of these errors is dependent on the body in question. For example, if the cross–flow drag is centred behind $L_{pp}/2$ then the errors shown would rotate by 90 °.

4.4 Roll Model

Surge, sway and yaw have been characterised, and the influence that these forces and moments have on roll has also been quantified, but only to a limited extent. This section describes two effects. The first is the roll angle influence on lift and drag. The second completes the roll mode analysis by describing a linear and nonlinear damping function.

4.4.1 Roll Angle Influence on Lift and Drag

The roll angle ϕ influences the lift and drag characteristics of the hull. Especially for ships with a low metacentric height, roll has a significant effect on the manoeuvring characteristics (Blanke and Jensen 1997) This influence emphasises the need for detailed modelling the of the roll–sway–yaw interactions. Extant work on this field can be found (e.g. Hirano and Takashina 1980). The approach taken here models the roll angle influence by further analogy to aerodynamics.

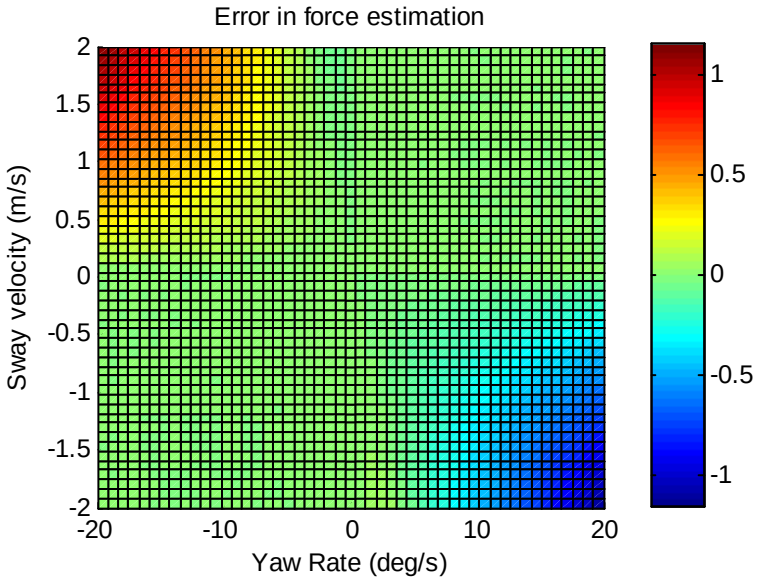

Figure 4.4: Structure of errors in Cross–flow approximation

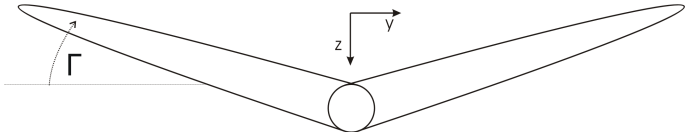

Figure 4.5: Wing with dihedral angle Γ

In an aircraft wing, the axial tilt (or v–shape) of a wing is called dihedral if tilted upwards, and anhedral if tilted downwards. Dihedral is depicted in Figure 4.5 by the symbol Γ.

This effect can be characterised by equating the roll angle with an angle of dihedral or anhedral: anhedral when the ship rolls into the sway direction, and dihedral when the ship away from the sway direction. The term dihedral will be used to mean both. The dihedral angle of a rolling hull is shown in Figure 4.6, where ϕ and Γ are conceptually the same.

The roll angle of the ship affects the circulatory lift and drag described in Sections 4.2.1 and 4.2.2, and these effects will now be described.

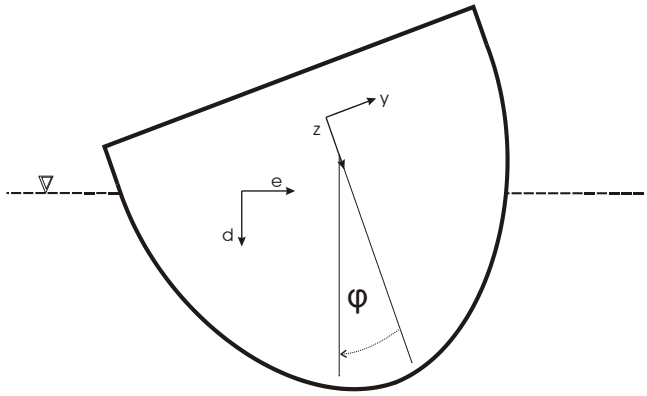

Figure 4.6: Roll-Angle/ Dihedral of Hull

Changes to Drag

Hoerner (1965) detailed the effect that an angle of dihedral has on the induced drag function using the following approximation:

$$C_{Di} = \frac{C_L^2}{\pi A_R \cos^2 \Gamma}, \tag{4.47}$$

where Γ is the angle of dihedral, C_L is the lift coefficient, and A_R is the aspect ratio of the wing. For application in this manoeuvring model, the same methodology is used to describe the roll angle in terms of this dihedral effect, i.e. $\Gamma = \phi$. This formula is used to augment the drag equation (4.22) as follows:

$$\begin{aligned} C_D(\phi, x) &= \frac{C}{\cos^2 \phi} \sin^2 \beta(x) && (4.48)\\ &= C \sin^2 \beta \left(1 + \tan^2 \phi\right) && (4.49)\\ \Rightarrow \Delta C_D(\phi, x) &= C \frac{(v + xr)^2}{U(x)^2} \tan^2 \phi && (4.50)\\ &\cong C \frac{(v + xr)^2}{U(x)^2} \phi^2, && (4.51) \end{aligned}$$

where C is a generic coefficient that is replaced later. This enters into the

drag equation as:

$$\begin{aligned}\Delta D(\phi, x) &= \frac{1}{2}\rho SCU(x)^2 \frac{(v+xr)^2}{U(x)^2}\phi^2 && (4.52)\\ &= \frac{1}{2}\rho SC(v+xr)^2\phi^2. && (4.53)\end{aligned}$$

Using $\tan^2\phi \cong \phi^2$ introduces errors of approximately 5% at $\phi = 15°$, but the errors escalate quickly above this. For large roll angles, such as manoeuvring in extreme seas, it becomes important to keep the trigonometric relationship, or to introduce an additional coefficient from the series expansion of the tan function:

$$\begin{aligned}\tan x &= x + \frac{x^3}{3} + \frac{2x^5}{15}... \quad |x| < \frac{\pi}{2} && (4.54)\\ \Rightarrow \tan\phi^2 &\cong \phi^2 + \frac{2}{3}\phi^4 && (4.55)\\ \Rightarrow \Delta D(\phi, x) &= \frac{1}{2}\rho S(v+xr)^2\left(\phi^2 C_{D\phi\phi} + \phi^4 C_{D\phi 4}\right). && (4.56)\end{aligned}$$

This noted, the drag function given in (4.53) is assumed to be good enough. In the body–fixed frame, the drag function is:

$$\begin{aligned}\Delta X_D(x) &= -\Delta D(\phi, x)\cos\beta(x) && (4.57)\\ &= -\Delta D(\phi, x)\frac{u}{U(x)}\\ &= -\frac{1}{2}\rho SC\frac{u}{U(x)}(v+xr)^2\phi^2\\ &\cong -\frac{1}{2}\rho SC(v+xr)^2\phi^2\\ \Rightarrow \Delta X_D &= X_{vv\phi\phi}v^2\phi^2 + X_{vr\phi\phi}vr\phi^2 + X_{rr\phi\phi}r^2\phi^2. && (4.58)\end{aligned}$$

$$\begin{aligned}\Delta Y_D(x) &= -\Delta D(\phi, x)\sin\beta(x) && (4.59)\\ &= -\Delta D(\phi, x)\frac{v+xr}{U}\\ &= -\frac{1}{2}\rho SC\frac{(v+xr)^3}{U(x)}\phi^2 && (4.60)\\ &\cong 0, && (4.61)\end{aligned}$$

where the small angle assumption $(v+xr)^3/U \cong 0$ has been applied.

Changes to Lift

The effect that dihedral has on lift is described in Hoerner and Borst's (1975) work on fluid dynamics, in which the generic equation describing the lift coefficient in relation to the angle of attack is given by:

$$\frac{d\alpha}{dC_L} = \frac{1}{2\pi \cos^2 \Gamma} + \frac{1}{\pi A_P \cos^2 \Gamma}. \tag{4.62}$$

We apply this equation and subtract the lift coefficient at zero angle of dihedral, using $\cos^2 \phi = 1 - \sin^2 \phi$ to give:

$$\begin{aligned} C_L(\phi, x) &= C \cos^2 \phi \sin \beta(x) && (4.63)\\ \Delta C_L(\phi, x) &= -C \sin^2 \phi \sin \beta(x) && (4.64)\\ &\cong C_{L\phi\phi}\phi^2 \frac{v + xr}{U(x)}. && (4.65) \end{aligned}$$

These terms enter into the original lift and drag equations to give:

$$\begin{aligned} \Delta L(\phi, x) &= \frac{1}{2}\rho U(x)^2 S \frac{v + xr}{U(x)} C_{L\phi\phi}\phi^2 && (4.66)\\ &= \frac{1}{2}\rho S U(x)(v + xr) C_{L\phi\phi}\phi^2. && (4.67) \end{aligned}$$

In the surge direction of the body–fixed frame these are:

$$\begin{aligned} \Delta X_L(x) &= \Delta L(x) \sin \beta(x) && (4.68)\\ &= \frac{1}{2}\rho S U(x) . (v + xr) C_{L\phi\phi}\phi^2 \frac{v + xr}{U(x)} \\ &= \frac{1}{2}\rho S (v + xr)^2 C_{L\phi\phi}\phi^2 && (4.69)\\ \Rightarrow X_L &= X_{vv\phi\phi} v^2\phi^2 + X_{vr\phi\phi} vr\phi^2 + X_{rr\phi\phi} r^2\phi^2. && (4.70) \end{aligned}$$

In the sway direction, this is:

$$\begin{aligned} Y_L(x) &= -\Delta L(x) \cos \beta(x) && (4.71)\\ &= -\frac{1}{2}\rho S U(x) . (v + xr) C_{L\phi\phi}\phi^2 \frac{u}{U(x)} \\ &= -\frac{1}{2}\rho S u (v + xr) C_{L\phi\phi}\phi^2 \\ \Rightarrow Y_L &= Y_{uv\phi\phi} uv\phi^2 + Y_{ur\phi\phi} ur\phi^2. && (4.72) \end{aligned}$$

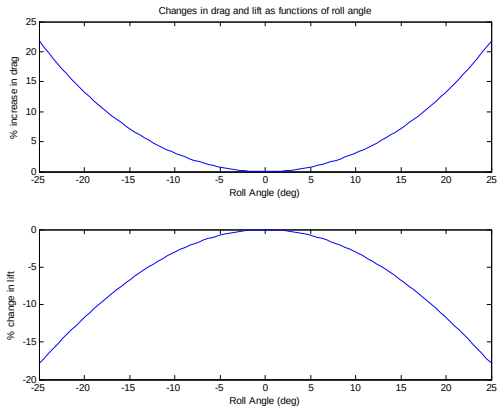

Figure 4.7: Roll influence on lift and drag

4.4.2 Overall Changes

The complete changes of lift and drag In the body fixed frame are given by:

$$\begin{aligned} \Delta X_{LD} &= \Delta X_D + \Delta X_L \\ \Delta Y_{LD} &= \Delta Y_D + \Delta Y_L. \end{aligned} \tag{4.73}$$

$$\Delta X_{LD} = X_{vv\phi\phi} v^2\phi^2 + X_{vr\phi\phi} vr\phi^2 + X_{rr\phi\phi} r^2\phi^2 \tag{4.74}$$

$$\Delta Y_{LD} = Y_{uv\phi\phi} uv\phi^2 + Y_{ur\phi\phi} ur\phi^2. \tag{4.75}$$

The effect that roll angle has on lift and drag generation is shown in Figure 4.7. The drag forces experienced by the ship can increase in the region of 10–15 % during a moderately aggressive manoeuvre, while the lift forces drop by a similar percentage, and so it is important to take this into account in the modelling process.

Collecting all the circulatory lift and drag forces together, in the body–

fixed frame the augmented circulatory lift and drag forces are:

$$\begin{aligned} X_{LD} &= X^L_{uu}u^2 + X^L_{uuu}u^3 + X^L_{vv}v^2 + X^L_{rr}r^2 + X^L_{rv}rv + X^L_{uvv}uv^2 \\ &\quad + X^L_{rvu}rvu + X^L_{urr}ur^2 + X^L_{vv\phi\phi}v^2\phi^2 + X^L_{vr\phi\phi}vr\phi^2 + X^L_{rr\phi\phi}r^2\phi^2 \end{aligned} \tag{4.76}$$

$$\begin{aligned} Y_{LD} &= Y^L_{uv}uv + Y^L_{ur}ur + Y^L_{uur}u^2r + Y^L_{uuv}u^2v + Y^L_{vvv}v^3 + Y^L_{rrr}r^3 \\ &\quad + Y^L_{rrv}r^2v + Y^L_{vvr}v^2r + Y^L_{uv\phi\phi}uv\phi^2 + Y^L_{ur\phi\phi}ur\phi^2 \end{aligned} \tag{4.77}$$

$$\begin{aligned} K_{LD} &= Y_{LD}z_{cp} = K^L_{uv}uv + K^L_{ur}ur + K^L_{uur}u^2r + K^L_{uuv}u^2v + K^L_{vvv}v^3 \\ &\quad + K^L_{rrr}r^3 + K^L_{rrv}r^2v + K^L_{vvr}v^2r + K^L_{uv\phi\phi}uv\phi^2 + K^L_{ur\phi\phi}ur\phi^2 \end{aligned} \tag{4.78}$$

$$\begin{aligned} N_{LD} &= Y_{LD}x_{cp} = N^L_{uv}uv + N^L_{ur}ur + N^L_{uur}u^2r + N^L_{uuv}u^2v + N^L_{vvv}v^3 \\ &\quad + N^L_{rrr}r^3 + N^L_{rrv}r^2v + N^L_{vvr}v^2r + N^L_{uv\phi\phi}uv\phi^2 + N^L_{ur\phi\phi}ur\phi^2. \end{aligned} \tag{4.79}$$

4.4.3 Roll Damping

The damping in roll remains to be modelled. During motion of the ship through water, energy is transported away from the ship in the form of gravity waves: for most degrees of freedom, this type of damping constitutes the majority of total damping. However, this is not the case for the roll mode: there are generally more complicated physical processes in play, and these are difficult to model.

There are at least five constituent components of roll damping: wave generation, skin friction, eddy creation, lift generation, and appendage damping (bilge keels or fins etc.). Some of these are depicted in Figure 4.8. These processes are highly complicated, and in general it is either impractical or impossible to model them in a sound theoretical manner. Empirical formulae are typically used instead. These can be modelled according to the results by Ikeda *et al.* (1976), Lloyd (1998) or Himeno (1981) as either a linear component plus a cubic, or a linear component plus a quadratic modulus term (Bass and Haddara 1988). This paper takes the cubic version (e.g. Perez 2005, Journée and Massie 2001):

$$K = K_p p + K_{ppp}p^3. \tag{4.80}$$

4.5 Total Damping Forces

The complete set of damping forces acting on the ship are then:

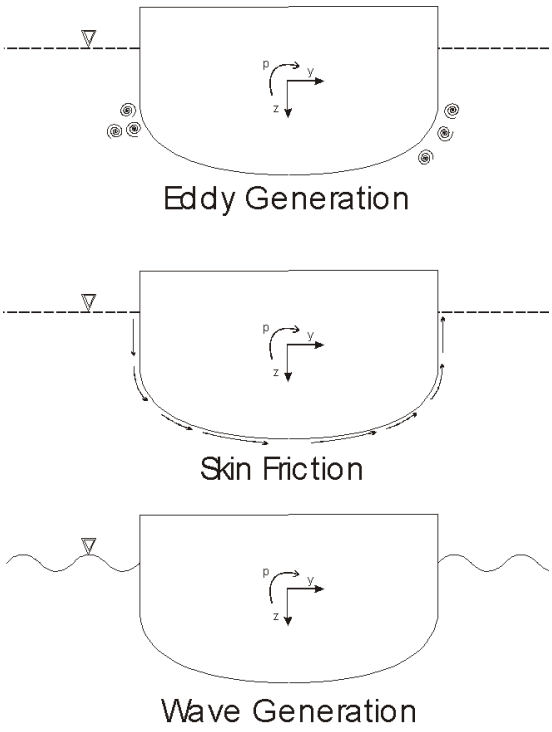

Figure 4.8: Sources of Roll Damping

Circulatory Lift and Drag These forces are described by equations (4.76)–(4.79). The roll angle influences are included.

Crossflow Drag Crossflow drag is modelled according to equations (4.44)–(4.46).

Roll Damping The damping in roll is given according to equation (4.80).

Chapter 5

Complete Models

The purpose of this chapter is to collate the results of the three preceding chapters. Finally, several models will be presented, which will then constitute the required models used in the second half of this thesis. The important regimes to model are:

Low–Frequency Model This model copes with low-frequency operations. The purpose of this model is to comprehensively model a ship travelling in calm water.

Model with Fluid Memory Effect This model is more complete, in that it accurately models operations in the presence of waves.

Reduced Order Models Simpler models are presented, for use in autopilot design.

5.1 Low–Frequency Model

This model is a 4–DOF model for use in calm waters. It is given by:

$$\dot{\boldsymbol{\eta}} = \mathbf{J}(\boldsymbol{\theta})\,\boldsymbol{\nu} \tag{5.1}$$

$$\mathbf{M}\dot{\boldsymbol{\nu}} + \mathbf{C}(\boldsymbol{\nu})\,\boldsymbol{\nu} + \mathbf{D}(\boldsymbol{\nu})\,\boldsymbol{\nu} + \mathbf{g}(\boldsymbol{\eta}) = \boldsymbol{\tau}, \tag{5.2}$$

where $\mathbf{M} \triangleq \mathbf{M}_{RB} + \bar{\mathbf{M}}_A$, $\mathbf{C}(\boldsymbol{\nu}) \triangleq \mathbf{C}_{RB}(\boldsymbol{\nu}) + \mathbf{C}_A^0(\boldsymbol{\nu})$. The added mass is given by:

$$\mathbf{M}_A = -\begin{bmatrix} X_{\dot{u}}^0 & 0 & 0 & 0 \\ 0 & Y_{\dot{v}}^0 & Y_{\dot{p}}^0 & Y_{\dot{r}}^0 \\ 0 & K_{\dot{v}}^0 & K_{\dot{p}}^0 & K_{\dot{r}}^0 \\ 0 & N_{\dot{v}}^0 & N_{\dot{p}}^0 & N_{\dot{r}}^0 \end{bmatrix} \tag{5.3}$$

$$\bar{\mathbf{M}}_A = \frac{1}{2}\left(\mathbf{M}_A + \mathbf{M}_A^\top\right). \tag{5.4}$$

The added mass Coriolis-centripetal matrix, calculated from (5.4), is:

$$\mathbf{C}_A^0(\boldsymbol{\nu}) \triangleq \begin{bmatrix} 0 & 0 & 0 & Y_{\dot{v}}^0 v + \frac{1}{2}\left(N_{\dot{v}}^0 + Y_{\dot{r}}^0\right) r \\ & & & +\frac{1}{2}\left(Y_{\dot{p}}^0 + K_{\dot{v}}^0\right) p \\ 0 & 0 & 0 & -X_{\dot{u}}^0 u \\ 0 & 0 & 0 & 0 \\ -Y_{\dot{v}}^0 v - \frac{1}{2}\left(N_{\dot{v}}^0 + Y_{\dot{r}}^0\right) r & & & \\ -\frac{1}{2}\left(Y_{\dot{p}}^0 + K_{\dot{v}}^0\right) p & X_{\dot{u}}^0 u & 0 & 0 \end{bmatrix} \tag{5.5}$$

$$\mathbf{C}_{RB}(\boldsymbol{\nu}) \triangleq \begin{bmatrix} 0 & 0 & 0 & mv \\ 0 & 0 & mw & -mu \\ 0 & -mw & 0 & I_y q \\ -mv & mu & -I_y q & 0 \end{bmatrix}. \tag{5.6}$$

The damping matrix $\mathbf{D}(\boldsymbol{\nu})$ is modelled as:

- Linear lift and drag, given by equations (4.76)–(4.79)
- Crossflow drag given by equations (4.44)–(4.46)
- Roll damping, given by equation (4.80)

One matrix formulation of this is:

$$\mathbf{D}(\boldsymbol{\nu}) = \begin{bmatrix} -X^L_{uu}u - X^L_{uuu}u^2 - X^L_{rvu}rv & -X^L_{vv}v - X^L_{rv}r - X^L_{uvv}uv - X^L_{vv\phi\phi}v\phi^2 - X^L_{vr\phi\phi}r\phi^2 \\ -Y^L_{uv\phi\phi}v\phi^2 - Y^L_{ur\phi\phi}r\phi^2 & -Y^L_{uv}u - Y^L_{uuv}u^2 - Y^L_{vvv}v^2 - Y^L_{rrv}r^2 - Y_{|v|v}|v| - Y_{|r|v}|r| \\ -K^L_{uv\phi\phi}v\phi^2 - K^L_{ur\phi\phi}r\phi^2 & -K^L_{uv}u - K^L_{uuv}u^2 - K^L_{vvv}v^2 - K^L_{rrv}r^2 - K_{|v|v}|v| - K_{|r|v}|r| \\ -N^L_{uv\phi\phi}v\phi^2 - N^L_{ur\phi\phi}r\phi^2 & -N^L_{uv}u - N^L_{uuv}u^2 - N^L_{vvv}v^2 - N^L_{rrv}r^2 - N_{|v|v}|v| - N_{|r|v}|r| \end{bmatrix}$$
$$\begin{bmatrix} 0 & -X^L_{rr}r - X^L_{urr}ur - X^L_{rr\phi\phi}r\phi^2 \\ 0 & -Y^L_{ur}u - Y^L_{uur}u^2 - Y^L_{rrr}r^2 - Y^L_{vvr}v^2 - Y_{|v|r}|v| - Y_{|r|r}|r| \\ -K_p - K_{ppp}p^2 & -K^L_{ur}u - K^L_{uur}u^2 - K^L_{rrr}r^2 - K^L_{vvr}v^2 - K_{|v|r}|v| - K_{|r|r}|r| \\ 0 & -N^L_{ur}u - N^L_{uur}u^2 - N^L_{rrr}r^2 - N^L_{vvr}v^2 - N_{|v|r}|v| - N_{|r|r}|r| \end{bmatrix}. \quad (5.7)$$

The restoring matrix, $\mathbf{g}(\boldsymbol{\eta})$ is given as:

$$\mathbf{g}(\boldsymbol{\eta}) = \begin{bmatrix} 0 \\ \rho g \int_0^z A_{wp}(\zeta)\, d\zeta \sin\phi \\ \rho g \nabla \overline{GM_T} \sin\phi\cos\phi \\ \rho g \nabla \left(-\overline{GM_L} + \overline{GM_T}\right) \sin\phi \end{bmatrix}. \quad (5.8)$$

A simpler form of this is:

$$\mathbf{g}(\boldsymbol{\eta}) = \begin{bmatrix} 0 \\ 0 \\ \rho g \nabla \overline{GM_T} \sin\phi \\ 0 \end{bmatrix}. \quad (5.9)$$

5.2 Model with Fluid Memory Effects

This is a model suitable for motion through waves. The unified model is given by:

$$\dot{\boldsymbol{\eta}} = \mathbf{J}(\boldsymbol{\theta})\boldsymbol{\nu} \quad (5.10)$$

$$\mathbf{M}\dot{\boldsymbol{\nu}} + \mathbf{C}(\boldsymbol{\nu})\boldsymbol{\nu} + \left(\bar{\mathbf{M}}^*_{\mathbf{A}} * \dot{\boldsymbol{\nu}}\right)(t) + \mathbf{D}(\boldsymbol{\nu})\boldsymbol{\nu} + \mathbf{g}(\boldsymbol{\eta}) = \boldsymbol{\tau}, \quad (5.11)$$

where $\mathbf{M} \triangleq \mathbf{M}_{RB} + \mathbf{M}_A^{\infty}$, and $\mathbf{C}(\boldsymbol{\nu}) \triangleq \mathbf{C}_{RB}(\boldsymbol{\nu}) + \mathbf{C}_A^{\infty}(\boldsymbol{\nu}) + \mathbf{C}_A^{*}(\boldsymbol{\nu})$, with these defined as:

$$\mathbf{M}_A^*(t) = -\begin{bmatrix} X_{\dot{u}}^*(t) & 0 & 0 & 0 \\ 0 & Y_{\dot{v}}^*(t) & Y_{\dot{p}}^*(t) & Y_{\dot{r}}^*(t) \\ 0 & K_{\dot{v}}^*(t) & K_{\dot{p}}^*(t) & K_{\dot{r}}^*(t) \\ 0 & N_{\dot{v}}^*(t) & N_{\dot{p}}^*(t) & N_{\dot{r}}^*(t) \end{bmatrix} \tag{5.12}$$

$$\bar{\mathbf{M}}_A^*(t) = \frac{1}{2}\left(\mathbf{M}_A^*(t) + \mathbf{M}_A^*(t)^{\top}\right) \tag{5.13}$$

$$\mathbf{M}_A^{\infty} = -\begin{bmatrix} X_{\dot{u}}^{\infty} & 0 & 0 & 0 \\ 0 & Y_{\dot{v}}^{\infty} & Y_{\dot{p}}^{\infty} & Y_{\dot{r}}^{\infty} \\ 0 & K_{\dot{v}}^{\infty} & K_{\dot{p}}^{\infty} & K_{\dot{r}}^{\infty} \\ 0 & N_{\dot{v}}^{\infty} & N_{\dot{p}}^{\infty} & N_{\dot{r}}^{\infty} \end{bmatrix}. \tag{5.14}$$

$$\mathbf{C}_A^{\infty}(\boldsymbol{\nu}) = \begin{bmatrix} 0 & 0 \\ 0 & 0 \\ 0 & 0 \\ -Y_{\dot{v}}^{\infty} v - \frac{1}{2}\left(N_{\dot{v}}^{\infty} + Y_{\dot{r}}^{\infty}\right) r & \\ -\frac{1}{2}\left(Y_{\dot{p}}^{\infty} + K_{\dot{v}}^{\infty}\right) p & X_{\dot{u}}^{\infty} u \\ \begin{matrix} 0 \\ 0 \\ 0 \end{matrix} & \begin{matrix} Y_{\dot{v}}^{\infty} v + \frac{1}{2}\left(N_{\dot{v}}^{\infty} + Y_{\dot{r}}^{\infty}\right) r \\ +\frac{1}{2}\left(Y_{\dot{p}}^{\infty} + K_{\dot{v}}^{\infty}\right) p \\ -X_{\dot{u}}^{\infty} u \\ 0 \\ 0 \end{matrix} \end{bmatrix} \tag{5.15}$$

$$\mathbf{C}_A^{*}(\boldsymbol{\nu}) = \begin{bmatrix} 0 & 0 \\ 0 & 0 \\ 0 & 0 \\ -\left(Y_{\dot{v}}^* * v\right)(t) & \\ -\left(Y_{\dot{p}}^* * p\right)(t) & \left(X_{\dot{u}}^* * u\right)(t) \\ -\left(Y_{\dot{r}}^* * r\right)(t) & \\ \begin{matrix} 0 \\ 0 \\ 0 \\ 0 \end{matrix} & \begin{matrix} \left(Y_{\dot{v}}^* * v\right)(t) + \left(Y_{\dot{p}}^* * p\right)(t) \\ +\left(Y_{\dot{r}}^* * r\right)(t) \\ -\left(X_{\dot{u}}^* * u\right)(t) \\ 0 \\ 0 \end{matrix} \end{bmatrix}. \tag{5.16}$$

5.3 Autopilot Models

The models presented here are for heading autopilot design. Both are yaw only nonlinear time-varying models.

Low-Frequency Model

$$\begin{aligned}
&(I_z - N_{\dot{r}})\,\dot{r} - N^L_{uv\phi\phi}uv\phi^2 - N^L_{uv}uv - N^L_{uuv}u^2v - N^L_{vvv}v^3 \\
&-N^L_{rrv}r^2v - N_{|v|v}\,|v|\,v - N_{|r|v}\,|r|\,v - N^L_{ur}ur - N^L_{uur}u^2r \\
&-N^L_{rrr}r^3 - N^L_{vvr}v^2r - N_{|v|r}\,|v|\,r - N_{|r|r}\,|r|\,r + \left(X^0_{\dot{u}} - Y^0_{\dot{v}}\right)uv \\
&-\frac{1}{2}\left(N^0_{\dot{v}} + Y^0_{\dot{r}}\right)ru - \frac{1}{2}\left(Y^0_{\dot{p}} + K^0_{\dot{v}}\right)p \;=\; N \qquad (5.17)\\
&\dot{\phi} \;=\; r \qquad (5.18)
\end{aligned}$$

Model with Fluid Memory Effects

$$\begin{aligned}
&(I_z - N_{\dot{r}})\,\dot{r} - N^L_{uv\phi\phi}uv\phi^2 - N^L_{uv}uv - N^L_{uuv}u^2v - N^L_{vvv}v^3 \\
&-N^L_{rrv}r^2v - N_{|v|v}\,|v|\,v - N_{|r|v}\,|r|\,v - N^L_{ur}ur - N^L_{uur}u^2r \\
&-N^L_{rrr}r^3 - N^L_{vvr}v^2r - N_{|v|r}\,|v|\,r - N_{|r|r}\,|r|\,r \\
&+\left(X^\infty_{\dot{u}} - Y^\infty_{\dot{v}}\right)uv - K^\infty_{\dot{v}}up - N^\infty_{\dot{v}}ru \\
&-\frac{1}{2}\left(Y^*_{\dot{v}} * v\right)(t)\,u - \frac{1}{2}\left(Y^*_{\dot{p}} * p\right)(t)\,u \\
&-\frac{1}{2}\left(Y^*_{\dot{r}} * r\right)(t)\,u + \frac{1}{2}\left(X^*_{\dot{u}} * u\right)(t)\,v \;=\; N \qquad (5.19)\\
&\dot{\phi} \;=\; r \qquad (5.20)
\end{aligned}$$

Part II

Identification of the Ship Model

Chapter 6

Planar Motion Mechanism Tests

The first part of this thesis developed an advanced model structure. The second part of this thesis complements the first by using experimental data to show that the work from Part I is valid

This chapter describes how the model derived in Part I of this thesis can be identified from captive model tests.

Validation and verification of a model might take a number of forms. Experimental procedures include full–scale tests, model–scale captive tests and free running tests. Each method has its advantages and disadvantages. Captive tests give great control over what is done, though limits what *can* be done. The quality of measurement data is excellent, typically with all states being measured. Full–scale experiments are of prohibitive expense, but provide the only true link to the physics involved in manoeuvring. The measurements involved in these tests are typically more deficient, often lacking in data for example in propeller thrust and other force measurements. Free–running model tests provide a tenuous link between the two. Clearly all three together are best, but this is immaterial, as all of them will rarely be available at any suitable price.

The datasource for this chapter is a set of commercially obtained PMM runs.

6.1 Experiment Description

The data used for analysis in this thesis stems from commercial planar motion mechanism (PMM) tests. These tests were performed on a scale

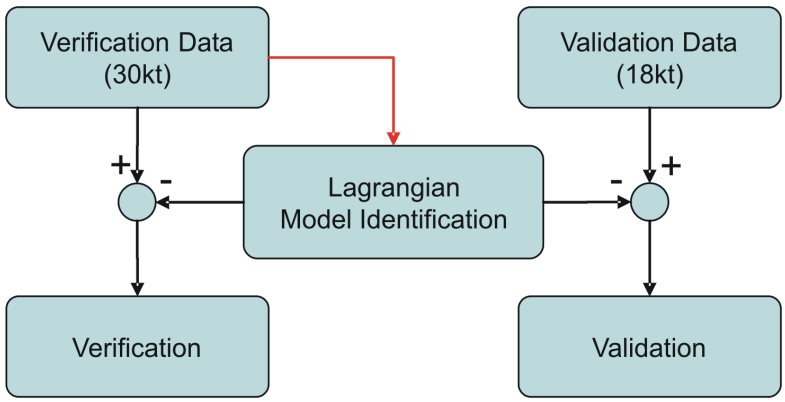

Figure 6.1: Flowchart illustrating identification methodology

model of a modern frigate. The model was free to move in heave and pitch, and was constrained in all other degrees of freedom.

The experimental results used in this thesis are put to two purposes:

Verification The process of verification entails making sure that the model can match a given dataset. By identifying the coefficients of the model, and then showing that the derived model is capable of replicating the dataset; the model can be shown to be viable.

Validation Validation entails testing the model against a completely different dataset; one that was not used in the derivation process. Matching this data well is a vital step in demonstrating the utility of the model. To verify that the model is in fact effective, the model is tested against a dataset not used in its derivation.

The test is to investigate whether the coefficients of the model, identified from some set of experiments, can replicate *other* experiments. If different experiments can be matched, this is highly suggestive of effective and physical modelling of the vessel. This process is illustrated in Figure 6.1. Note that the validation data is not used to derive the Lagrangian model.

Two distinct regimes were tested. The first at 30kt and the second at 18kt. This significant difference in speed allows an estimation of how effective the derived model is.

Furthermore, a PMM model was purchased, which had been fitted to

this same dataset. This model gives a kind of benchmark or test–case to compare to the Lagrangian model.

A variety of PMM test runs were used. Each type of test emphasises different dynamic characteristics.

Pure Drift Pure drift simply sets the model at a fixed oblique angle, and tows the vessel along. Static derivatives such as X_{uu} or $Y_{|v|v}$ are isolated from any influence from yaw motion.

Pure Sway A pure sway test tows the model forwards, while moving solely in sway, with the heading fixed at zero. These are usually sinusoidal oscillations, but in principle can be any motion whatsoever. This test, then, isolates the sway dynamics from the yaw dynamics. An example test is shown here in Figure 6.2.

Pure Yaw A pure yaw test tows the model forwards while moving in yaw. The sidewards motion is compensated for: there is no sway velocity. An example is shown in Figure 6.3.

Mixed Sway and Yaw This test has the ship at a set sway velocity, while the model yaws. In essence it is a generalisation of pure yaw, except the model is held at a nonzero sway velocity. It is shown in Figure 6.4.

6.2 Parameterisation

Prior to identifying the model, it is parameterised into a suitable form. The basis for this parameterisation is the model given in Section 5.1.

$$\begin{aligned}
\theta_x &= \left[\; X^0_{\dot{u}} \quad Y^0_{\dot{v}} \quad \tfrac{1}{2}\left(N^0_{\dot{v}} + Y^0_{\dot{r}}\right) \quad X^L_{uu} \right. \\
&\qquad \left. X^L_{uuu} \quad X^L_{rvu} \quad X^L_{vv} \quad X^L_{rv} \quad X^L_{uvv} \;\right] && (6.1)\\
\theta_y &= \left[\; Y^0_{\dot{v}} \quad \tfrac{1}{2}\left(Y^0_{\dot{r}} + N^0_{\dot{v}}\right) \quad X^0_{\dot{u}} \quad Y^L_{uv} \quad Y^L_{uuv} \quad Y^L_{vvv} \quad Y^L_{rrv} \right. \\
&\qquad \left. Y^L_{ur} \quad Y^L_{uur} \quad Y^L_{rrr} \quad Y^L_{vvr} \quad Y_{|v|v} \quad Y_{|r|v} \quad Y_{|v|r} \quad Y_{|r|r} \;\right] && (6.2)\\
\theta_k &= \left[\; \tfrac{1}{2}\left(Y_{\dot{p}} + K_{\dot{v}}\right) \quad \tfrac{1}{2}\left(K_{\dot{r}} + N_{\dot{p}}\right) \quad K^L_{uv} \quad K^L_{uuv} \quad K^L_{vvv} \quad K^L_{rrv} \right. \\
&\qquad \left. K^L_{ur} \quad K^L_{uur} \quad K^L_{rrr} \quad K^L_{vvr} \quad K_{|v|v} \quad K_{|r|v} \quad K_{|v|r} \quad K_{|r|r} \;\right] && (6.3)\\
\theta_n &= \left[\; \tfrac{1}{2}\left(N_{\dot{v}} + Y_{\dot{r}}\right) \quad N_{\dot{r}} \quad Y^0_{\dot{v}} \quad X_{\dot{u}} \quad \tfrac{1}{2}\left(N^0_{\dot{v}} + Y_{\dot{r}}\right) \quad N^L_{uv} \quad N^L_{uuv} \quad N^L_{vvv} \right. \\
&\qquad \left. N^L_{rrv} \quad N^L_{ur} \quad N^L_{uur} \quad N^L_{rrr} \quad N^L_{vvr} \quad N_{|v|v} \quad N_{|r|v} \quad N_{|v|r} \quad N_{|r|r} \;\right] && (6.4)
\end{aligned}$$

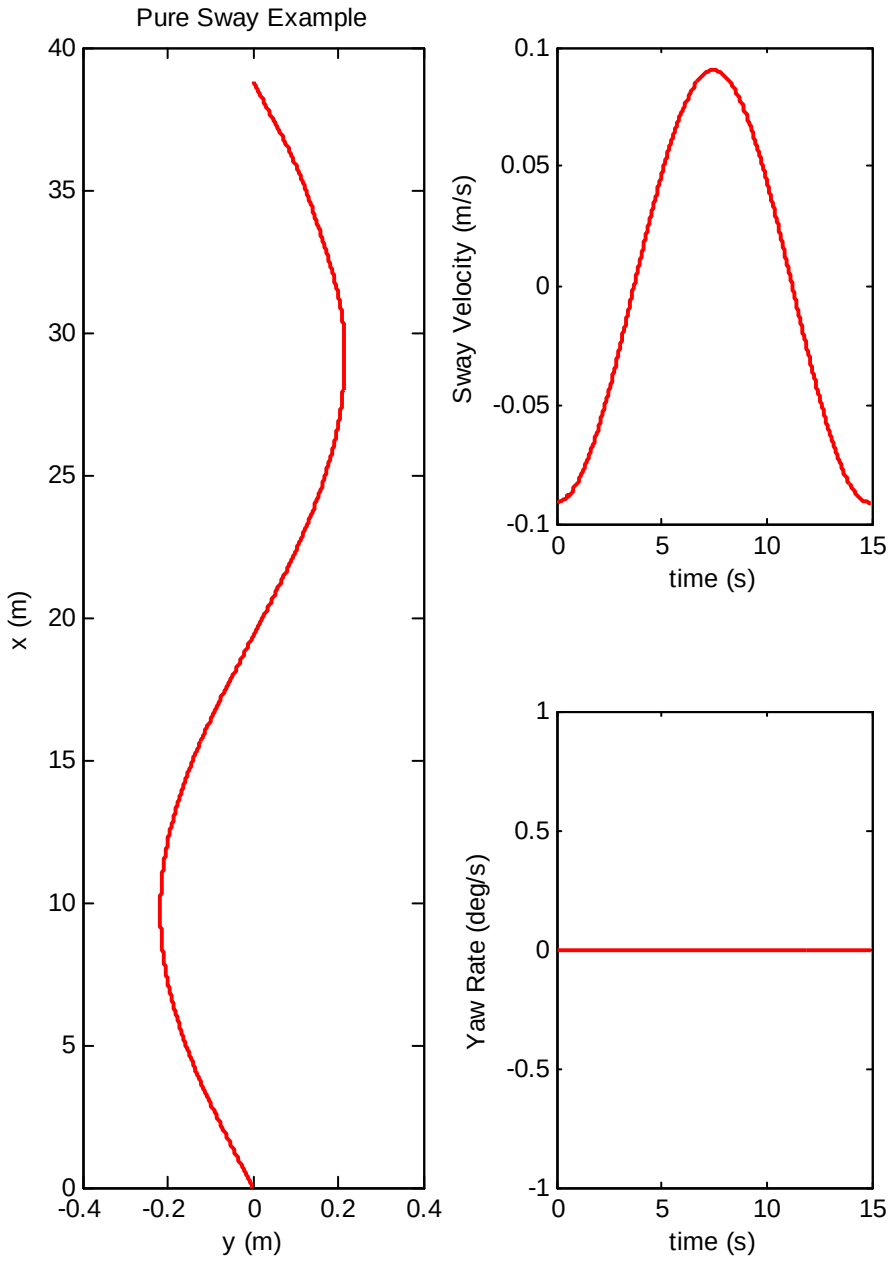

Figure 6.2: A pure sway test. Note that there is no yaw motion, only sway.

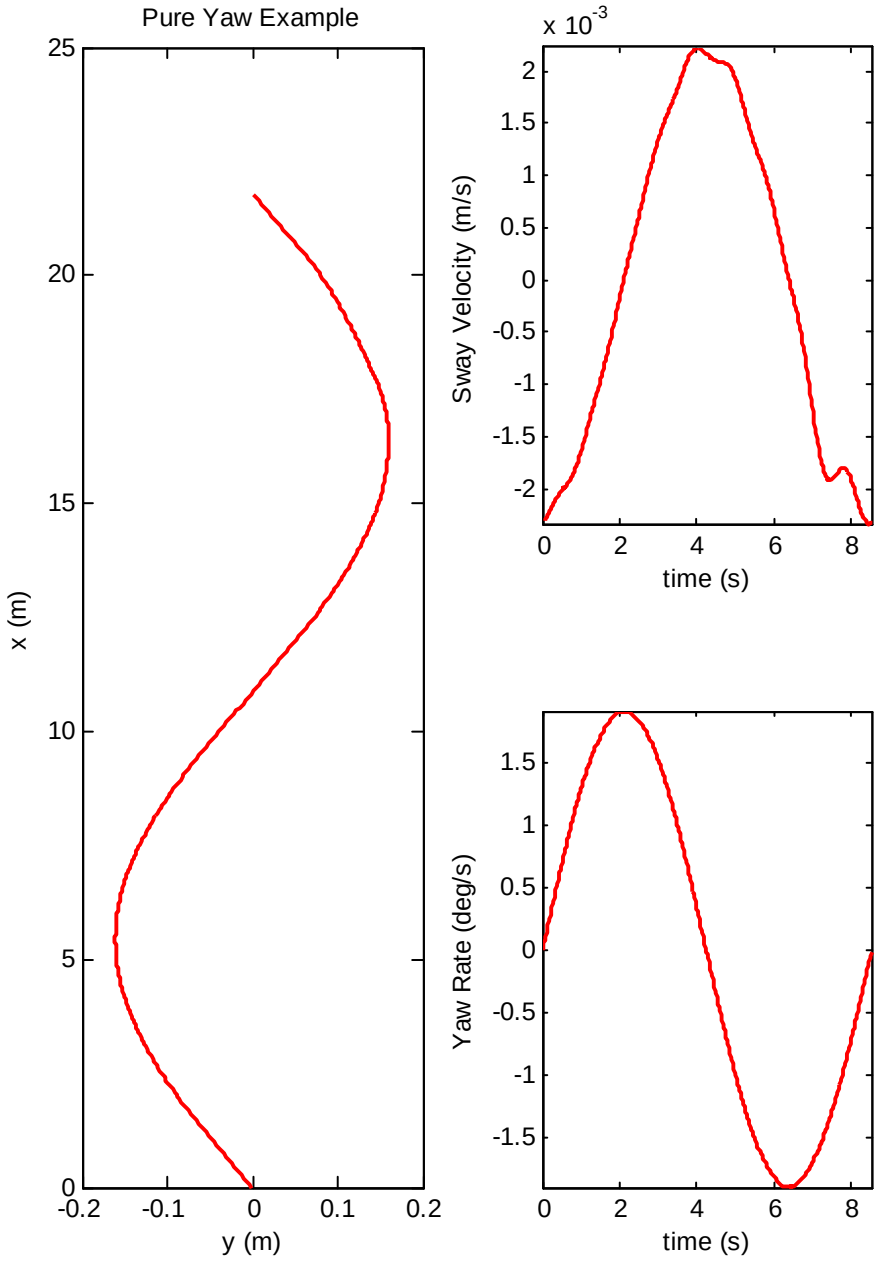

Figure 6.3: An example of pure yaw motion. Note that $v \simeq 0\ m/s$.

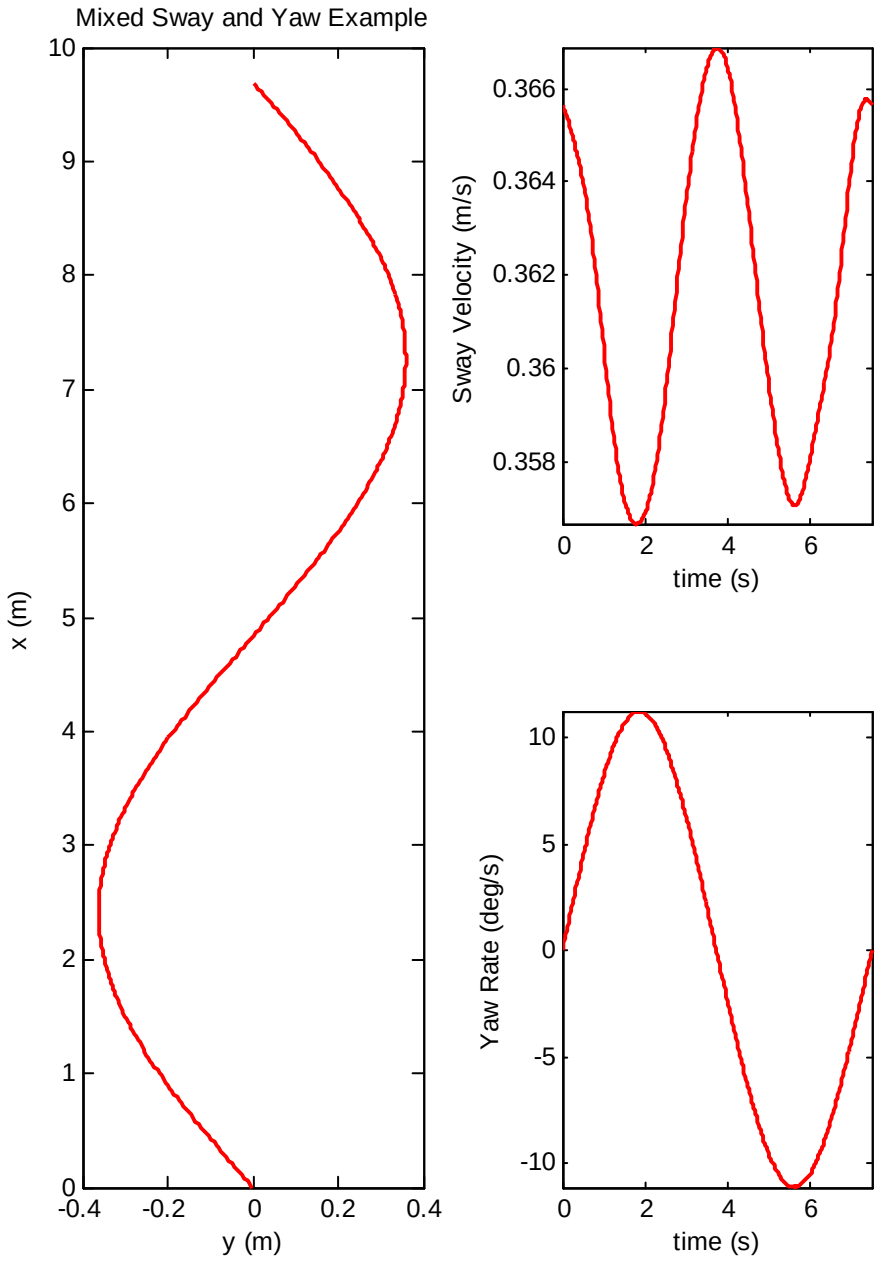

Figure 6.4: Example of yaw motion at a drift angle. Note that v is fixed at a nonzero value.

This is not the final structure applied in computation. Take the surge parameters: $Y^0_{\dot{v}}$ and X^L_{rv} are both multiplied by rv. It therefore seems that the two are indistinguishable, but this is not the case. The sway added–mass appears trivially in the sway equation, and so when all functions are considered together, this parameter is identifiable. There are several instances of this, such as the pair $X^0_{\dot{u}}$ and Y^L_{ur} in the sway equation, but again these pairs present no actual problem if all degrees of freedom are treated simultaneously.

The total parameter vector is then:

$$\begin{aligned}\theta_t \;=\; \Big[\; & X^0_{\dot{u}} \quad Y^0_{\dot{v}} \quad \tfrac{1}{2}\left(N^0_{\dot{v}} + Y^0_{\dot{r}}\right) \quad \tfrac{1}{2}\left(Y_{\dot{p}} + K_{\dot{v}}\right) \quad \tfrac{1}{2}\left(K_{\dot{r}} + N_{\dot{p}}\right) \quad N_{\dot{r}} \\ & X^L_{uu} \quad X^L_{uuu} \quad X^L_{rvu} \quad X^L_{vv} \quad X^L_{rv} \quad X^L_{uvv} \quad Y^L_{uv} \quad Y^L_{uuv} \\ & Y^L_{vvv} \quad Y^L_{rrv} \quad Y^L_{ur} \quad Y^L_{uur} \quad Y^L_{rrr} \quad Y^L_{vvr} \quad Y_{|v|v} \quad Y_{|r|v} \\ & Y_{|v|r} \quad Y_{|r|r} \quad K^L_{uv} \quad K^L_{uuv} \quad K^L_{vvv} \quad K^L_{rrv} \quad K^L_{ur} \quad K^L_{uur} \\ & K^L_{rrr} \quad K^L_{vvr} \quad K_{|v|v} \quad K_{|r|v} \quad K_{|v|r} \quad K_{|r|r} \quad N^L_{uv} \quad N^L_{uuv} \\ & N^L_{vvv} \quad N^L_{rrv} \quad N^L_{ur} \quad N^L_{uur} \quad N^L_{rrr} \quad N^L_{vvr} \quad N_{|v|v} \quad N_{|r|v} \\ & \qquad\qquad N_{|v|r} \quad N_{|r|r} \;\Big]\,. \end{aligned} \tag{6.5}$$

6.3 Identification Results

The regression algorithm used to derive the unknown parameters is the large-scale algorithm within the *lsqcurvefit* function of the *Matlab*© *Optimization Toolbox* (Matlab 2006). This is a *subspace trust region method*, details of which can be found in the works on the *interior-relective Newton method* by Coleman and Li (1996). The data fitting is carried out by solving for the θ_t that best fits the cost function:

$$\min_{\theta_t} \frac{1}{2} \left| \mathbf{F}\left(\theta_t, \boldsymbol{\nu}, \dot{\boldsymbol{\nu}}\right) - \boldsymbol{\tau}_m \right|^2 .$$

Once the coefficients have been found from this analysis, they can be used to reconstruct the PMM test. A capability to do so indicates that the Lagrangian model matches up well with the physical system and hence verifies the structure of the model. This same process is carried out on a different set of test data that was not used in the regression analyses: if the model works even for data that was not included in the regression analysis, the Lagrangian model's suitability is assured.

6.3.1 Verification

This section shows the Lagrangian model compared to its source data. Note that in dynamic tests, several runs are combined into single plots. This is done for reasons of brevity, and is the reason why there are apparent discontinuities in the force and moment data.

The steady drift motion, datapoints of which are shown in Figure 6.5, shows a very good match across a wide range of sideslip angles.

Pure sway is depicted in Figure 6.6. The two datasets match up well. The coupling from sway velocity to yaw moment is evidently dealt with very effectively. These moments are quite large, and there is very little noticeable difference between the experimental data and the Lagrangian model. The coefficients that are of importance here are those such as N^L_{uuv} and N^L_{vvv}.

The discontinuities seen in the plots are due to the merging of separate PMM runs. In the individual tests, the forces change smoothly.

The table below shows the root mean square error in the modelled forces.

DOF	Surge (N)	Sway (N)	Yaw (N)	Roll (N.m)
RMS Error	1.4	10.3	4.3	1.1

RMS Errors from Figure 6.6

The pure yaw is shown in Figure 6.7. These two sets of test data also match up very well.

In comparison to the source data, the surge forces are rather muted in the Lagrangian model. There is more oscillatory behaviour in the source dataset. This suggests that the direct coupling of yaw to surge is slightly underestimated. The fit is still within a few percent.

The roll mode shows noticeable errors, but in this experiment the moments in roll are extremely small; peaking at about 8 N.m. The direct coupling of yaw to roll does not appear to be very significant.

In sway, the forces are quite high, so the coupling from yaw to sway is very important to model.

The RMS errors for the pure yaw case are shown in the following table. The errors are very low, even for sway and yaw.

DOF	Surge (N)	Sway (N)	Yaw (N)	Roll (N.m)
RMS Error	2.8	5.9	9.5	1.8

RMS Errors from Figure 6.7

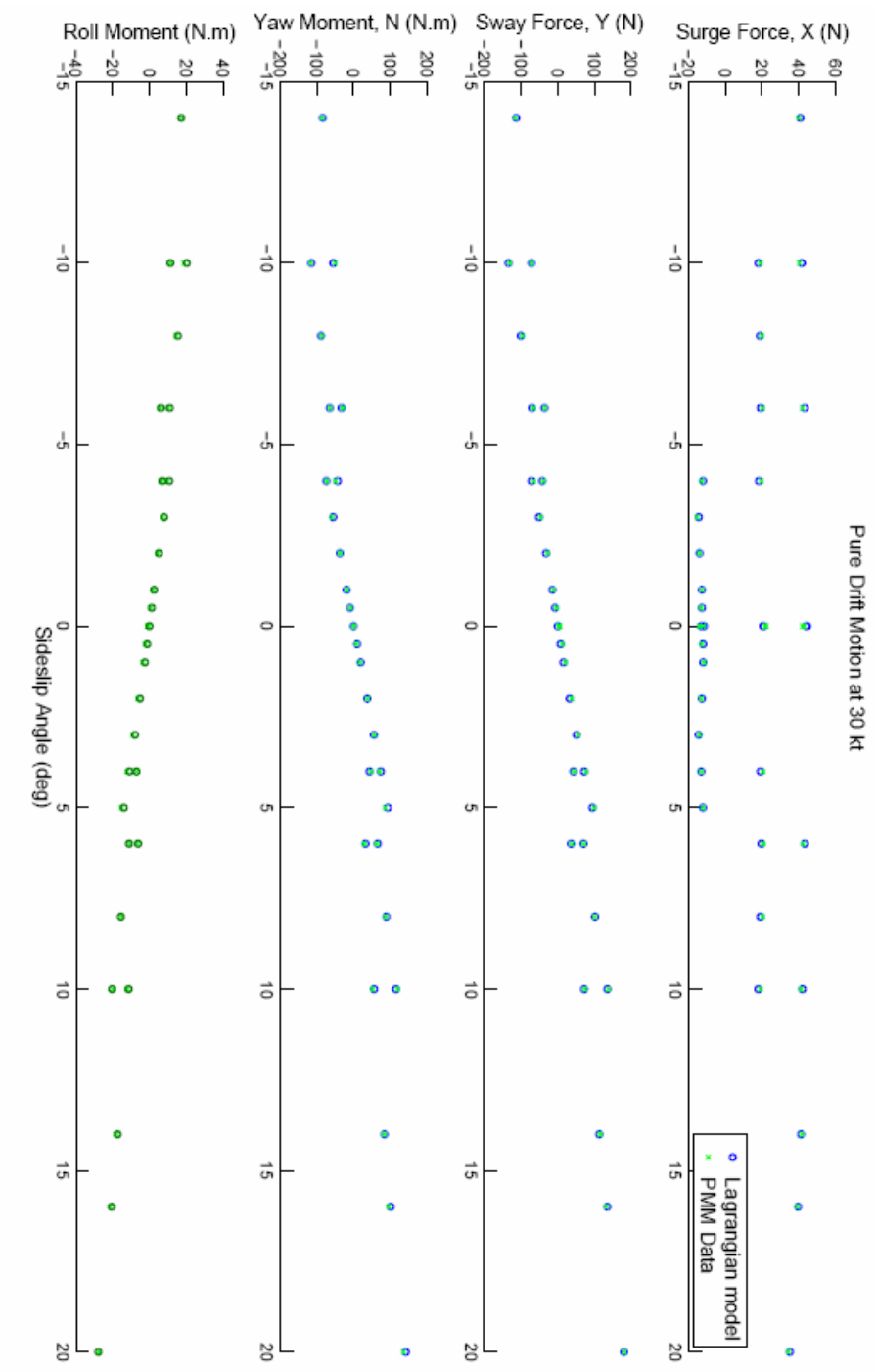

Figure 6.5: Lagrangian model verified with 30 kt steady drift motion

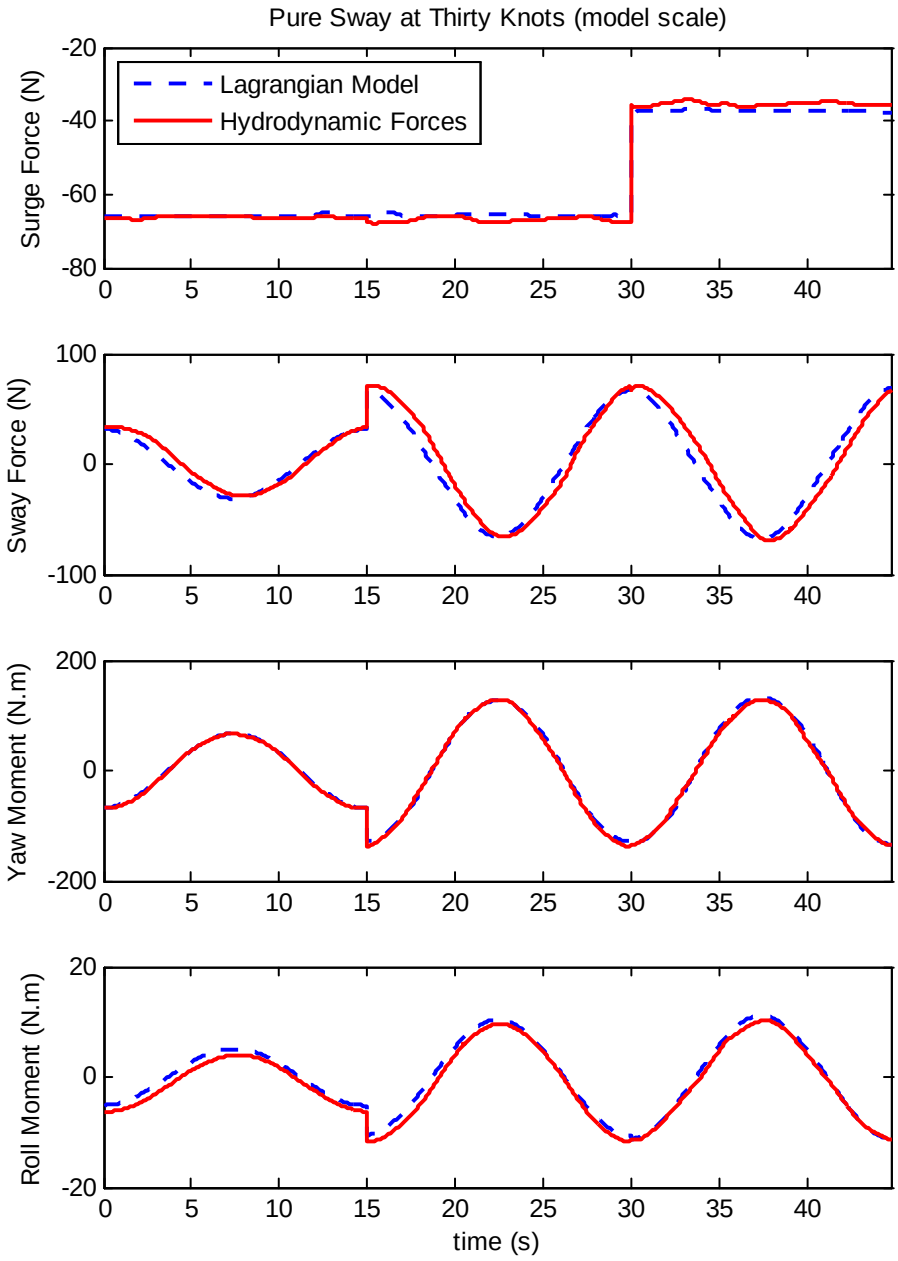

Figure 6.6: Verification of model in pure sway motion.

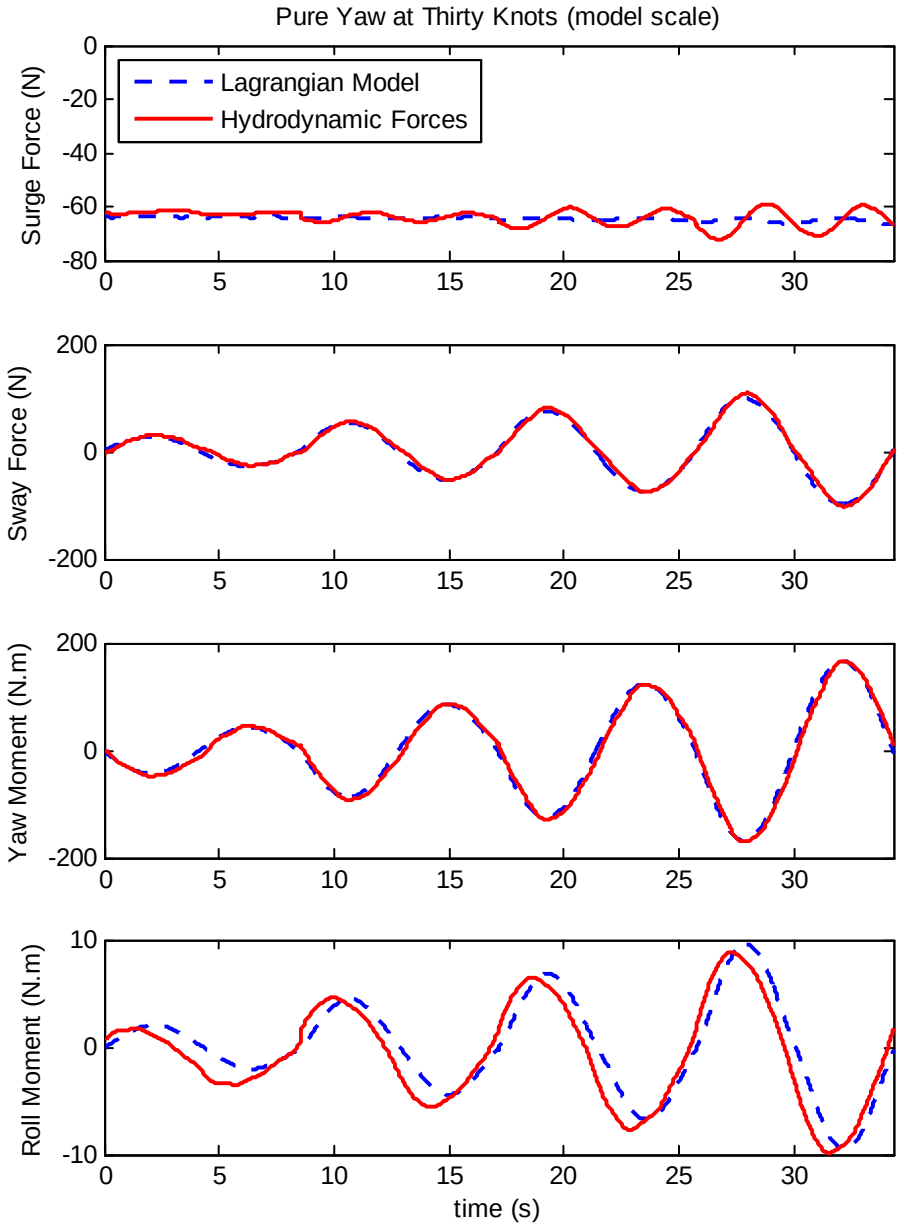

Figure 6.7: Verification of model in pure yaw motion.

Figure 6.8 shows mixed sway and yaw motion. This is the experiment that is most difficult to fit to. The model is moving in surge, sway and yaw all at once, and so all coupling terms are important.

It is worthwhile to compare the magnitude of the forces and moments in the mixed sway yaw case to those of the earlier cases. In Figures 6.6 and 6.7, the typical forces are much smaller than here. This fact demonstrates that it is not sufficient to model the vessel using sway and yaw separately. Dealing with these modes of motion in isolation gives a very poor indication of the forces during regular manoeuvring. The coupled sway–yaw effects have a large effect on the forces and moments observed. Coefficients such as X^L_{rvu} and $N_{|v|r}$ are therefore extremely important.

The high number of discontinuities within the test data is again due to the merging of many PMM runs into one dataset. During each PMM run the forces are smooth.

This strongly suggests the importance of coupled sway–yaw effects. Dealing with sway and then yaw in isolation gives a very poor indication of the effects that take place when both are in action.

DOF	Surge (N)	Sway (N)	Yaw (N)	Roll (N.m)
RMS Error	7.1	8.8	14.1	2.4

RMS Errors from Figure 6.8

6.3.2 Validation

The model is validated using a dataset taken from 18 kt experiments. None of the data presented in this section was used to derive coefficients for the model. The goal of this section is to ascertain whether the Lagrangian model can replicate this unknown data.

Pure yaw experiments are shown in Figure 6.9, while mixed sway and yaw experiments are shown in Figure 6.10. The matching is also very effective at the reduced speed.

The pure yaw test follows very closely in sway, roll and yaw. The match in surge is a little poorer. The source data oscillates much more, which implies that the surge–yaw couplings are being undermodelled at this speed, and so there is a likely Reynold's Number dependence within coefficients like X^L_{urr} and X^L_{rr}. This said, the forces are so small at this speed that the differences are quite negligible.

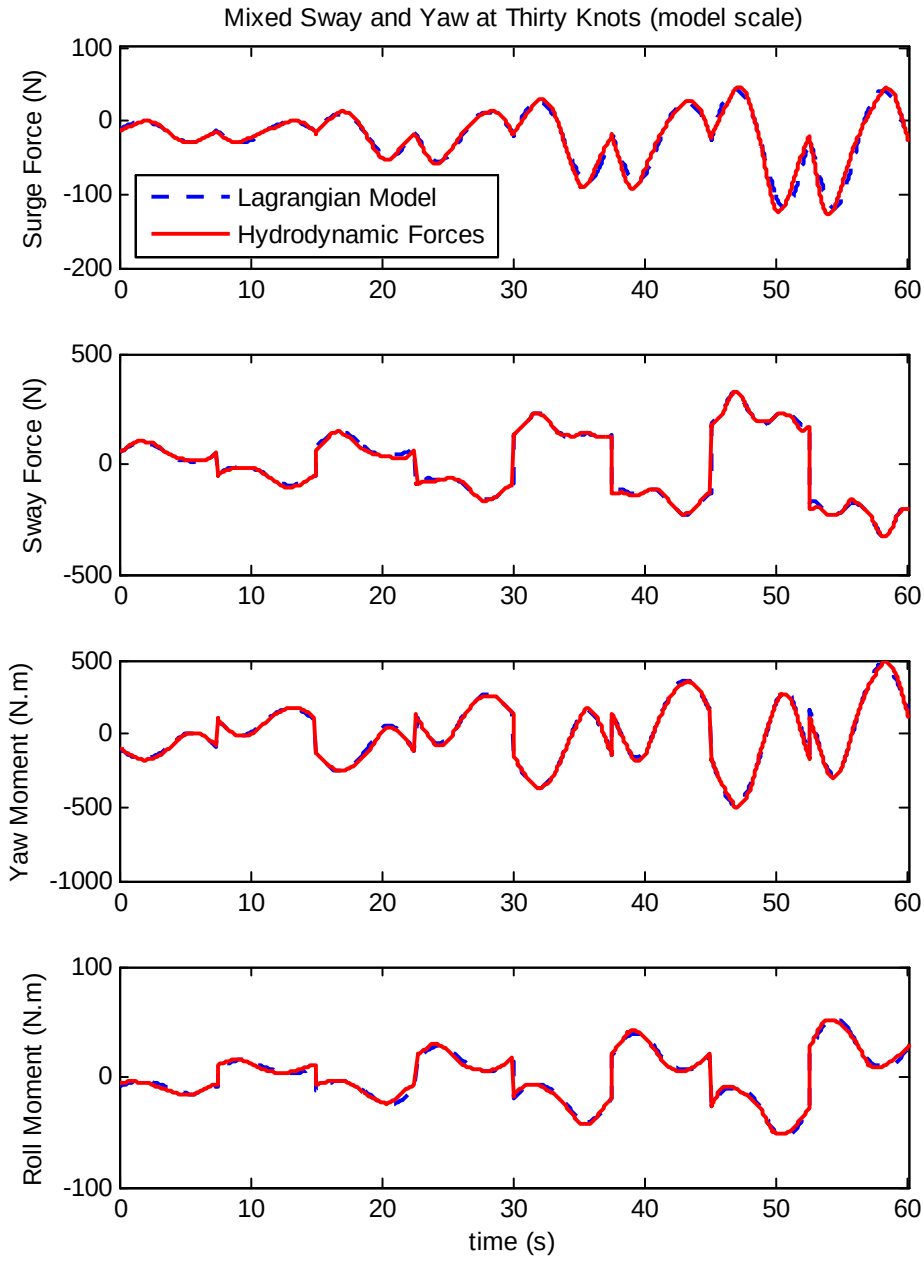

Figure 6.8: Verification of model in mixed sway and yaw motion.

In mixed sway and yaw, the match is thoroughly effective. The accuracy within aggressive manoeuvres is impressive.

DOF	Surge (N)	Sway (N)	Yaw (N)	Roll (N.m)
RMS Error	3.0	2.3	7.2	1.2

RMS Errors from Figure 6.9

DOF	Surge (N)	Sway (N)	Yaw (N)	Roll (N.m)
RMS Error	4.6	4.5	7.9	1.4

RMS Errors from Figure 6.10

6.3.3 Comparison to Pre–existing Model

The conventional PMM derived model, purchased along with the PMM data, was used as a benchmark to compare to.

This model itself is a 4–DOF model, but the surge motion is solely for perturbations about the steady cruise speed. Due to this, the surge motion was not analysed, as no useful information could be derived in comparing the two.

In closeness of fit, the two are often comparable, but the new model shows significant improvement in several respects.

The difference between the two is most marked in the aggressive sway–yaw manoeuvres.

The roll modelling in the Lagrangian model is always tighter, and this is especially the case in pure–yaw motion. This demonstrates the more effective coupling from surge and yaw to roll.

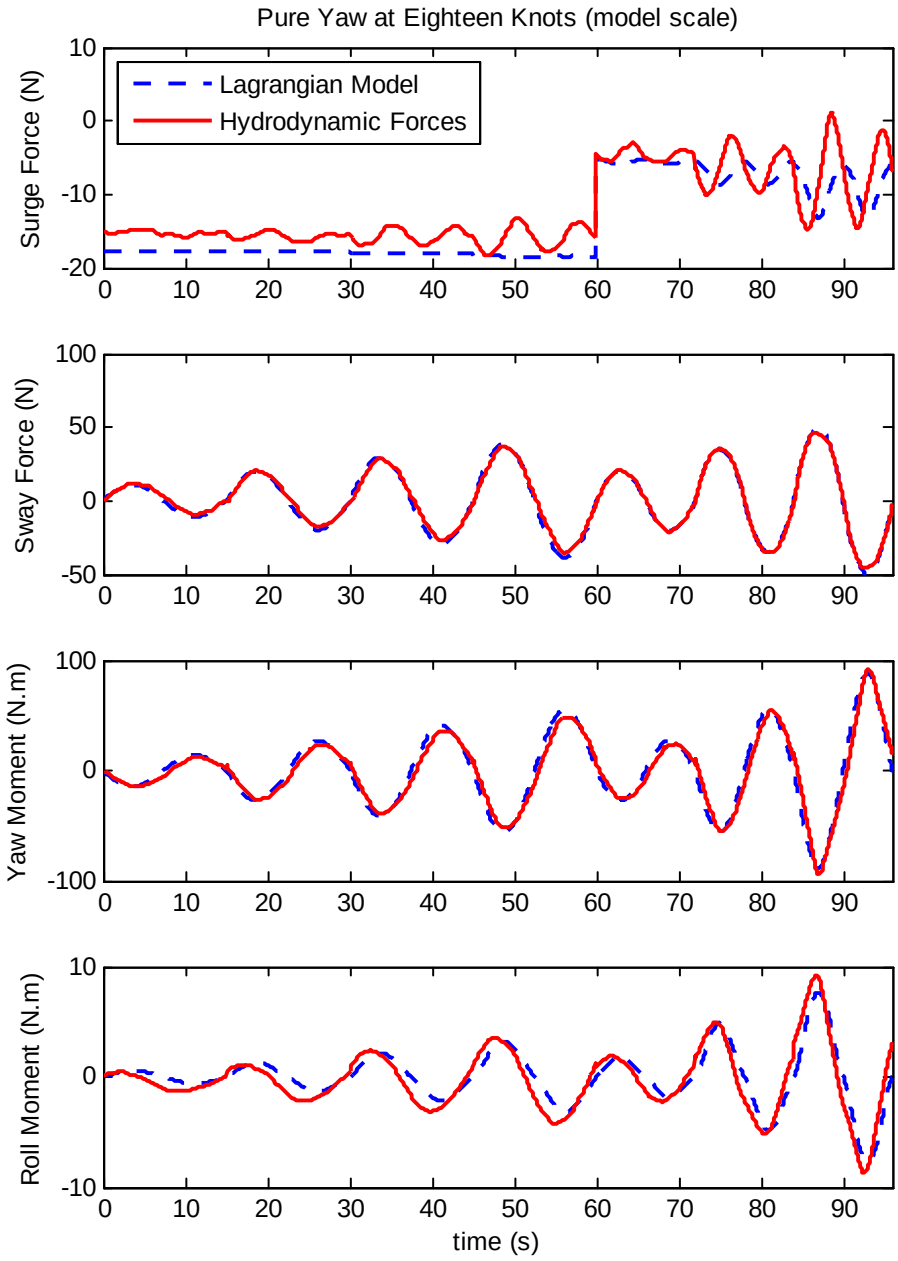

Figure 6.9: Model performance at 18 knots pure yaw.

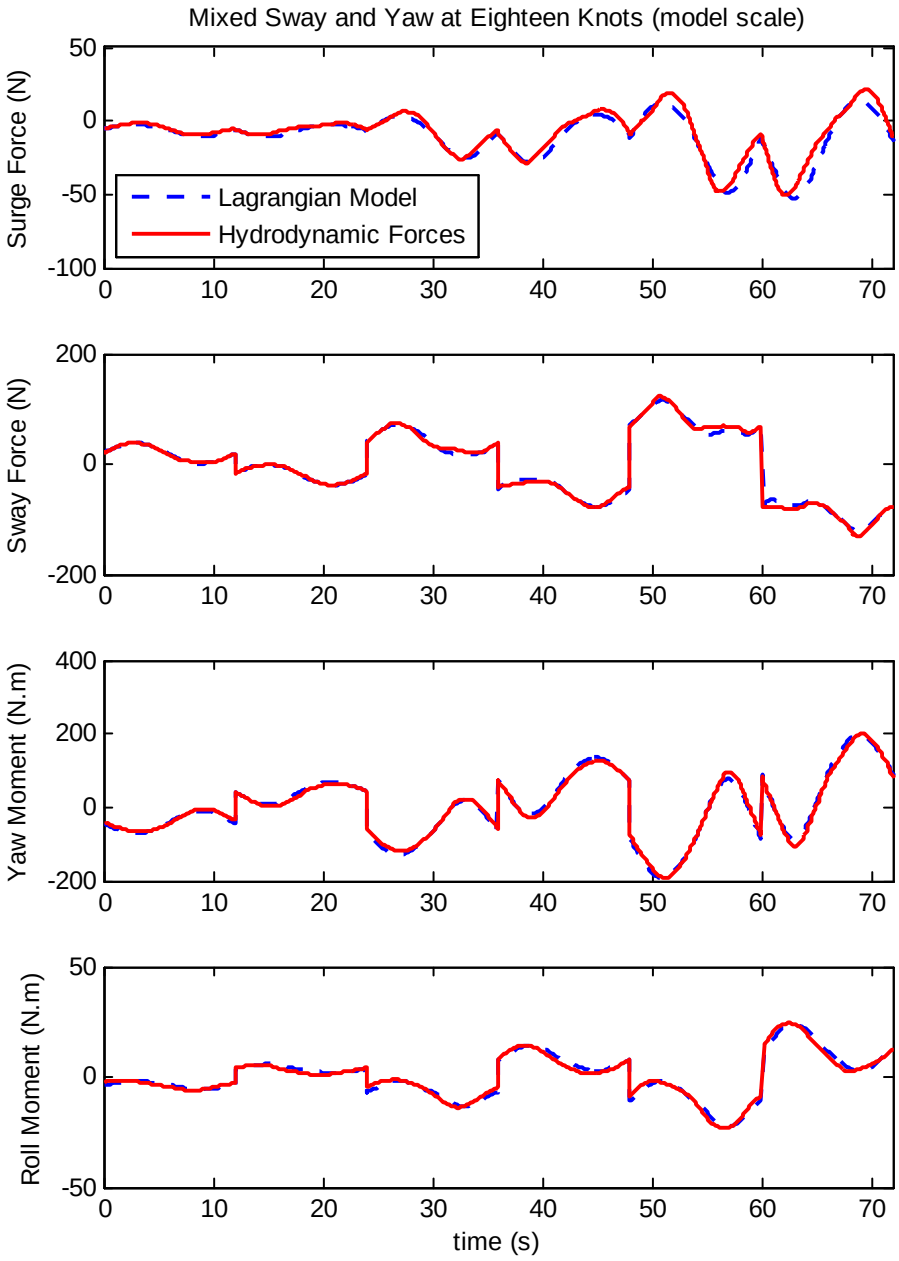

Figure 6.10: Model performance at 18 knots mixed sway and yaw.

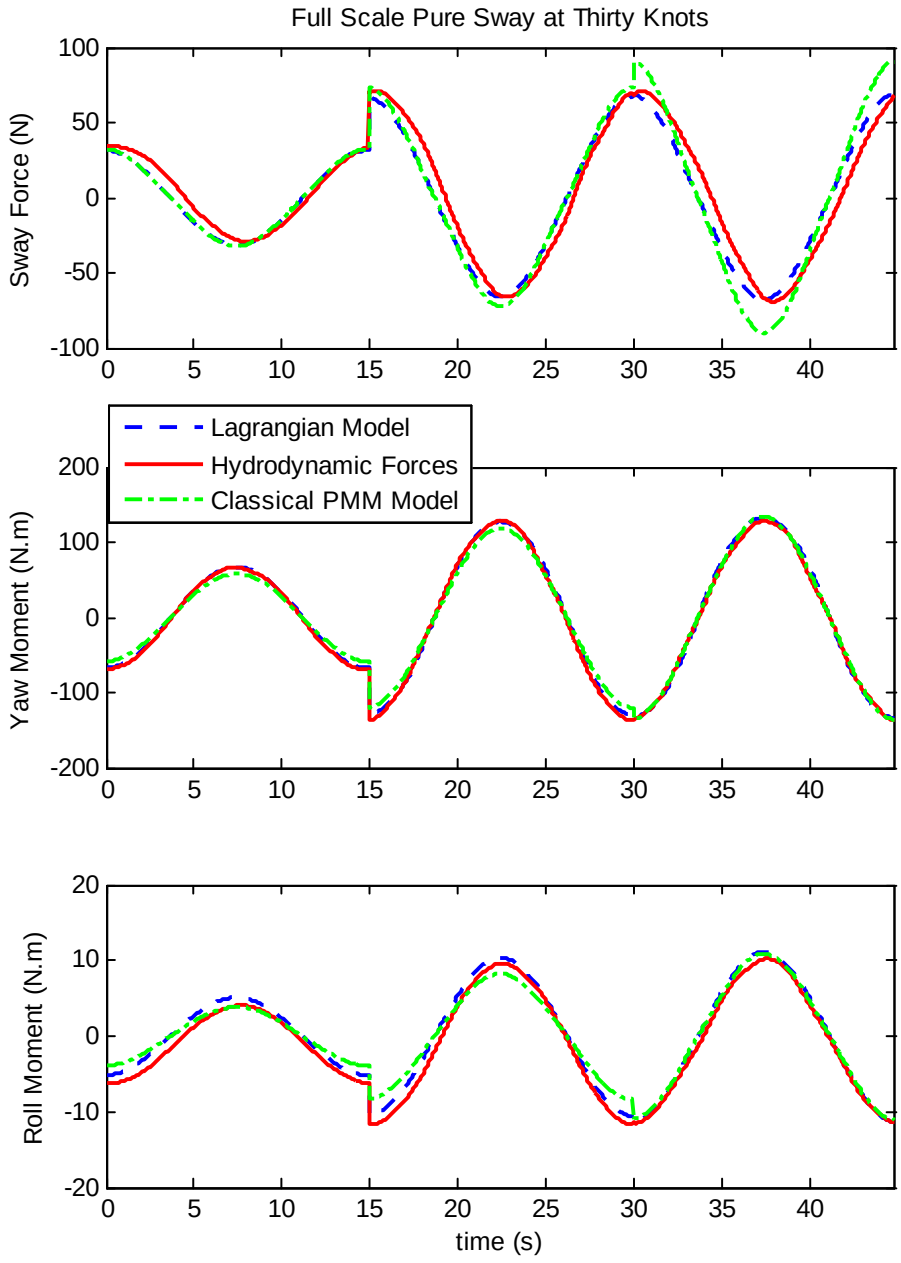

Figure 6.11: Comparison between model types in pure sway motion at 30kt.

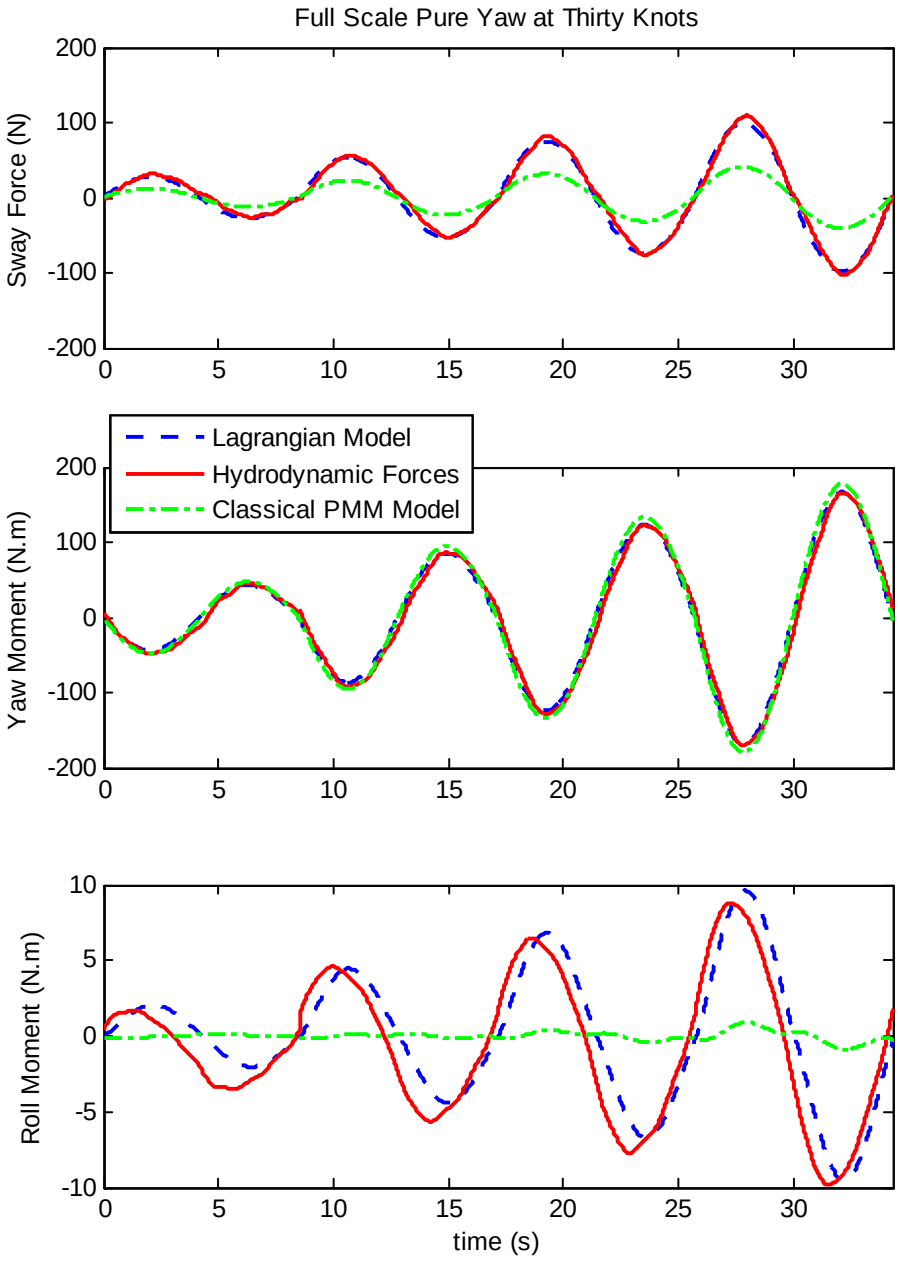

Figure 6.12: Comparison between model types in pure yaw motion at 30kt.

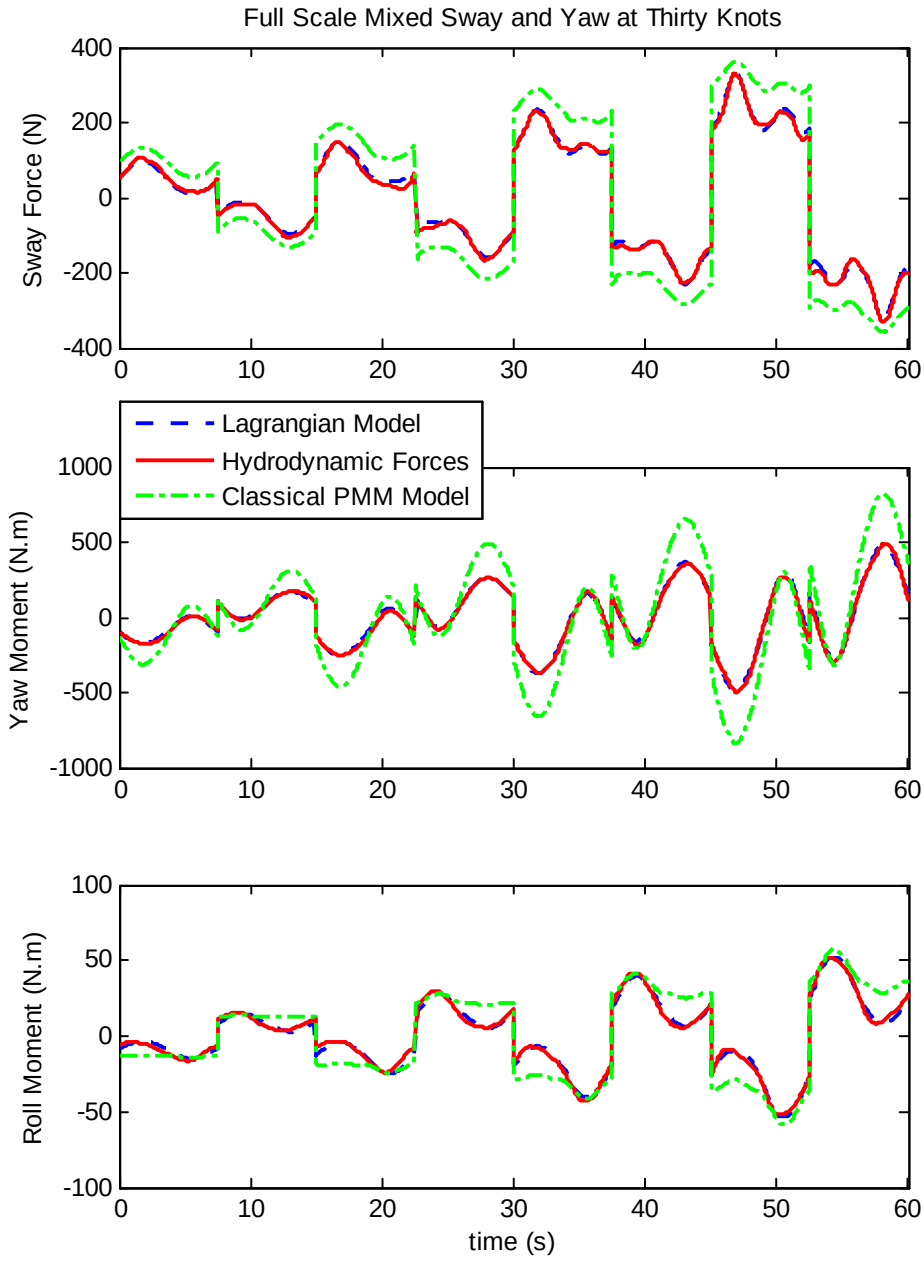

Figure 6.13: Comparison between model types in mixed sway and yaw motion at 30kt.

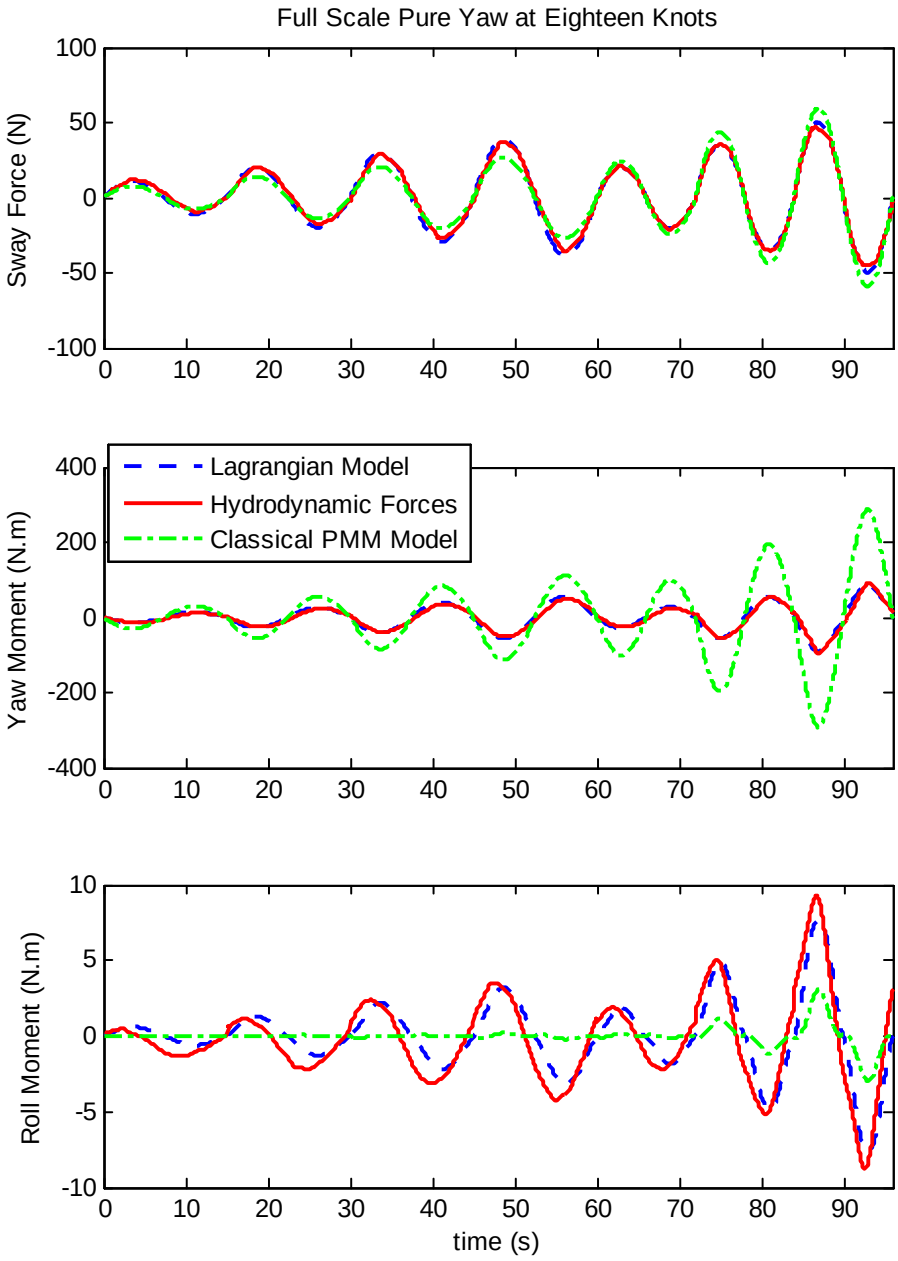

Figure 6.14: Comparison between model types in pure yaw motion at 18kt.

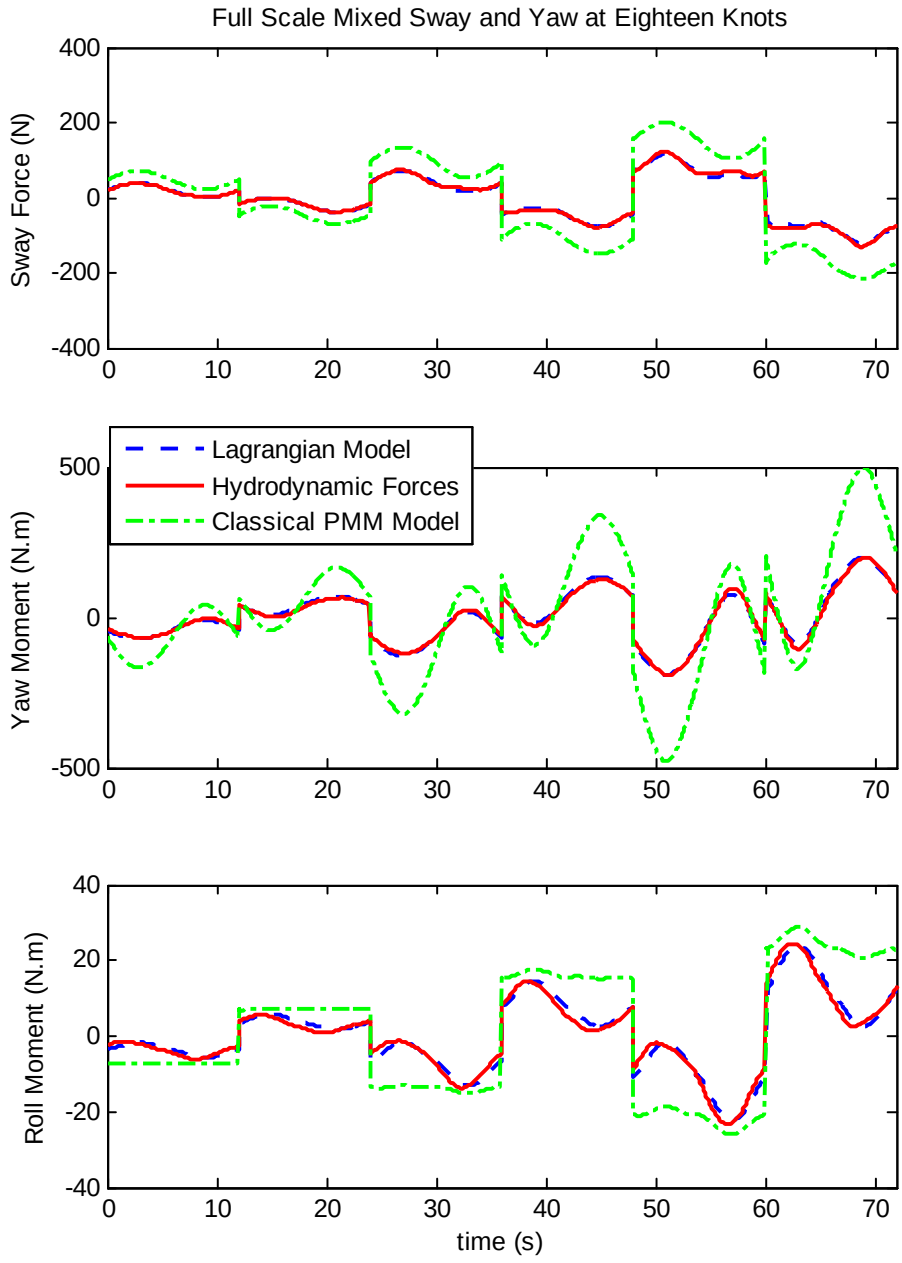

Figure 6.15: Comparison between model types in mixed sway and yaw motion at 18kt.

Chapter 7

Full–scale Trials

The tests presented in this chapter are additional verification tests. The source for this data is a set of full–scale trials on a trimaran. The results presented in this chapter verify that the model is sufficiently advanced by showing that it can match full–scale test data.

7.1 Vessel Details

Full–scale tests were carried out on the *Benchijigua Express*; an Austal–designed 127m long trimaran for use in vehicle and passenger transport. The ship is shown in Figure 7.1. This is a high speed vessel; operating at up to 40 kt.

The tests were carried out off the west coast of Australia, near Fremantle.

7.2 Test Details

In this chapter, the test data is far less ideal than in Chapter 6. The PMM tests had all force, position, velocity and acceleration measurements with virtually no noise whatsoever. In contrast, the full–scale tests were carried out in relatively calm water, but with significantly worse measurement technology available. Although the sea was fairly calm, there was still noticeable swell, and in addition the tests were carried out in an area known to have fairly significant current.

Position measurements were recorded from a global positioning system. These were augmented with roll angle and yaw rate measurements which

Figure 7.1: The H260 *Benchijigua Express,* courtesy of Austal Ships.

were derived from the vessel's ride control system. The unknown velocities were calculated by taking the derivatives of the measured positions.

The data available is a set of zig–zag tests. The vessel began from a steady forward speed at around 35 kt.

A much reduced order model is implemented in this chapter. There are a number of reasons why this is advisable. Firstly, the range of motions to be simulated is limited: only a few zig–zag oscillations are available. There is no real need for the full model to explain the test data. Secondly, the quality of the measured data is far poorer. There are no measurements of acceleration, and the control forces are similarly generated from calculation alone.

The parameter vector in this test is given by:

$$\begin{aligned}\theta_t \;=\; \big[\; & X^0_{\dot u} \quad Y^0_{\dot v} \quad \tfrac{1}{2}\left(N^0_{\dot v} + Y^0_{\dot r}\right) \quad \tfrac{1}{2}\left(Y_{\dot p} + K_{\dot v}\right) \quad \tfrac{1}{2}\left(K_{\dot r} + N_{\dot p}\right) \quad N_{\dot r} \\ & X^L_{uu} \quad X^L_{rvu} \quad Y^L_{uv} \quad Y^L_{ur} \quad Y_{|v|v} \quad Y_{|r|v} \\ & Y_{|v|r} \quad Y_{|r|r} \quad K^L_{uv} \quad K^L_{ur} \quad K_{|v|v} \quad K_{|r|v} \\ & K_{|v|r} \quad K_{|r|r} \quad N^L_{uv} \quad N^L_{ur} \quad N_{|v|v} \quad N_{|r|v} \quad N_{|v|r} \quad N_{|r|r} \;\big] \end{aligned} \tag{7.1}$$

Once again, the problem is to minimise:

$$\min_{\theta_t} \frac{1}{2} \left| \mathbf{F}\left(\theta_t, \boldsymbol{\nu}, \dot{\boldsymbol{\nu}}\right) - \boldsymbol{\tau}_m \right|^2 .$$

This minimisation problem was carried out using a genetic algorithm from (Passino 2005).

7.3 Results

To quantify the performance the coefficient of determination R^2 was calculated. This coefficient is defined as follows:

$$R^2 = \frac{\sum \left(\hat{D} - \bar{D}\right)^2}{\sum \left(\hat{D} - D\right)^2 + \sum \left(\hat{D} - \bar{D}\right)^2}, \tag{7.2}$$

where D and $\bar{D}$ are the measured data and the mean respectively, and $\hat{D}$ is the estimate of the data that the model generates. Each number is defined on $[0, 1]$ and gives an indicator of what proportion of the data is replicable.The values are shown below:

Data	R^2 Error
u	0.91
v	0.45
p	0.86
r	0.97
ϕ	0.94
ψ	0.90

R^2 from Figures 7.2 and 7.3

The match is generally very good. The match in sway is rather poorer than the rest. There are far more oscillations in the sway velocity, and it is unclear if this is purely due to differentiated noise.

7.4 Comments

The dynamics involved in the zig–zag tests are not very rich. The need for such an advanced model is therefore not necessary. The same test–data could just as well be replicated with an older model. The results presented in this chapter only show that the model is no less capable. Cautious optimism is the only sentiment that can be taken from the results presented in this chapter.

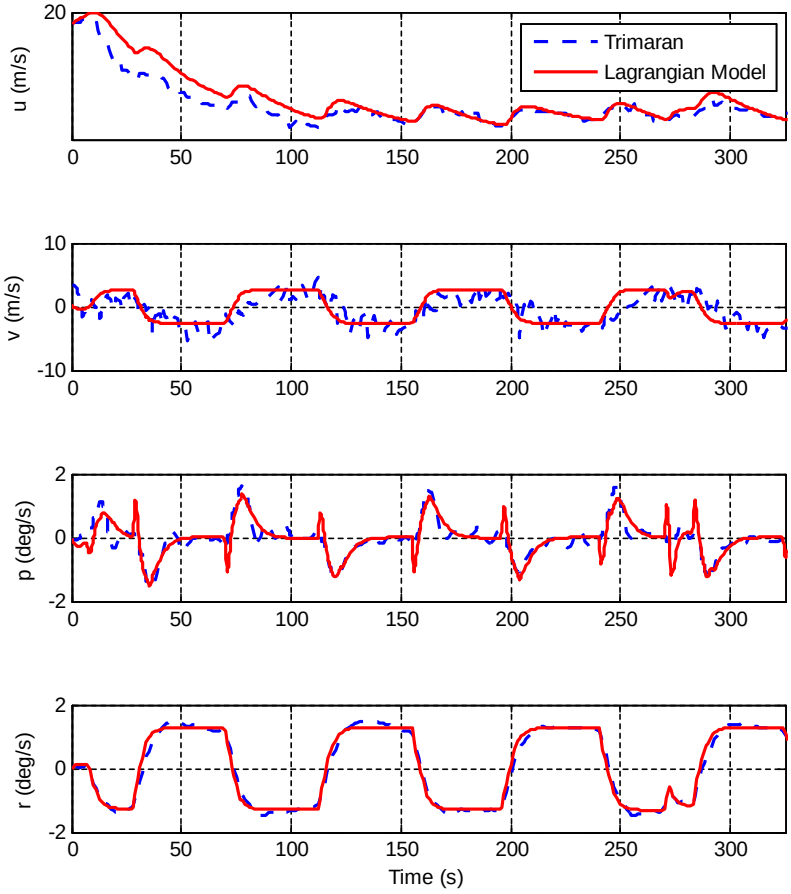

Figure 7.2: Body–fixed velocities during zig–zag manoeuvre

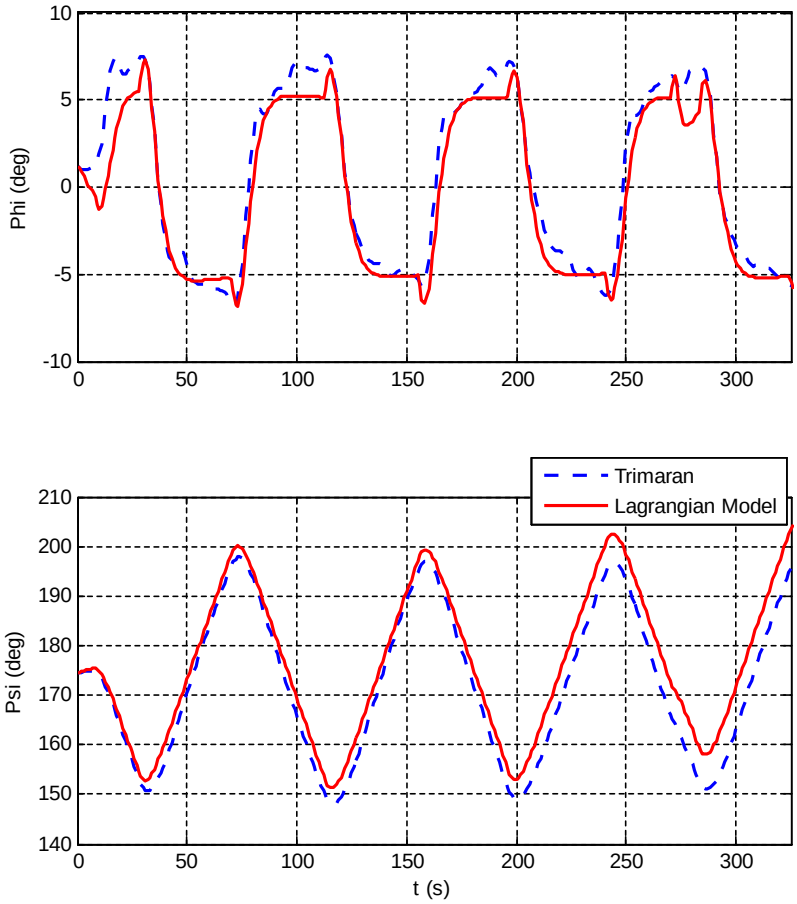

Figure 7.3: Roll angle and heading angle during zig–zag tests.

Chapter 8

Conclusions

The thesis has focused on modelling manoeuvring vessels. The goal was to discover a physically motivated model structure. Using lift and drag theory, a complex and advanced model of a ship was derived. The structure of the model makes it well–suited to a variety of simulation and control tasks.

The focus of the first part was to derive a model structure: the focus was not on the numerical determination of its parameters. The second part of the thesis was then to use experimental data to evaluate the model's abilities. The model was tested against a variety of high–quality PMM test data, and performed very well. It proved capable of replicating the test data by which it was derived. Furthermore, it proved capable of replicating additional tests. This one set of coefficients were shown to work very well across a wide speed range.

Full–scale tests on a high performance trimaran were presented. The Lagrangian model was shown to be capable of matching these tests effectively, further demonstrating its strengths.

In addition to these results, Kirchhoff's Equations were applied to derive an advanced yet useful formulation of the equations of motion. The end result is a generally applicable mathematical framework for manoeuvring through the seas.

The motivation throughout was to restore physicality to the modelling process, and a good deal of success has been enjoyed in this.

8.1 Future Work

The main body of work in the thesis can be improved upon with more experimental data. Very recent trends give the future of the field an optimistic

air. The SIMMAN conference (*SIMMAN* 2008) made available extensive sets of test data for several vessels, giving the community a free and open resource for use as a benchmark.

The dynamics of the roll mode were not able to be evaluated using the PMM data, although the full scale verification did identify some of these dynamics. Furthermore, only a single vessel was tested. Extensive testing is certainly desirable.

At no point in this thesis was online identification contemplated. There is a long history of using these methods for manoeuvring ships. Applying these methods to such an extensive model is no easy task. Progress in this area would be very useful.

Additionally, although a new framework for the equations of motion was presented, no attempt was made to tie this to any hydrodynamic code. Such an approach could lead to quick and effective development of simulation tools.

Bibliography

Abkowitz, M. A. (1964). Lectures on Ship Hydrodynamics - Steering and Maneuverability. Technical Report Hy-5. Hydro- and Aerodynamic's Laboratory. Lyngby, Denmark.

Abkowitz, M. A. (1975). System Identification Techniques for Ship Maneuvering Trials. In: *Proceeding of Symposium on Control Theory and Navy Applications*. Monterey, CA. pp. 337–393.

Abkowitz, M. A. (1980). Measurement of Hydrodynamic Characteristics from Ship Maneuvring Trials by System Identification. In: *Transactions on SNAME, 88:283–318*.

Anon. (1992). Atmospheric and space flight vehicle coordinate systems. Technical Report R-004-1992. ANSI/AIAA.

Aranha, J.A.P., S. da Silva, M.R. Martins and A.J.P. Leite (2001). A weathervane ship under wave and current action: an experimental verification of the wave drift damping formula. *Applied Ocean Research* **23**, 103–110.

Archimedes (2007). *The Works of Archimedes*. Kessinger Publishing Co. edited by T.L. Heath.

Arfken, G. (1985). *Mathematical Methods for Physicists*. 198-200. 3rd ed.. Academic Press.

Aristotle (*ca.* 330 B.C.). *On Physics*. 2004 ed.. Kessinger Publishing.

Ayaz, Z, D. Vassalos, J. Kostas and J. Spyrou (2006). Maneouvring behaviour of ships in extreme astern seas. *Journal of Ocean Engineering* **33**, 2381–2434.

Bailey, P.A., W.G. Price and P. Temarel (1997). A unified mathematical model describing the manoeuvring of a ship travelling in a seaway. *Transactions of the Royal Institute of Naval Architects* **140**, 131–149.

Bass, D. W. and M.R. Haddara (1988). Nonlinear models of ship roll damping. *International Shipbuilding Progress* **35**(401), 5–24.

Bech, M. I. and L. Wagner Smith (1969). Analogue Simulation of Ship Maneuvers. Technical Report Hy-14. Hydro- and Aerodynamics Laboratory. Lyngby, Denmark.

Berg, Tor Einar and T.U. Utnes (1978). A note on added mass calculation in connection with linear theory for the manoeuvring ship. Technical report. Norwegian Technical University. NTH, Trondheim.

Bernoulli, D. (1738). *Hydrodynamica*. 2004 ed.. Dover Books. Joint publication of Hydrodynamica and Hydraulica.

Bernoulli, Jakob (1703). Dèmonstration gènèrale du centre de balancement ou d'oscillation, tirèe de la nature du levier. *Mèmoires de l' Acadèmie des Sciences*.

Bernoulli, John (1743). *Hydraulica*. 2004 ed.. Dover Books. Joint publication of Hydrodynamica and Hydraulica.

Beukelman, W. and J.M.J. Journee (2001). Hydrodynamic transverse loads on ships in deep and shallow waters. In: *22nd International Conference on Hydrodynamics and Aerodynamics in Marine Engineering*.

Birkhoff, G. (1960). *Hydrodynamics-A Study in Logic, Fact and Similitude*. Princeton University Press. Princeton, New Jersey.

Bishop, R. E. D., W. G. Price and P. Temarel (1984). A functional representation of fluid actions on ships. *International Shipbuilding Progress* **31**, 239–249.

Bishop, R.E.D. and W.G. Price (1981). On the use of equilibrium axes and body axes in the dynamics of a rigid ship. *Journal of Mechanical Engineering Science* **23**(5), 243–256.

Blanke, M. (1981). Ship Propulsion Losses Related to Automated Steering and Prime Mover Control. PhD thesis. The Technical University of Denmark, Lyngby.

Blanke, M. and A. G. Jensen (1997). Dynamic Properties of Container Vessel with Low Metacentric Height. *Transactions of the Institute of Measurement and Control* **TIMC-19**(2), 78–93.

Bouguer, P. (1746). *Traitè du Navire*.

Bracewell, R. (1999). *The Fourier Transform and Its Applications*. 3rd ed.. McGraw–Hill. New York.

Christensen, A. and M. Blanke (1986). A Linearized State-Space Model in Steering and Roll of a High-Speed Container Ship. Technical Report 86-D-574. Servolaboratoriet, Technical University of Denmark. Denmark.

Clarke, D. (2003). The foundations of steering and maneuvering. In: *Proceedings of the IFAC Conference on Control Applications*. Plenary talk.

Clarke, D., P. Gedling and G. Hine (1983). The application of manoeuvring criteria in hull design using linear theory. In: *Proceedings of the Royal Institute of Naval Architects*. Royal Institute of Naval Architects. pp. 45–68.

Cohen, M. and Drabkin, I.E., Eds.) (1948). *Source Book in Greek Science*. McGraw-Hill Book Company Inc. First Edition.

Coleman, T.F and Y. Li (1996). An interior, trust region approach for nonlinear minimization subject to bounds. *SIAM Journal on Optimization* **6**, 418–445.

Craig, J. J. (1989). *Introduction to Robotics*. Addison-Wesley. Reading, Massachusetts.

Cummins, W.E. (1962). The impulse response function and ship motions. Technical Report 1661. David Taylor Model Basin, Hydromechanics Laboratory, USA.

Davidson, K. S. M. and L. I. Schiff (1946). Turning and Course Keeping Qualities. *Transactions of SNAME*.

di Casalè, Giovanni (1346). *On the Velocity of the Motion of Alteration*.

Duhem, P. (1917). Research on the history of physical theories. *Synthese* **83**(2), 189–200. Essay from 1917, reprinted May 1990.

Egeland, O. and J. T. Gravdahl (2002). *Modeling and Simulation for Automatic Control*. Marine Cybernetics. Trondheim, Norway.

Euler, L. (1749). *Scientia Navalis*. 1980 ed.. Birkhäuser Basel. written *ca. 1738*, edited by C. Truesdell.

Euler, L. (1750). Discovery of a new principal of mechanics. *Mèmoires de l' Acadèmie des Sciences* **Par. XXIII**, 196.

Euler, L. (1776). Novi Commentarii Academiae Scientairum Imperialis Petropolitane. - **Vol. XX**, 189.

Faltinsen, O. M. (1990). *Sea Loads on Ships and Offshore Structures*. Cambridge University Press.

Faltinsen, O.M. (2006*a*). *Hydrodynamics of High-Speed Vessels*. Cambridge University Press. New York City, NY, USA.

Faltinsen, O.M. (2006*b*). *Hydrodynamics of High-Speed Vessels*. Cambridge University Press. New York City, NY, USA.

Fedayevsky, K.K. and G.V. Sobolev (1963). *Control and Stability in Ship Design*. State Union Shipbuilding Publishing House. Leningrad, USSR.

Ferreiro, L. (2006). *Ships and Science: The Birth of Naval Architecture in the Scientific Revolution*. MIT Press.

Fossen, T. I. (1994). *Guidance and Control of Ocean Vehicles*. John Wiley and Sons Ltd. ISBN 0-471-94113-1.

Fossen, T. I. (2002*a*). *Marine Control Systems: Guidance, Navigation and Control of Ships, Rigs and Underwater Vehicles*. Marine Cybernetics AS. Trondheim, Norway. ISBN 82-92356-00-2.

Fossen, T. I. (2002*b*). *Marine Control Systems: Guidance, Navigation and Control of Ships, Rigs and Underwater Vehicles*. 3rd. printing onwards ed.. Marine Cybernetics AS. Trondheim, Norway. ISBN 82-92356-00-2.

Fossen, T.I. (2005). A nonlinear unified state space model for ship maneuvering and control in a seaway. *Journal of Bifurcation and Chaos*.

Galilei, Galileo (*ca.* 1602). *On Motion and Mechanics*. 1960 ed.. University of Wisconsin Press.

Galileo (1638). *Dialogue Concerning Two New Sciences*. Elsevier.

Golding, B., A. Ross and T.I. Fossen (2006). Identification of nonlinear viscous damping terms for marine vessels. In: *IFAC SYSID'06*.

Goldstein, H., C. P. Poole and J. L. Safko (1953). *Classical Mechanics*. 3rd edition, 2001 ed.. Addison-Wesley. Reading, MA, USA. "Euler Angles in Alternate Conventions".

Gradshteyn, I. S. and I. M. Ryzhik (2000). *Tables of Integrals, Series, and Products*. 6th ed.. Academic Press. San Diego, CA, USA.

Herman, L.K. (1995). The history, definition and pecularities of the earth centered inertial (eci) coordinate frame and the scales that measure time. In: *Proceedings of the IEEE Aerospace Applications Conference*. Vol. 2. Aspen, CO, USA. pp. 233–263.

Himeno, Y. (1981). Prediction of ship roll damping- state of the art. Technical report. Department of Naval Architecture and Marine Engineering. University of Michigan.

Hirano, M. and J. Takashina (1980). A calculation of ship turning motion taking coupling effect due to heel into consideration. *Trans. West-Japan Soc. of Naval Architects* **59**, 77–81.

Hoerner, S.F. (1965). *Fluid Dynamic Drag: Theoretical, Experimental and Statistical Information*. Hoerner Fluid Dynamics.

Hoerner, Sighard F. and H.V. Borst (1975). *Fluid-Dynamic Lift: Information on Lift and its Derivatives in Air and in Water*. Hoerner Fluid Dynamics. Bakersfield, CA 93390, USA.

Hooft, J.P. (1994). The cross-flow drag on a manoeuvring ship. *Ocean Engineering* **21**(3), 329–342.

Hwang, Wei-Yuan (1980). Application of System Identification to Ship Maneuvering. PhD thesis. Massachussetts Institute of Technology.

Ikeda, Y., K. Komatsu, Y. Himeno and N. Tanaka (1976). On roll damping force of ship: Effects of friction of hull and normal force of bilge keels. *J. Kansai Society of Naval Architects* **142**, 54–66.

Imlay, F. H. (1961). The Complete Expressions for Added Mass of a Rigid Body Moving in an Ideal Fluid. Technical Report DTMB 1528. David Taylor Model Basin. Washington D.C.

Inoue, S., M. Hirano and K. Kijima (1981). Hydrodynamic derivatives on ship manoeuvring. *International Shipbuilding Progress* **28**(321), 112–125.

Jones, R.T. (1946). Properties of low-aspect ratio wings at speeds below and above the speed sounds. Technical Report 835. National Advisory Committee for Aeronautics (NACA).

Journée, J.M.J. and W.W. Massie (2001). *Offshore Hydromechanics*. Delft University of Technology. The Netherlands.

Källström, C. G. and K. J. Åström (1981). Experiences of system identification applied to ship steering. *Automatica* **17**(1), 187–198.

Karasuno, K. and K. Igarashi (1990). Physical mathematical models of hydro- or aero-dynamic forces acting on ships moving in an oblique direction. In: *Proc. of MARSIM & ICSM '90*. Tokyo, Japan.

Kelvin, William Thomson and Peter Guthrie Tait (1896). *Treatise on Natural Philosophy*. Vol. 1. Adamant Media Corporation.

Khalil, H. K. (2002). *Nonlinear Systems*. MacMillan. New York.

Kijima, K., N. Yasuaki and T. Masaki (1990*a*). Prediction method of ship manoeuvrability in deep water. In: *Proceedings of Marsim & ISCM 90*. Tokyo, Japan.

Kijima, K., T. Katsuno, Y. Nakiri and Y. Furukawa (1990*b*). On the manoeuvring performance of a ship with the parameter of loading condition. *Journal of the Society of Naval Architects of Japan* **168**, 141–148.

Kirchhoff, G. (1869). *Über die Bewegung eines Rotationskorpers in einer Flussigkeit*. Crelle's Journal, No. 71, pp. 237–273. *(in German).*

Kreyszig, Erwin (1999). Advanced Engineering Mathematics. *John Wiley & Sons, Inc.*

Krstic, M., I. Kanellakopoulos and P. V. Kokotovic (1995). Nonlinear and Adaptive Control Design. *John Wiley and Sons Ltd. New York.*

Lagrange, J. L. (1788). Mècanique Analytique (Analytical Mechanics). *Boston Studies in the Philosophy of Science. 2001 ed.. Springer.*

Lamb, H. (1932). Hydrodynamics. *Cambridge University Press. London.*

Leite, A.J.P., J.A.P Aranha, C. Umeda and M.B. de Conti (1998). Current forces in tankers and bifurcation of equilibrium of turret systems: hydrodynamic model and experiments. Applied Ocean Research **20**, *145–156.*

*Lewis, E. V., Ed.) (1989*a*).* Principles of Naval Architecture. *2nd ed.. Society of Naval Architects and Marine Engineers (SNAME).*

*Lewis, E.V., Ed.) (1989*b*).* Principles of Naval Architecture. *2nd ed.. Society of Naval Architects and Marine Engineers (SNAME).*

Lifshitz, E. M. and L. D. Landau (1982). Course of Theoretical Physics : Mechanics. *3rd edition ed.. Butterworth-Heinemann.*

Lloyd, A.R.J.M. (1998). Seakeeping: Ship behaviour in rough weather. *A.R.J.M. Lloyd. 26 Spithead Avenue, Gosport, Hampshire, UK.*

Mach, E. (1883). The science of mechanics: A critical and historical account of its development. *Open Court Publishing Company. Chicago, IL, USA. 1960 printing.*

Matlab (2006). Optimization Toolbox Manual. *The Mathworks, Inc. Version 3.1.*

Matsuura, J.P.J., K. Nimishoto, M.M. Brenitsas and L.O. Garza-Rios (2000). Comparative assessment of hydrodynamic models in slow-motion mooring dynamics. Journal of Offshore Mechanics and Arctic Engineering **122**, *109–117.*

Meirovitch, L. and M. K. Kwak (1989). State Equations for a Spacecraft With Flexible Appendages in Terms of Quasi-Coordinates. Applied Mechanics Reviews **42***(11), 161–170.*

Milne-Thomson, L. M. (1968). Theoretical Hydrodynamics. *MacMillan Education Ltd. London.*

*MMG (1977*a*). MMG report I. Technical Report 575. Journal of the Society of Naval Architects of Japan.*

*MMG (1977*b*). MMG report II. Technical Report 577. Journal of the Society of Naval Architects of Japan.*

*MMG (1977*c*). MMG report III. Technical Report 578. Journal of the Society of Naval Architects of Japan.*

*MMG (1977*d*). MMG report IV. Technical Report 579. Journal of the Society of Naval Architects of Japan.*

MMG (1980). MMG report V. Technical Report 616. Journal of the Society of Naval Architects of Japan.

Munk, M. M. (1936). Aerodynamics Theory: Aerodynamics of Airships*. Vol. VI. Berlin: Springer. ed. W. F. Durand.*

Naidu, D. S. (2003). Optimal Control Systems*. CRC Press. ISBN 0-8493-0892-5.*

Newman, J. N. (1977). Marine Hydrodynamics*. MIT Press. Cambridge, MA.*

Noll, W. (2006). On the past and future of natural phiosophy. Journal of Elasticity **84***(1), 1–11.*

Nomoto, K., T. Taguchi, K. Honda and S. Hirano (1957). On the Steering Qualities of Ships. Technical report. International Shipbuilding Progress, Vol. 4.

Norrbin, N. (1971). Theory and observations on the use of a mathematical model for ship manoeuvring in deep and confined water. Technical Report 63. Swedish State Shipbuilding Experimental Tank. Gothenburg.

Norrbin, N. H. (1963). On the Design and Analyses of the Zig-Zag Test on Base of Quasi Linear Frequency Response. Technical Report B 104-3. The Swedish State Shipbuilding Experimental Tank (SSPA). Gothenburg, Sweden.

Norrbin, N. H. (1970). Theory and Observation on the use of a Mathematical Model for Ship Maneuvering in Deep and Confined Waters. In: Proc. of the 8th Symposium on Naval Hydrodynamics*. Pasadena, California.*

Obokata, J. (1987). On the basic design of single point mooring systems. Journal of the Society of Naval Architects of Japan **161***, 183–195. In Japanese.*

Obokata, J. and N. Sasaki (1982). On the horizontal slow oscillations and the dynamic stability of a ship moored to single point moorings. Transactions of the West-Japan Society of Naval Architects **186***, 87–93. In Japanese.*

Obokata, J., N. Sasaki and J. Nagashima (1981). On the estimation of current force induced on a ship hull by some tests. Journal of the Kansai Society of Naval Architects of Japan **180**, *47–57. In Japanese.*

Ogilvie, T.F. (1964). Recent progress towards the understanding and prediction of ship motions. In: 5th Symposium on Naval Hydrodynamics. *pp. 3–79.*

Ortega, R., A. J. van der Schaft, I. Mareels and B. Maschke (2001). Putting energy back in control. IEEE Control Systems Magazine *pp. 18–33.*

Passino, K. M. (2005). Biomimicry for Optimization, Control and Automation. *Springer–Verlag. London.*

Pereira, M. (2006). Instruments for marine navigation: A historical perspective. In: Proc. of the 7th IFAC Conference on Manoeuvring and Control of Marine Craft (MCMC).

Perez, T. (2005). Ship Motion Control: Course Keeping and Roll Stabilisation Using Rudder and Fins. *Advances in Industrial Control. Springer-Verlag. London, UK.*

Perez, Tristan and Thor I. Fossen (2007). Kinematic models for manoeuvring and seakeeping of marine vessels. Modeling, Identification and Control **28***(1), 19–30.*

Pesce, C. P. (2003). The application of lagrange equations to mechanical systems with mass explicitly dependent on position. Journal of Applied Mechanics **70**, *751–756.*

Pesce, C. P. and E. A. Tannuri (2006). The lagrange equations for systems with mass varying explicitly with position: Some applications to offshore engineering. Journal of the Brazilian Society of Mechanical Sciences and Engineering **28***(4), 496–504.*

Philoponus, John (517). On Aristotle's Physics. *Ancient Commentators on Aristotle. 2006 ed.. Gerald Duckworth & Co. Ltd.*

Refsnes, J. E. G. (2008). Nonlinear Model-Based Control of Slender Body AUVs. PhD thesis. NTNU. Trondheim, Norway. Thesis 2008:60.

Ross, A., T. Perez and T.I. Fossen (2006). Clarification of the low-frequency modelling concept for marine craft. In: Conference on Maneouvring and Control of Marine Craft (MCMC).

Sagatun, S. I. (1992). Modeling and Control of Underwater Vehicles: A Lagrangian Approach. PhD thesis. The Norwegian Institute of Technology. Trondheim, Norway.

Sagatun, S. I. and T.I. Fossen (1991). Lagrangian Formulation of Underwater Vehicles' Dynamics. In: Proceedings of the IEEE International Conference on Systems, Man and Cybernetics. *Charlottesville, VA. pp. 1029–1034.*

SIMMAN *(2008). Denmark.*

Simos, A.N., C.P. Pesce, M.M. Bernitsas and S.B. Cohen (2002). Hydrodynamic model induced differences in spm post pitchfork bifurcation paths. Journal of Offshore Engineering and Arctic Engineering **124**, *174–178.*

Sir Isaac Newton (1687). Philosophiæ Naturalis Principia Mathematica. *1995, 3rd ed.. Prometheus Books. Amherst, NY, USA. Translated by Andrew Motte.*

Skjetne, R., Ø. Smogeli and T.I. Fossen (2004). A nonlinear ship maneuvering model: Identification and adaptive control with experiments for a model ship. Modeling, Identification and Control (MIC) **25**, *3–27.*

Slotine, J. J. E. and W. Li (1991). Applied Nonlinear Control. *Prentice-Hall Int. Englewood Cliffs, New Jersey 07632.*

Smogeli, Ø. N. (2006). Control of Marine Propellers: From Normal to Extreme Conditions. PhD thesis. Norwegian University of Science and Technology (NTNU). Trondheim, Norway.

Son, K. H. and K. Nomoto (1982). On the Coupled Motion of Steering and Rolling of a High Speed Container Ship. Naval Architect of Ocean Engineering **20**, *73–83. From J.S.N.A., Japan, Vol. 150, 1981.*

Sorabji, R., Ed.) (1987). Philoponus and the Rejection of Aristotelian Science. *Cornell University Press. Essay: Philoponus' Impetus Theory in the Arabic Tradition by F. Zimmerman.*

*Sørensen, A. J. (2005*a*).* Marine Cybernetics: Modelling and Control. *5th ed.. Department of Marine Technology, NTNU, Trondheim. UK-05-76.*

*Sørensen, A. J. (2005*b*). Structural issues in the design and operation of marine control systems.* Annual Reviews in Control **29***(1), 125–149.*

Takashina, J. (1986). Ship maneuvering motion due to tugboats and its mathematical model. Journal of the Society of Naval Architects of Japan **160**, *93–104. In Japanese.*

Tanaka, S. (1995). On the hydrodynamic forces acting on a ship at large drift angles. Transactions of the West-Japan Society of Naval Architects **91**, *81–94. In Japanese.*

Tick, L. J. (1959). Differential equations with frequency-dependent coefficients. Journal of Ship Research.

Truesdell, C. (1968). Essays in the History of Mechanics. *Springer-Verlag. Berlin, Germany.*

Truesdell, C. (1988). Great Scientists of Old as Heretics in the Scientific Method. *University of Virginia Press.*

van der Schaft, A.J. (1999). $\mathcal{L}_2$-Gain and Passivity Techniques in Nonlinear Control. *Springer-Verlag. Berlin.*

Vitruvius (ca. 27 B.C.). Ten Books on Architecture. *2001 ed.. Cambridge University Press.*

Wallace, W.A. (1981). Prelude to Galileo. *D. Reidel Publishing Company. 190 Old Derby Street, Hingham, MA 02043, USA.*

Weisstein, E. W. (2008). Euler angles. Technical report. Mathworld– A Wolfram Web Resource. http://mathworld.wolfram.com/EulerAngles.html.

White, Sir William H. (1877). A manual of naval architecture: For the use of officers of the Royal Navy, officers of the mercantile marine, shipbuilders and shipowners. *J. Murray. London, UK.*

Wichlund, K. Y., O. J. Sørdalen and O. Egeland (1995). Control Properties of Underactuated Vehicles. In: Proceedings of the IEEE Int. Conf. on Robotics and Automation. *Nagoya, Japan. pp. 2009–2014.*

Wiener, N. (1948). Cybernetics: Or Control and Communication in the Animal and the Machine. *2nd edition, 1965 ed.. MIT Press.*

Williams Jr., James H. (1996). Fundamentals of Applied Dynamics*. John Wiley & Sons, Inc.*

World Geodetic System (1984). Its Definition and Relationships with Local Geoedtic Systems. DMA TR 8350.2, 2nd ed., Defense Mapping Agency, Fairfax, VA.

Appendix A

Derivation of Kirchhoff's Equations

The kinetic energy of an object with mass $\mathbf{M}$ is given by:

$$T = \frac{1}{2}\boldsymbol{\nu}^\top \mathbf{M}\boldsymbol{\nu}.$$

Since this is quadratic in $\boldsymbol{\nu}$, we can apply Euler's Theorem on homogeneous functions (Kreyszig 1999) to state that:

$$\begin{aligned} \boldsymbol{\nu}\frac{\partial T}{\partial \boldsymbol{\nu}} &= 2T \\ \Rightarrow \boldsymbol{\nu}_1\frac{\partial T}{\partial \boldsymbol{\nu}_1} + \boldsymbol{\nu}_2\frac{\partial T}{\partial \boldsymbol{\nu}_2} &= 2T. \end{aligned}$$

It can be shown (see the proof in Section 18.32 of Milne-Thomson 1968) that the time rate of change of the impulse wrench $(\boldsymbol{\xi}, \boldsymbol{\lambda})$ can be related to the force-torque couple $(\boldsymbol{\tau}_1, \boldsymbol{\tau}_2)$ by:

$$\frac{\partial \boldsymbol{\xi}}{\partial t} = \boldsymbol{\tau}_1 \tag{A.1}$$

$$\frac{\partial \boldsymbol{\lambda}}{\partial t} = \boldsymbol{\tau}_2. \tag{A.2}$$

Consider the motion of $\{b\}$, relative to $\{n\}$: the latter fixed in space, and the former fixed to the body (see Section 2.1.1). Without loss of generality, the analysis begins with the two frames coincident: $o_b = o_n$ at $t = t_0$. The translational effects can be decoupled from the rotational effects by taking infinitesimal changes of each. The two can then be treated separately.

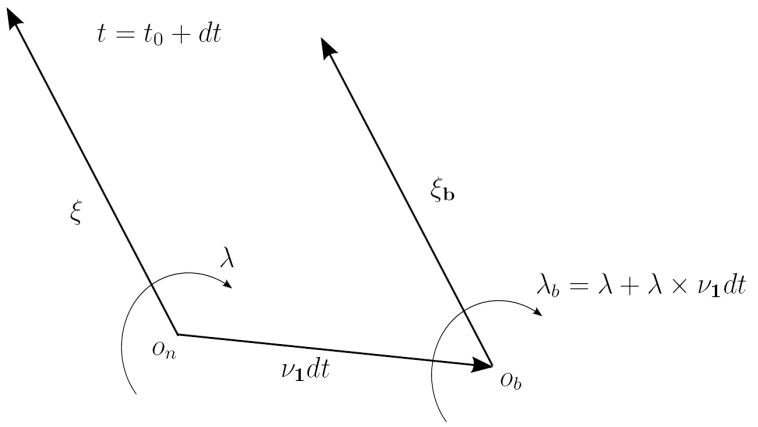

Figure A.1: An infinitesimal translation of the origin

Take the impulse wrench $(\boldsymbol{\xi}, \boldsymbol{\lambda})$ and translate it infinitesimally by the amount $\boldsymbol{\nu}_1 dt$. This is shown in Figure A.1. The translation does not affect the vector $\boldsymbol{\xi}_b$, but at $t = t_0 + dt$ alters the moment impulse $\boldsymbol{\lambda}_b$ by the amount $\boldsymbol{\nu}_1 dt \times \boldsymbol{\xi}$. That is, an infinitesimal translation gives:

$$(\boldsymbol{\xi}_b, \boldsymbol{\lambda}_b) = (\boldsymbol{\xi}, \boldsymbol{\lambda}) \quad t = t_0 \tag{A.3}$$

$$(\boldsymbol{\xi}_b, \boldsymbol{\lambda}_b) = (\boldsymbol{\xi}, \boldsymbol{\lambda} + \boldsymbol{\nu_1} dt \times \boldsymbol{\lambda}) \quad t = t_0 + dt. \tag{A.4}$$

Therefore, a translation induces an increment in the impulse term $\boldsymbol{\lambda}_b$ of $\mathbf{S}(\boldsymbol{\nu}_1)\boldsymbol{\lambda}$.

Take the same impulse wrench and rotate it infintesimally by the amount $\boldsymbol{\nu}_2 dt$. This is depicted in Figure A.2. The rotation alters $\boldsymbol{\xi}$ by $\boldsymbol{\nu}_2 dt \times \boldsymbol{\xi}$, and $\boldsymbol{\lambda}$ by $\boldsymbol{\nu}_2 dt \times \boldsymbol{\lambda}$.

$$(\boldsymbol{\xi}_b, \boldsymbol{\lambda}_b) = (\boldsymbol{\xi}, \boldsymbol{\lambda}) \quad t = t_0 \tag{A.5}$$

$$(\boldsymbol{\xi}_b, \boldsymbol{\lambda}_b) = (\boldsymbol{\xi} + \boldsymbol{\nu}_2 dt \times \boldsymbol{\xi}, \boldsymbol{\lambda} + \boldsymbol{\nu}_2 dt \times \boldsymbol{\lambda}) \quad t = t_0 + dt. \tag{A.6}$$

The two increments are therefore $\mathbf{S}(\boldsymbol{\nu}_2)\boldsymbol{\xi}$ and $\mathbf{S}(\boldsymbol{\nu}_2)\boldsymbol{\lambda}$ respectively.

The time rate of change of $(\boldsymbol{\xi}, \boldsymbol{\lambda})$ with respect to the $\{n\}$–frame is $d\boldsymbol{\xi}/dt$ and $d\boldsymbol{\lambda}/dt$ respectively. Collecting these with the two preceeding

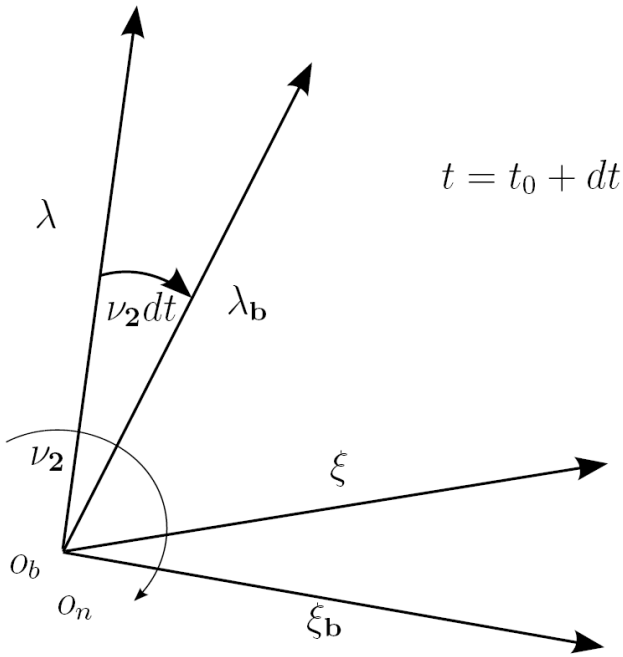

Figure A.2: An infinitesimal rotation of the origin

paragraphs' results gives:

$$\begin{aligned}\frac{\partial \boldsymbol{\xi}}{\partial t} &= \frac{d\boldsymbol{\xi}}{dt} + \mathbf{S}(\boldsymbol{\nu}_2)\,\boldsymbol{\xi} \\ \frac{\partial \boldsymbol{\lambda}}{\partial t} &= \frac{d\boldsymbol{\lambda}}{dt} + \mathbf{S}(\boldsymbol{\nu}_2)\,\boldsymbol{\lambda} + \mathbf{S}(\nu_1)\,\boldsymbol{\xi}.\end{aligned}$$

Applying (A.1)–(A.2) gives:

$$\frac{d\boldsymbol{\xi}}{dt} + \mathbf{S}(\boldsymbol{\nu}_2)\,\boldsymbol{\xi} = \boldsymbol{\tau}_1 \tag{A.7}$$

$$\frac{d\boldsymbol{\lambda}}{dt} + \mathbf{S}(\boldsymbol{\nu}_2)\,\boldsymbol{\lambda} + \mathbf{S}(\nu_1)\,\boldsymbol{\xi} = \boldsymbol{\tau}_2. \tag{A.8}$$

These constitute the equations of motion which relate the impulse wrench to the forces *in the body fixed frame*. The final step to be taken is to relate these equations to the kinetic energy.

An application of a force-torque couple over an infinitesimal time, δt, gives a corresponding increase in the velocities of $(\boldsymbol{\nu}_1 + \delta\boldsymbol{\nu}_1, \boldsymbol{\nu}_2 + \delta\boldsymbol{\nu}_2)$, at which time the impulse wrench will have changed to $(\boldsymbol{\xi} + \delta\boldsymbol{\xi}, \boldsymbol{\lambda}+\delta\boldsymbol{\lambda})$. Over the infinitesimal distance, the work done (i.e., the increment in kinetic energy) will be:

$$\boldsymbol{\nu}_1\delta\boldsymbol{\xi} + \boldsymbol{\nu}_2\delta\boldsymbol{\lambda} = \frac{\partial T}{\partial \boldsymbol{\nu}_1}\delta\boldsymbol{\nu}_1 + \frac{\partial T}{\partial \boldsymbol{\nu}_1}\delta\boldsymbol{\nu}_2 = \delta T. \tag{A.9}$$

If the linear and angular velocities are taken to be $\delta\boldsymbol{\nu}_1$ and $\delta\boldsymbol{\nu}_2$, then we can set $\delta = h$, where h is an alternative infintesimal scalar. By again applying Euler's Theorem we can see that $\delta\boldsymbol{\xi} = h\boldsymbol{\xi}$ and $\delta\boldsymbol{\lambda} = h\boldsymbol{\lambda}$. Similarly, $\delta T = 2hT$. This gives:

$$\boldsymbol{\nu}_1\boldsymbol{\xi} + \boldsymbol{\nu}_2\boldsymbol{\lambda} = \frac{\partial T}{\partial \boldsymbol{\nu}_1}\boldsymbol{\nu}_1 + \frac{\partial T}{\partial \boldsymbol{\nu}_2}\boldsymbol{\nu}_2 = 2T.$$

An additional infinitesimal variation then gives:

$$\boldsymbol{\nu}_1\delta\boldsymbol{\xi} + \boldsymbol{\xi}\delta\boldsymbol{\nu}_1 + \boldsymbol{\nu}_2\delta\boldsymbol{\lambda} + \boldsymbol{\lambda}\delta\boldsymbol{\nu}_2 = 2\delta T \tag{A.10}$$

Subtracting (A.9) from (A.10) gives the result:

$$\boldsymbol{\xi}\delta\boldsymbol{\nu}_1 + \boldsymbol{\lambda}\delta\boldsymbol{\nu}_2 = \delta T = \frac{\partial T}{\partial \boldsymbol{\nu}_1}\delta\boldsymbol{\nu}_1 + \frac{\partial T}{\partial \boldsymbol{\nu}_2}\delta\boldsymbol{\nu}_2$$

This then relates the impulse wrench $(\boldsymbol{\xi}, \boldsymbol{\lambda})$ to the kinetic energy as follows:

$$\boldsymbol{\xi} \equiv \frac{\partial T}{\partial \boldsymbol{\nu}_1} \tag{A.11}$$

$$\boldsymbol{\lambda} \equiv \frac{\partial T}{\partial \boldsymbol{\nu}_2} \tag{A.12}$$

First the equations of motion were derived in terms of the impulse wrench $(\boldsymbol{\xi}, \boldsymbol{\lambda})$, seen in equations (A.7)–(A.8). Now this impulse wrench has been derived in terms of the partial derivatives of the kinetic energy of the system, shown in (A.11) and (A.12).

The final step is then to substitute these relations back into (A.7)–(A.8). This gives:

$$\frac{d}{dt}\frac{\partial T}{\partial \boldsymbol{\nu}_1} + \mathbf{S}\left(\boldsymbol{\nu}_2\right)\frac{\partial T}{\partial \boldsymbol{\nu}_1} = \boldsymbol{\tau}_1 \tag{A.13}$$

$$\frac{d}{dt}\frac{\partial T}{\partial \boldsymbol{\nu}_2} + \mathbf{S}\left(\boldsymbol{\nu}_2\right)\frac{\partial T}{\partial \boldsymbol{\nu}_2} + \mathbf{S}\left(\nu_1\right)\frac{\partial T}{\partial \boldsymbol{\nu}_1} = \boldsymbol{\tau}_2. \tag{A.14}$$

These equations of motion are Kirchhoff's (1869) equations. Given a starting point of the kinetic energy T, these equations describe the relationship between the forces acting on a body, and the motion induced.

Appendix B

Equations of Motion

The equations of motion given in this chapter are derived by applying equations (A.13)–(A.14) to the kinetic energy of a system.

B.1 6–DOF Rigid Body Equations of Motion

Using

$$\mathbf{M}_{RB} = \begin{bmatrix} m & 0 & 0 & 0 & m.z_g & -m.y_g \\ 0 & m & 0 & -m.z_g & 0 & m.x_g \\ 0 & 0 & m & m.y_g & -m.x_g & 0 \\ 0 & -m.z_g & m.y_g & I_x & -I_{xy} & I_{xz} \\ m.z_g & 0 & -m.x_g & -I_{yx} & I_y & -I_{zy} \\ -m.y_g & m.x_g & 0 & I_{zx} & -I_{zy} & I_z \end{bmatrix}$$

gives the kinetic energy as $T = 1/2\boldsymbol{\nu}^\top \mathbf{M}_{RB}\boldsymbol{\nu}$. Using this in (A.13)–(A.14) gives the equations of motion to be:

$$\dot{\boldsymbol{\eta}} = \mathbf{J}(\boldsymbol{\theta})\,\boldsymbol{\nu} \tag{B.1}$$

$$\mathbf{M}_{RB}\dot{\boldsymbol{\nu}} + \mathbf{C}_{RB}(\boldsymbol{\nu})\,\boldsymbol{\nu} = \boldsymbol{\tau}_{RB}, \tag{B.2}$$

where the matrix function $\mathbf{C}_{RB}(\boldsymbol{\nu})$ is given by:

$$\mathbf{C}_{RB}(\boldsymbol{\nu}) = \begin{bmatrix} 0 & 0 & 0 \\ 0 & 0 & 0 \\ 0 & 0 & 0 \\ -m(y_g q + z_g r) & m(x_g q - w) & m(x_g r + v) \\ m(y_g p + w) & -m(z_g r + x_g p) & m(y_g r - u) \\ m(z_g p - v) & m(z_g q + u) & -m(x_g p + y_g q) \end{bmatrix} \begin{bmatrix} m(y_g q + z_g r) & -m(x_g q - w) & -m(x_g r + v) \\ -m(y_g p + w) & m(z_g r + x_g p) & -m(y_g r - u) \\ -m(z_g p - v) & -m(z_g q + u) & m(x_g p + y_g q) \\ 0 & I_{xz} p + I_z r & -I_y q \\ -I_{xz} p - I_z r & 0 & I_x p + I_{xz} r \\ I_y q & -I_x p - I_{xz} r & 0 \end{bmatrix}. \tag{B.3}$$

The rigid body equations of motion retain this form throughout the rest of this appendix.

B.2 6–DOF Low–Frequency Motion

The added–mass at low frequency is given by:

$$\mathbf{M}_A^0 = -\begin{bmatrix} X_{\dot{u}}^0 & X_{\dot{v}}^0 & X_{\dot{w}}^0 & X_{\dot{p}}^0 & X_{\dot{q}}^0 & X_{\dot{r}}^0 \\ Y_{\dot{u}}^0 & Y_{\dot{v}}^0 & Y_{\dot{w}}^0 & Y_{\dot{p}}^0 & Y_{\dot{q}}^0 & Y_{\dot{r}}^0 \\ Z_{\dot{u}}^0 & Z_{\dot{v}}^0 & Z_{\dot{w}}^0 & Z_{\dot{p}}^0 & Z_{\dot{q}}^0 & Z_{\dot{r}}^0 \\ K_{\dot{u}}^0 & K_{\dot{v}}^0 & K_{\dot{w}}^0 & K_{\dot{p}}^0 & K_{\dot{q}}^0 & K_{\dot{r}}^0 \\ M_{\dot{u}}^0 & M_{\dot{v}}^0 & M_{\dot{w}}^0 & M_{\dot{p}}^0 & M_{\dot{q}}^0 & M_{\dot{r}}^0 \\ N_{\dot{u}}^0 & N_{\dot{v}}^0 & N_{\dot{w}}^0 & N_{\dot{p}}^0 & N_{\dot{q}}^0 & N_{\dot{r}}^0 \end{bmatrix}. \tag{B.4}$$

The total kinetic energy in low frequency motion is then:

$$T = \frac{1}{2}\boldsymbol{\nu}^\top \left(\mathbf{M}_{RB} + \bar{\mathbf{M}}_A^0\right)\boldsymbol{\nu}. \tag{B.5}$$

Applying equations (A.13)–(A.14) gives:

$$\dot{\boldsymbol{\eta}} = \mathbf{J}(\boldsymbol{\theta})\,\boldsymbol{\nu} \tag{B.6}$$

$$\left(\mathbf{M}_{RB} + \bar{\mathbf{M}}_A^0\right)\dot{\boldsymbol{\nu}} + \left(\mathbf{C}_{RB}(\boldsymbol{\nu}) + \mathbf{C}_A^0(\boldsymbol{\nu})\right)\boldsymbol{\nu} = \boldsymbol{\tau}^b, \tag{B.7}$$

where the inertial component is given by:

$$\bar{\mathbf{M}}_A^0 = \frac{1}{2}\left(\mathbf{M}_A^0 + \left(\mathbf{M}_A^0\right)^\top\right).$$

The Coriolis–centripetal matrix function $\mathbf{C}_A^0(\boldsymbol{\nu})$ is given by:

$$\mathbf{C}_A^0(\boldsymbol{\nu}) = \begin{bmatrix} 0 & 0 & 0 & 0 & -a_3 & a_2 \\ 0 & 0 & 0 & a_3 & 0 & -a_1 \\ 0 & 0 & 0 & -a_2 & a_1 & 0 \\ 0 & -a_3 & a_2 & 0 & -b_3 & b_2 \\ a_3 & 0 & -a_1 & b_3 & 0 & -b_1 \\ -a_2 & a_1 & 0 & -b_2 & b_1 & 0 \end{bmatrix}, \tag{B.8}$$

where

$$\begin{aligned} a_1 &= X_{\dot{u}}u + \frac{1}{2}(X_{\dot{v}} + Y_{\dot{u}})v + \frac{1}{2}(X_{\dot{w}} + Z_{\dot{u}})w \\ &\quad + \frac{1}{2}(X_{\dot{p}} + K_{\dot{u}})p + \frac{1}{2}(X_{\dot{q}} + M_{\dot{u}})q + \frac{1}{2}(X_{\dot{r}} + N_{\dot{u}})r \qquad \text{(B.9)} \\ a_2 &= \frac{1}{2}(Y_{\dot{u}} + X_{\dot{v}})u + Y_{\dot{v}}v + \frac{1}{2}(Y_{\dot{w}} + Z_{\dot{v}})w \\ &\quad + \frac{1}{2}(Y_{\dot{p}} + K_{\dot{v}})p + \frac{1}{2}(Y_{\dot{q}} + M_{\dot{v}})q + \frac{1}{2}(Y_{\dot{r}} + N_{\dot{v}})r \qquad \text{(B.10)} \\ a_3 &= \frac{1}{2}(Z_{\dot{u}} + X_{\dot{w}})u + \frac{1}{2}(Z_{\dot{v}} + Y_{\dot{w}})v + Z_{\dot{w}}w \\ &\quad + \frac{1}{2}(Z_{\dot{p}} + K_{\dot{w}})p + \frac{1}{2}(Z_{\dot{q}} + M_{\dot{w}})q + \frac{1}{2}(Z_{\dot{r}} + N_{\dot{w}})r \qquad \text{(B.11)} \\ b_1 &= \frac{1}{2}(K_{\dot{u}} + X_{\dot{p}})u + \frac{1}{2}(K_{\dot{v}} + Y_{\dot{p}})v + \frac{1}{2}(K_{\dot{w}} + Z_{\dot{p}})w \\ &\quad + K_{\dot{p}}p + \frac{1}{2}(K_{\dot{q}} + M_{\dot{p}})q + \frac{1}{2}(K_{\dot{r}} + N_{\dot{p}})r \qquad \text{(B.12)} \\ b_2 &= \frac{1}{2}(M_{\dot{u}} + X_{\dot{q}})u + \frac{1}{2}(M_{\dot{v}} + Y_{\dot{q}})v + \frac{1}{2}(M_{\dot{w}} + Z_{\dot{q}})w \\ &\quad + \frac{1}{2}(M_{\dot{p}} + K_{\dot{q}})p + M_{\dot{q}}q + \frac{1}{2}(M_{\dot{r}} + N_{\dot{q}})r \qquad \text{(B.13)} \\ b_3 &= \frac{1}{2}(N_{\dot{u}} + X_{\dot{r}})u + \frac{1}{2}(N_{\dot{v}} + Y_{\dot{r}})v + \frac{1}{2}(N_{\dot{w}} + Z_{\dot{r}})w \\ &\quad + \frac{1}{2}(N_{\dot{p}} + K_{\dot{r}})p + \frac{1}{2}(N_{\dot{q}} + M_{\dot{r}})q + N_{\dot{r}}r. \qquad \text{(B.14)} \end{aligned}$$

B.3 Equations of Motion with Fluid Memory Effects

This section uses the results from Section 3.2. The time–domain representation of added–mass in the unified model is given by:

$$\mathbf{M}_A(t) = \frac{1}{\sqrt{2\pi}}\mathbf{M}_A^*(t) + \frac{1}{\sqrt{2\pi}}\mathbf{M}_A^\infty,$$

with the matrices given by:

$$\mathbf{M}_A^*(t) = -\begin{bmatrix} X_{\dot{u}}^*(t) & X_{\dot{v}}^*(t) & X_{\dot{w}}^*(t) & X_{\dot{p}}^*(t) & X_{\dot{q}}^*(t) & X_{\dot{r}}^*(t) \\ Y_{\dot{u}}^*(t) & Y_{\dot{v}}^*(t) & Y_{\dot{w}}^*(t) & Y_{\dot{p}}^*(t) & Y_{\dot{q}}^*(t) & Y_{\dot{r}}^*(t) \\ Z_{\dot{u}}^*(t) & Z_{\dot{v}}^*(t) & Z_{\dot{w}}^*(t) & Z_{\dot{p}}^*(t) & Z_{\dot{q}}^*(t) & Z_{\dot{r}}^*(t) \\ K_{\dot{u}}^*(t) & K_{\dot{v}}^*(t) & K_{\dot{w}}^*(t) & K_{\dot{p}}^*(t) & K_{\dot{q}}^*(t) & K_{\dot{r}}^*(t) \\ M_{\dot{u}}^*(t) & M_{\dot{v}}^*(t) & M_{\dot{w}}^*(t) & M_{\dot{p}}^*(t) & M_{\dot{q}}^*(t) & M_{\dot{r}}^*(t) \\ N_{\dot{u}}^*(t) & N_{\dot{v}}^*(t) & N_{\dot{w}}^*(t) & N_{\dot{p}}^*(t) & N_{\dot{q}}^*(t) & N_{\dot{r}}^*(t) \end{bmatrix} \tag{B.15}$$

$$\mathbf{M}_A^\infty = -\begin{bmatrix} X_{\dot{u}}^\infty & X_{\dot{v}}^\infty & X_{\dot{w}}^\infty & X_{\dot{p}}^\infty & X_{\dot{q}}^\infty & X_{\dot{r}}^\infty \\ Y_{\dot{u}}^\infty & Y_{\dot{v}}^\infty & Y_{\dot{w}}^\infty & Y_{\dot{p}}^\infty & Y_{\dot{q}}^\infty & Y_{\dot{r}}^\infty \\ Z_{\dot{u}}^\infty & Z_{\dot{v}}^\infty & Z_{\dot{w}}^\infty & Z_{\dot{p}}^\infty & Z_{\dot{q}}^\infty & Z_{\dot{r}}^\infty \\ K_{\dot{u}}^\infty & K_{\dot{v}}^\infty & K_{\dot{w}}^\infty & K_{\dot{p}}^\infty & K_{\dot{q}}^\infty & K_{\dot{r}}^\infty \\ M_{\dot{u}}^\infty & M_{\dot{v}}^\infty & M_{\dot{w}}^\infty & M_{\dot{p}}^\infty & M_{\dot{q}}^\infty & M_{\dot{r}}^\infty \\ N_{\dot{u}}^\infty & N_{\dot{v}}^\infty & N_{\dot{w}}^\infty & N_{\dot{p}}^\infty & N_{\dot{q}}^\infty & N_{\dot{r}}^\infty \end{bmatrix}. \tag{B.16}$$

The components of these are defined according to the notation in Section 3.2. The kinetic energy of the total system is then

$$T_A = \frac{1}{2}\boldsymbol{\nu}^\top\left(\mathbf{M}_{RB} + \mathbf{M}_A^\infty\right)\boldsymbol{\nu} + \sqrt{\frac{\pi}{2}}\left(\boldsymbol{\nu}^\top * \bar{\mathbf{M}}_A^* * \boldsymbol{\nu}\right)(t), \tag{B.17}$$

where

$$\bar{\mathbf{M}}_A^*(t) \triangleq \frac{1}{2}\left(\mathbf{M}_A^*(t) + \mathbf{M}_A^*(t)^\top\right).$$

Applying equations (A.13)–(A.14) gives:

$$\dot{\boldsymbol{\eta}} = \mathbf{J}(\boldsymbol{\theta})\boldsymbol{\nu} \tag{B.18}$$

$$\left(\mathbf{M}_{RB} + \mathbf{M}_A^\infty\right)\dot{\boldsymbol{\nu}} + \left(\mathbf{C}_{RB}(\boldsymbol{\nu}) + \mathbf{C}_A^\infty(\boldsymbol{\nu}) + \mathbf{C}_A^*(\boldsymbol{\nu})\right)\boldsymbol{\nu} = \boldsymbol{\tau}. \tag{B.19}$$

The Coriolis–centripetal matrices are formed as follows:

$$\mathbf{C}_A^\infty(\boldsymbol{\nu}) = \begin{bmatrix} 0 & 0 & 0 & 0 & -a_3^\infty & a_2^\infty \\ 0 & 0 & 0 & a_3^\infty & 0 & -a_1^\infty \\ 0 & 0 & 0 & -a_2^\infty & a_1^\infty & 0 \\ 0 & -a_3^\infty & a_2^\infty & 0 & -b_3^\infty & b_2^\infty \\ a_3^\infty & 0 & -a_1^\infty & b_3^\infty & 0 & -b_1^\infty \\ -a_2^\infty & a_1^\infty & 0 & -b_2^\infty & b_1^\infty & 0 \end{bmatrix},$$

where

$$
\begin{aligned}
a_1^{\infty} &\triangleq X_{\dot{u}}^{\infty} u + Y_{\dot{u}}^{\infty} v + Z_{\dot{u}}^{\infty} w + K_{\dot{u}}^{\infty} p + M_{\dot{u}}^{\infty} q + N_{\dot{u}}^{\infty} r && \text{(B.20)}\\
a_2^{\infty} &\triangleq X_{\dot{v}}^{\infty} u + Y_{\dot{v}}^{\infty} v + Z_{\dot{v}}^{\infty} w + K_{\dot{v}}^{\infty} p + M_{\dot{v}}^{\infty} q + N_{\dot{v}}^{\infty} r && \text{(B.21)}\\
a_3^{\infty} &\triangleq X_{\dot{w}}^{\infty} u + Y_{\dot{w}}^{\infty} v + Z_{\dot{w}}^{\infty} w + K_{\dot{w}}^{\infty} p + M_{\dot{w}}^{\infty} q + N_{\dot{w}}^{\infty} r && \text{(B.22)}\\
b_1^{\infty} &\triangleq X_{\dot{p}}^{\infty} u + Y_{\dot{p}}^{\infty} v + Z_{\dot{p}}^{\infty} w + K_{\dot{p}}^{\infty} p + M_{\dot{p}}^{\infty} q + N_{\dot{p}}^{\infty} r && \text{(B.23)}\\
b_2^{\infty} &\triangleq X_{\dot{q}}^{\infty} u + Y_{\dot{q}}^{\infty} v + Z_{\dot{q}}^{\infty} w + K_{\dot{q}}^{\infty} p + M_{\dot{q}}^{\infty} q + N_{\dot{q}}^{\infty} r && \text{(B.24)}\\
b_3^{\infty} &\triangleq X_{\dot{r}}^{\infty} u + Y_{\dot{r}}^{\infty} v + Z_{\dot{r}}^{\infty} w + K_{\dot{r}}^{\infty} p + M_{\dot{r}}^{\infty} q + N_{\dot{r}}^{\infty} r; && \text{(B.25)}
\end{aligned}
$$

and $\mathbf{C}_A^* (\boldsymbol{\nu})$ is:

$$
\mathbf{C}_A^* (\boldsymbol{\nu}) = \begin{bmatrix}
0 & 0 & 0 & 0 & -a_3^* & a_2^* \\
0 & 0 & 0 & a_3^* & 0 & -a_1^* \\
0 & 0 & 0 & -a_2^* & a_1^* & 0 \\
0 & -a_3^* & a_2^* & 0 & -b_3^* & b_2^* \\
a_3^* & 0 & -a_1^* & b_3^* & 0 & -b_1^* \\
-a_2^* & a_1^* & 0 & -b_2^* & b_1^* & 0
\end{bmatrix}, \qquad \text{(B.26)}
$$

where

$$
\begin{aligned}
a_1^* &\triangleq \frac{1}{2}\left(X_{\dot{u}}^* * u\right)(t) + \frac{1}{2}\left(X_{\dot{v}}^* * v\right)(t) + \frac{1}{2}\left(X_{\dot{w}}^* * w\right)(t) \\
&\quad + \frac{1}{2}\left(X_{\dot{p}}^* * p\right)(t) + \frac{1}{2}\left(X_{\dot{q}}^* + * q\right)(t) + \frac{1}{2}\left(X_{\dot{r}}^* * r\right)(t) && \text{(B.27)}\\
a_2^* &\triangleq \frac{1}{2}\left(Y_{\dot{u}}^* * u\right)(t) + \frac{1}{2}\left(Y_{\dot{v}}^* * v\right)(t) + \frac{1}{2}\left(Y_{\dot{w}}^* * w\right)(t) \\
&\quad + \frac{1}{2}\left(Y_{\dot{p}}^* * p\right)(t) + \frac{1}{2}\left(Y_{\dot{q}}^* + M_{\dot{v}}\right)(t) + \frac{1}{2}\left(Y_{\dot{r}}^* + N_{\dot{v}}\right)(t) && \text{(B.28)}\\
a_3^* &\triangleq \frac{1}{2}\left(Z_{\dot{u}}^* * u\right)(t) + \frac{1}{2}\left(Z_{\dot{v}}^* * v\right)v + \frac{1}{2}\left(Z_{\dot{w}}^* * w\right)(t) \\
&\quad + \frac{1}{2}\left(Z_{\dot{p}}^* * p\right)(t) + \frac{1}{2}\left(Z_{\dot{q}}^* * q\right)(t) + \frac{1}{2}\left(Z_{\dot{r}}^* * r\right)(t) && \text{(B.29)}
\end{aligned}
$$

$$
\begin{aligned}
b_1^* \triangleq\ & \frac{1}{2}\left(K_{\dot{u}}^* * u\right)(t) + \frac{1}{2}\left(K_{\dot{v}}^* * v\right)(t) + \frac{1}{2}\left(K_{\dot{w}}^* * w\right)(t) \\
& + \frac{1}{2}\left(K_{\dot{p}}^* * p\right)(t) + \frac{1}{2}\left(K_{\dot{q}}^* * q\right)(t) + \frac{1}{2}\left(K_{\dot{r}}^* * N_{\dot{p}}\right)(t) \qquad \text{(B.30)} \\
b_2^* \triangleq\ & \frac{1}{2}\left(M_{\dot{u}}^* * u\right)(t) + \frac{1}{2}\left(M_{\dot{v}}^* * v\right)(t) + \frac{1}{2}\left(M_{\dot{w}}^* * w\right)(t) \\
& + \frac{1}{2}\left(M_{\dot{p}}^* * p\right)(t) + \frac{1}{2}\left(M_{\dot{q}}^* * q\right)(t) + \frac{1}{2}\left(M_{\dot{r}}^* * r\right)(t) \qquad \text{(B.31)} \\
b_3^* \triangleq\ & \frac{1}{2}\left(N_{\dot{u}}^* * u\right)(t) + \frac{1}{2}\left(N_{\dot{v}}^* * v\right)(t) + \frac{1}{2}\left(N_{\dot{w}}^* * w\right)(t) \\
& + \frac{1}{2}\left(N_{\dot{p}}^* * p\right)(t) + \frac{1}{2}\left(N_{\dot{q}}^* * q\right)(t) + \frac{1}{2}\left(N_{\dot{r}}^* * r\right)(t). \qquad \text{(B.32)}
\end{aligned}
$$

Appendix C

PMM Test Data

The PMM tests from Chapter 6 are shown here in full. This set of tests was carried out on a 1:35.48 scale model of a modern frigate.

All data presented is nondimensional. The procedure for nondimensionalisation is:

$$
\begin{aligned}
u' &= \frac{u}{U_0} \\
v' &= \frac{v}{U_0} \\
r' &= \frac{r}{U_0/L_{pp}} \\
t' &= \frac{t}{L_{pp}/U_0} \\
X' &= \frac{X}{\frac{1}{2}\rho U_n^2 L_{pp}^2} \\
Y' &= \frac{Y}{\frac{1}{2}\rho U_n^2 L_{pp}^2} \\
K' &= \frac{K}{\frac{1}{2}\rho U_n^2 L_{pp}^3} \\
N' &= \frac{N}{\frac{1}{2}\rho U_n^2 L_{pp}^3}
\end{aligned}
$$

C.1 Thirty Knot Tests

C.1.1 Pure Sway

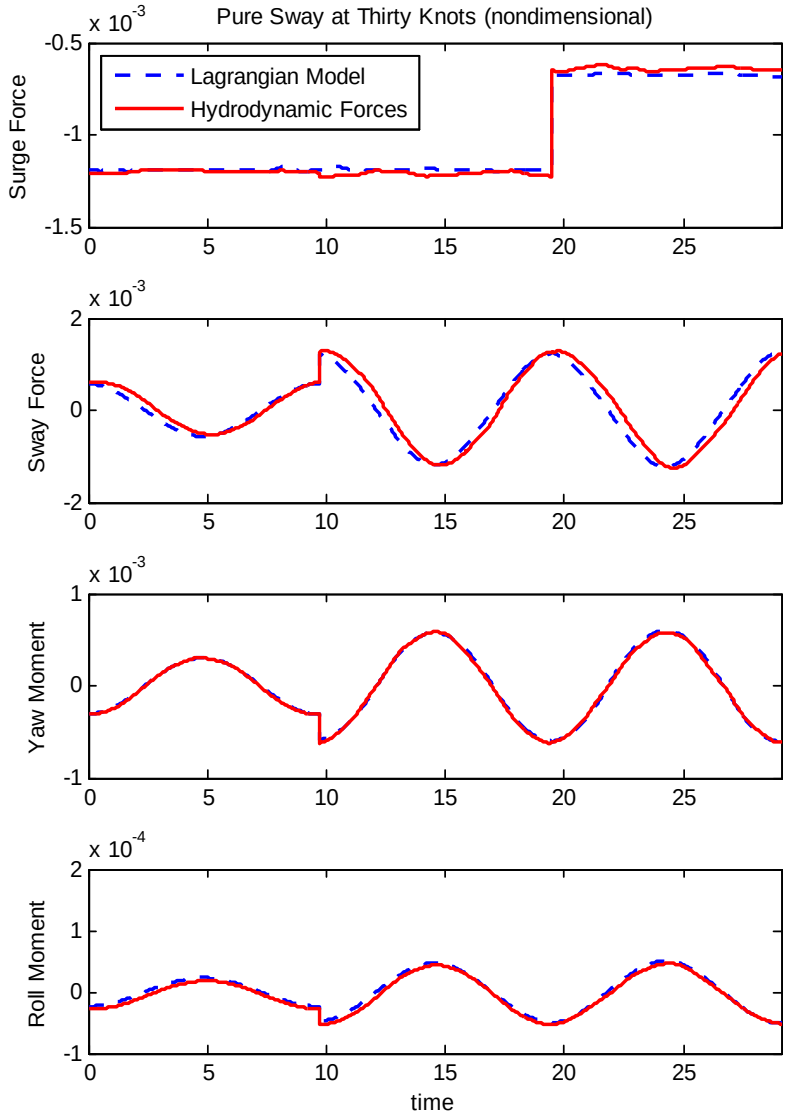

30kt, pure sway motion.

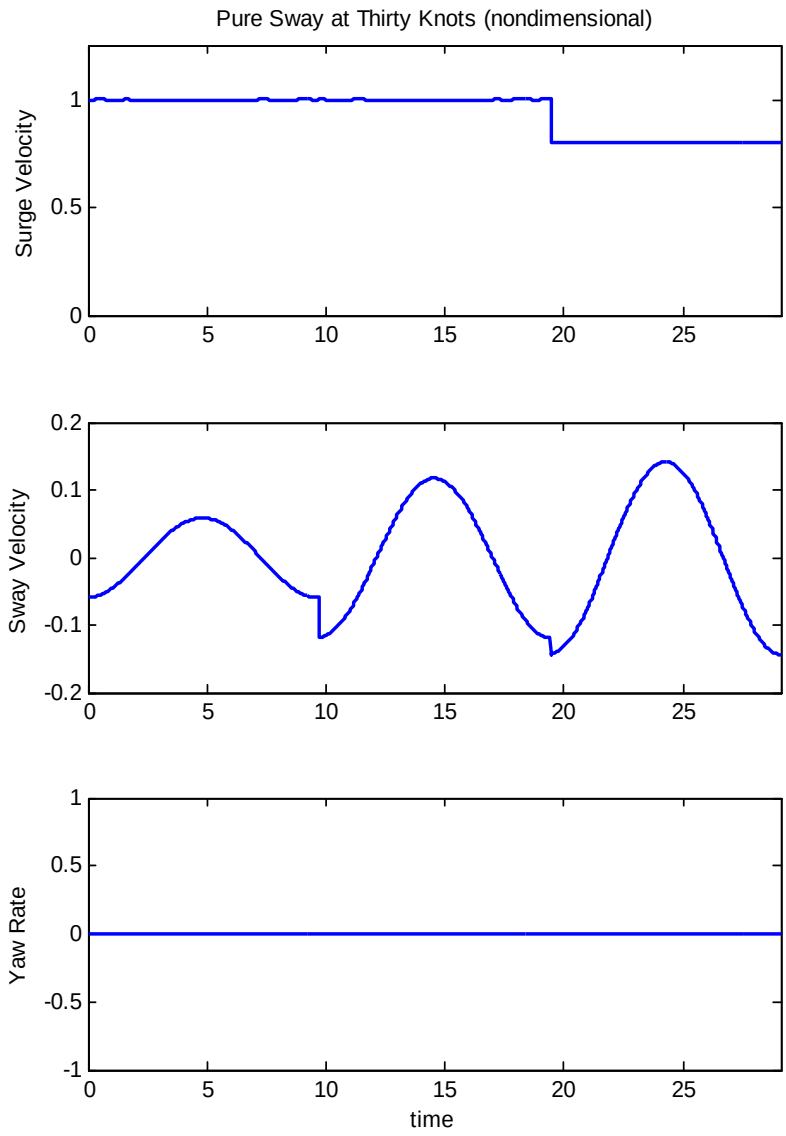

Velocities during 30kt pure sway motion.

C.1.2 Pure Yaw

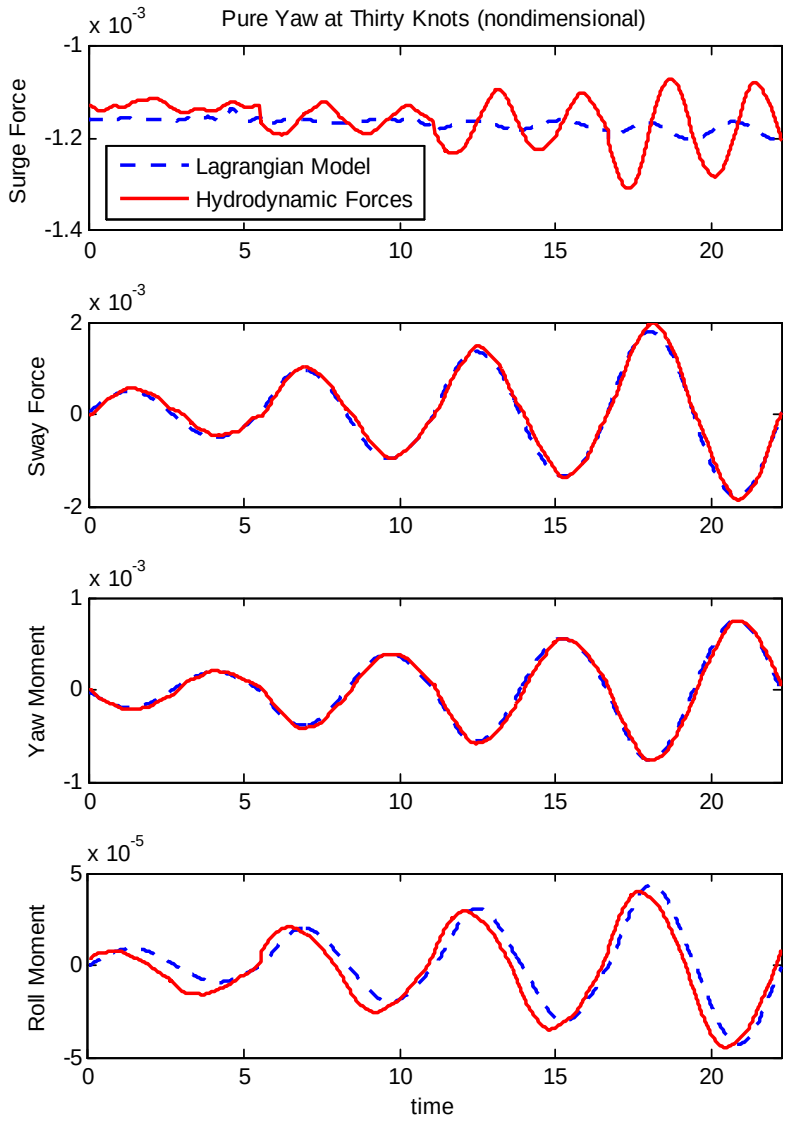

30kt pure yaw motion.

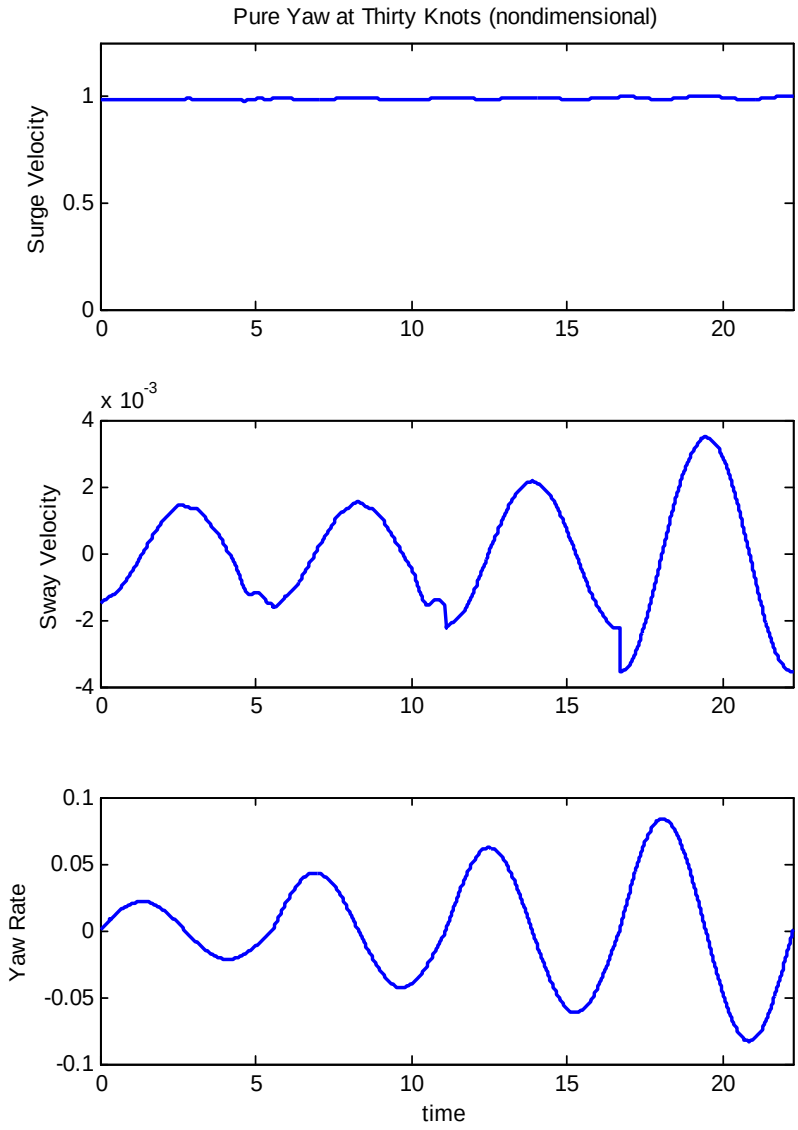

Velocities during 30kt pure yaw motion.

C.1.3 Mixed Sway and Yaw

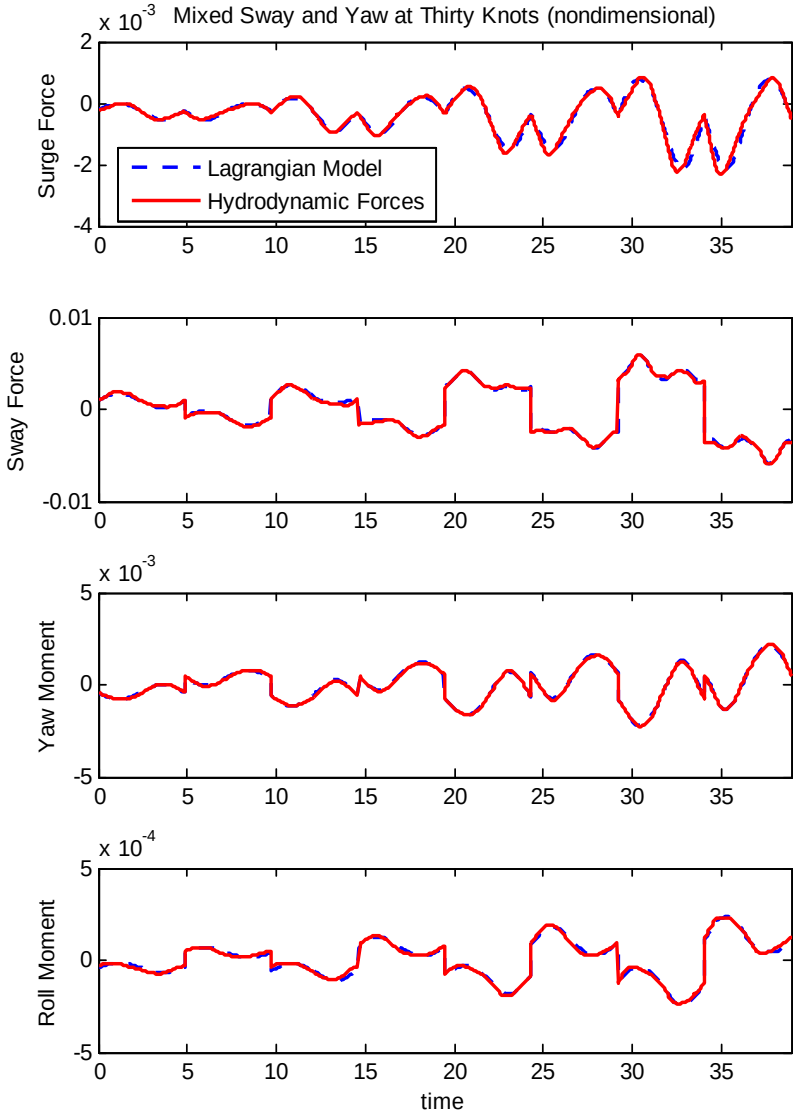

30kt mixed sway and yaw motion.

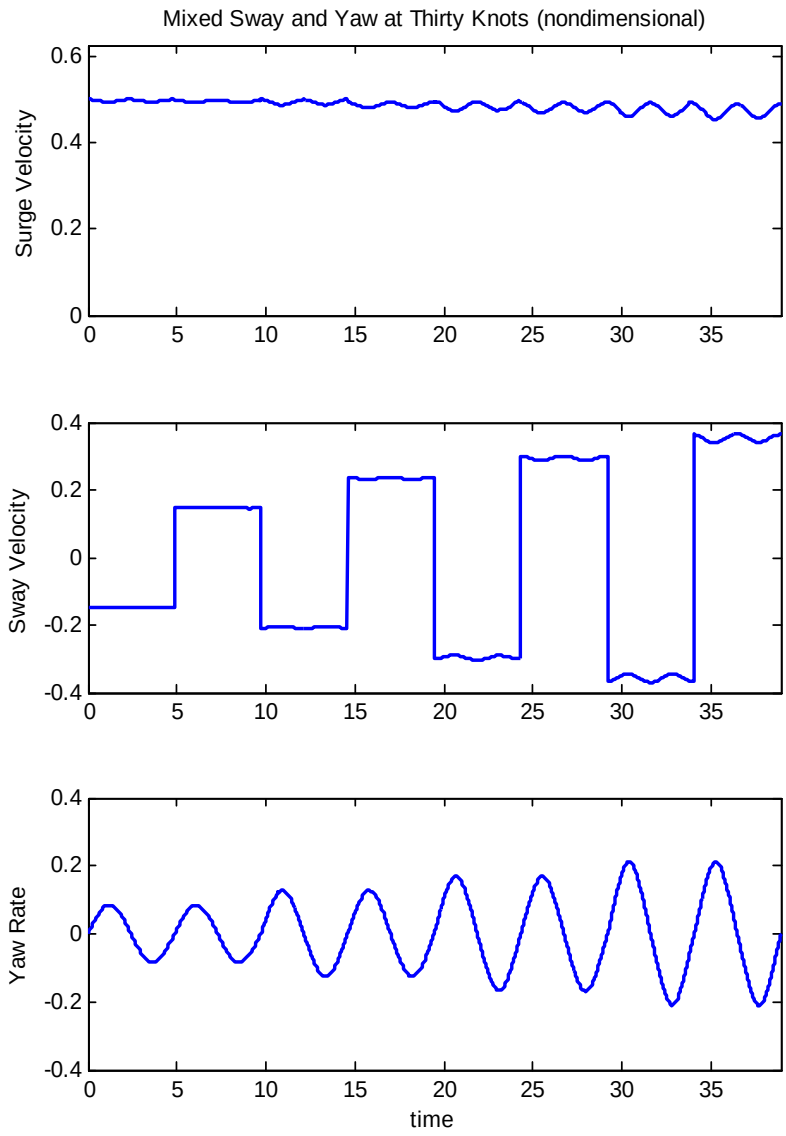

Velocities during 30kt mixed sway and yaw motion.

C.2 Eighteen Knot Tests

C.2.1 Pure Yaw

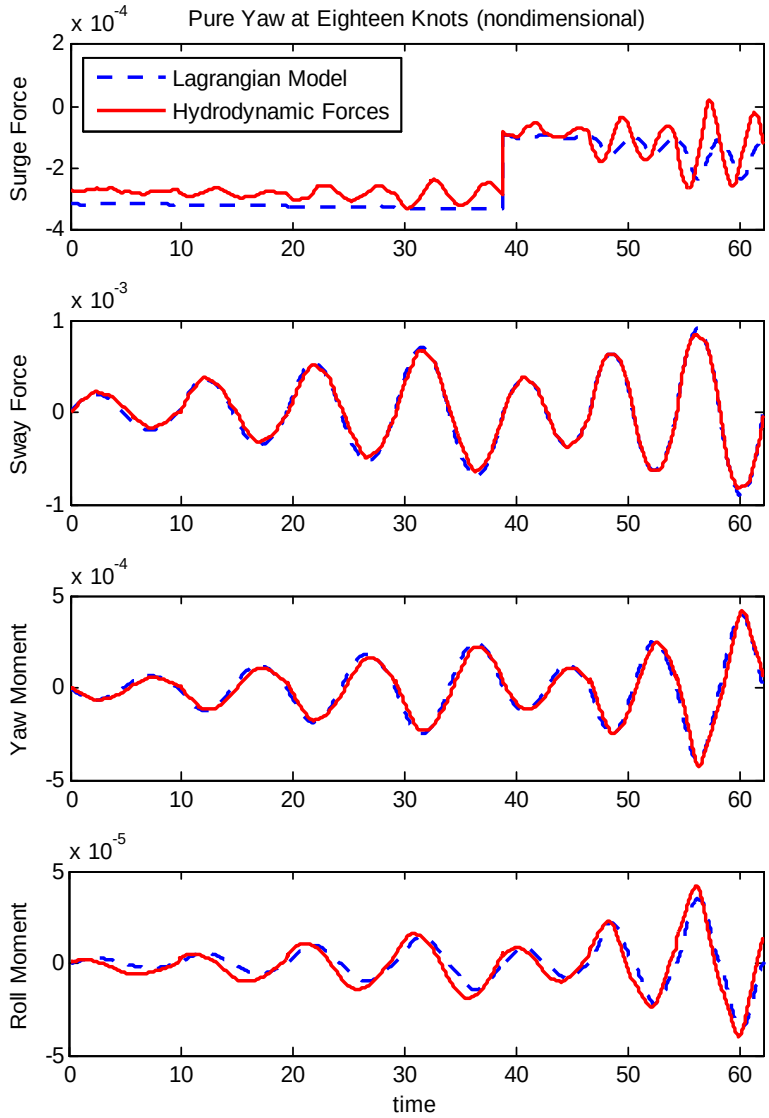

Pure yaw motion at 18kt.

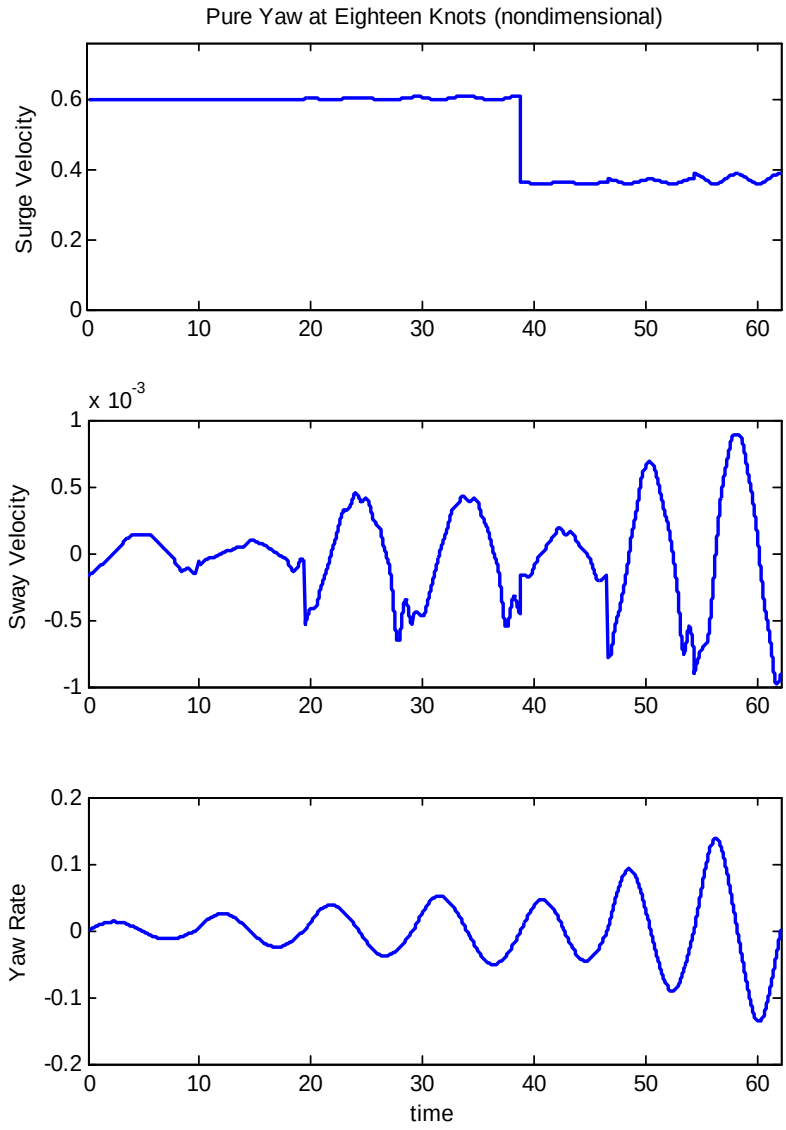

Velocities during pure yaw motion at 18kt.

C.2.2 Mixed Sway and Yaw

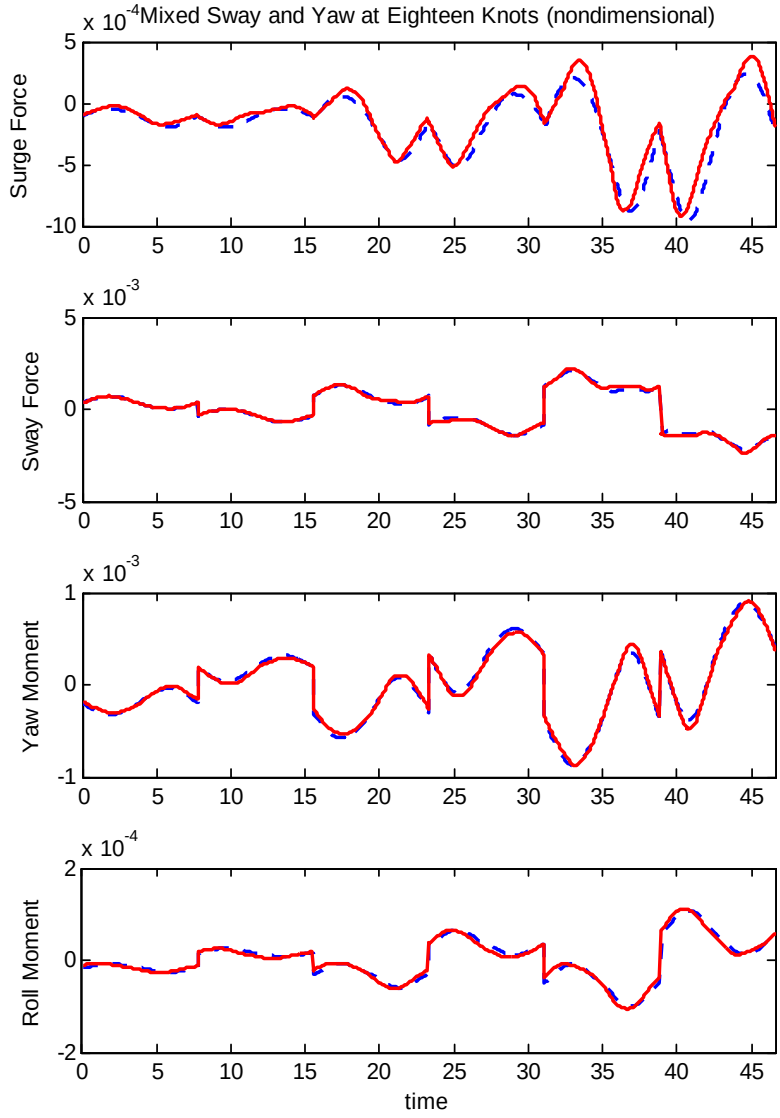

Mixed sway and yaw motion at 18kt.

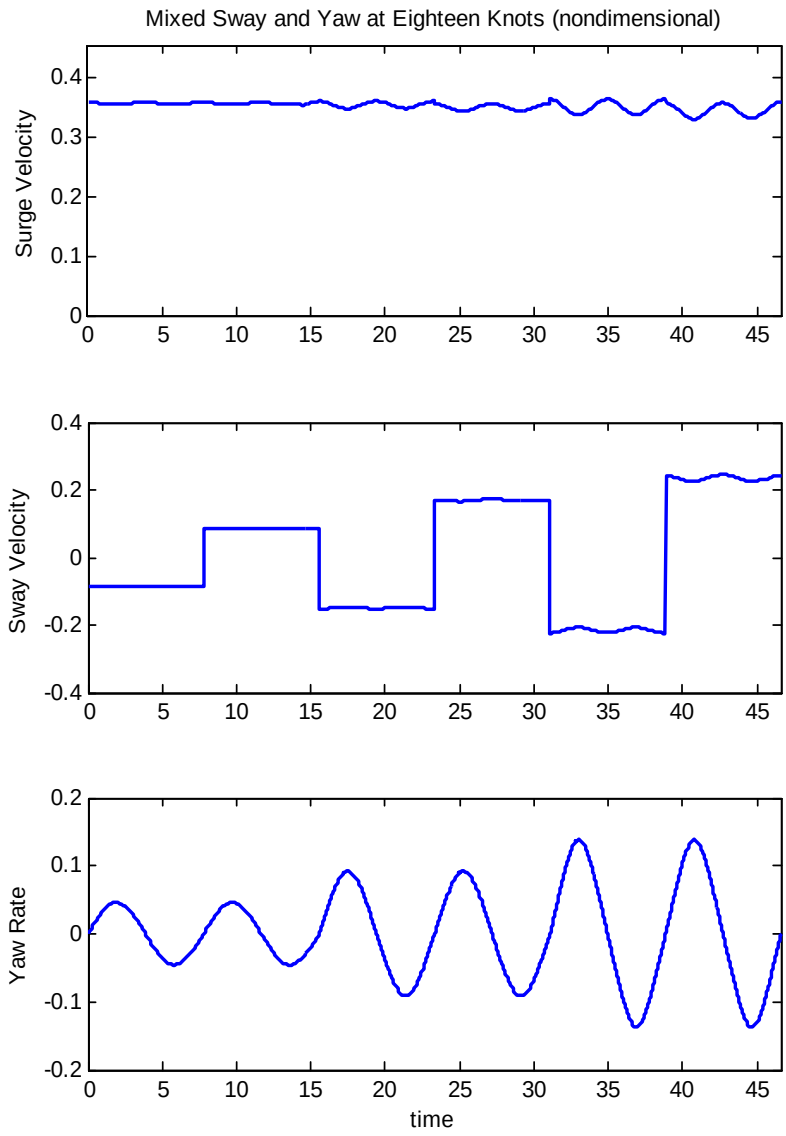

Velocities during mixed sway and yaw motion at 18kt.